

1 **Vulnerability of amphibians to global warming**

2 Patrice Pottier^{1,2*}, Michael R. Kearney³, Nicholas C. Wu⁴, Alex R. Gunderson⁵, Julie E. Rej⁵, A.
3 Nayelli Rivera-Villanueva^{6,7}, Pietro Pollo¹, Samantha Burke¹, Szymon M. Drobniak^{1,8+}, and
4 Shinichi Nakagawa^{1,9+}

5
6 ¹ Evolution & Ecology Research Centre, School of Biological, Earth and Environmental
7 Sciences, University of New South Wales, Sydney, New South Wales, Australia.

8 ² Division of Ecology and Evolution, Research School of Biology, The Australian National
9 University, Canberra, Australian Capital Territory, Australia

10 ³ School of BioSciences, The University of Melbourne, Melbourne, Victoria, Australia

11 ⁴ Hawkesbury Institute for the Environment, Western Sydney University, Richmond, New South
12 Wales, Australia

13 ⁵ Department of Ecology and Evolutionary Biology, Tulane University, New Orleans, Louisiana,
14 USA

15 ⁶ Centro Interdisciplinario de Investigación para el Desarrollo Integral Regional Unidad Durango
16 (CIIDIR), Instituto Politécnico Nacional, Durango, México

17 ⁷ Laboratorio de Biología de la Conservación y Desarrollo Sostenible de la Facultad de Ciencias
18 Biológicas, Universidad Autónoma de Nuevo León, Monterrey, México

19 ⁸ Institute of Environmental Sciences, Jagiellonian University, Kraków, Poland.

20 ⁹ Department of Biological Sciences, University of Alberta, Edmonton, Alberta, Canada.

21 *Corresponding author

22 +These authors supervised the work equally

23 Corresponding author: Patrice Pottier (p.pottier@unsw.edu.au)

24 **ORCID**

25 Patrice Pottier <https://orcid.org/0000-0003-2106-6597>

26 Michael R. Kearney <https://orcid.org/0000-0002-3349-8744>

27 Nicholas C. Wu <https://orcid.org/0000-0002-7130-1279>

28 Alex R. Gunderson <https://orcid.org/0000-0002-0120-4246>

29 Julie E. Rej <https://orcid.org/0000-0002-3670-067X>

30 A. Nayelli Rivera-Villanueva <https://orcid.org/0000-0002-9190-4317>

31 Pietro Pollo <https://orcid.org/0000-0001-6555-5400>

32 Samantha Burke <https://orcid.org/0000-0001-6902-974X>

33 Szymon M. Drobniak <https://orcid.org/0000-0001-8101-6247>

34 Shinichi Nakagawa <https://orcid.org/0000-0002-7765-5182>

35 **Summary**

36 Amphibians are the most threatened vertebrates, yet their resilience to rising temperatures
37 remains poorly understood^{1,2}. This is primarily because knowledge of thermal tolerance is
38 taxonomically and geographically biased³, compromising global climate vulnerability
39 assessments. Here, we employed a phylogenetically-informed data imputation approach to
40 predict the heat tolerance of 60% of amphibian species and assessed their vulnerability to daily
41 temperature variation in thermal refugia. We found that 104 out of 5203 species (2%) are currently
42 exposed to overheating events in shaded terrestrial conditions. Despite accounting for heat
43 tolerance plasticity, a 4°C global temperature increase would create a step-change in impact
44 severity, pushing 7.5% of species beyond their physiological limits. In the Southern Hemisphere,
45 tropical species encounter disproportionately more overheating events, while non-tropical species
46 are more susceptible in the Northern Hemisphere. These findings challenge evidence for a
47 general latitudinal gradient in overheating risk⁴⁻⁶ and underscore the importance of considering
48 climatic variability in vulnerability assessments. We provide conservative estimates assuming
49 access to cool shaded microenvironments. Therefore, the impacts of global warming will likely
50 exceed our projections. Our microclimate-explicit analyses demonstrate that vegetation and water
51 bodies are critical in buffering amphibians during heat waves. Immediate action is needed to
52 preserve and manage these microhabitat features.

53 **Keywords**

54 Anura, Caudata, critical thermal maximum, behavioral thermoregulation, behavioural
55 thermoregulation, microclimate selection, biophysical modelling, global analysis, thermal safety
56 margin, warming tolerance, extreme heat events, climate change.

57

58 **Main text**

59 Climate change has pervasive impacts on biodiversity, yet the extent and consequences of this
60 environmental crisis vary spatially and taxonomically^{7,8}. For ectothermic species, such as
61 amphibians, the link between climate warming and body temperature is clear, with immediate
62 effects on physiological processes⁹. Over 40% of amphibian species are currently listed as
63 threatened, and additional pressures due to escalating thermal extremes may further increase
64 their extinction risk^{2,10}. Therefore, it is vital to assess the resilience of amphibians to climate
65 change to prioritise where and how conservation actions are taken.

66 Accurate assessments of resilience to climate change require adequate data on thermal
67 tolerance and environmental exposure^{5,6,11}. However, the most exhaustive dataset on
68 amphibian heat tolerance limits only covers 7.5% of known species and is geographically
69 biased towards temperate regions³ (Fig. 1). This discrepancy is problematic, considering the
70 high species richness in the tropics and the mounting evidence that tropical ectotherms are
71 most susceptible to rising temperatures^{4-6,12,13}. Such sampling biases call into question the
72 reliability of inferences in under-sampled areas and have implications for conservation
73 strategies. Given the rapid pace of climate change and the finite resources available for
74 research, acquiring sufficient empirical data to fill these knowledge gaps within a realistic
75 timeframe is increasingly untenable^{14,15}. Therefore, alternative methods to identify the
76 populations and areas most susceptible to thermal stress are critically needed in a rapidly
77 warming climate.

78 Climate vulnerability assessments also require environmental data with high spatial and
79 temporal resolution, particularly because extreme heat is more likely to trigger overheating
80 events than increased mean temperatures¹⁶⁻¹⁸. When heat tolerance limits are known, cutting-
81 edge approaches in biophysical ecology allow fine-scale vulnerability assessments that account
82 for morphology, behaviour, and microhabitat setting in both historical and future climate
83 projections^{19,20}. While broadly applicable, biophysically informed analyses are particularly
84 relevant for amphibians, whose body temperatures depend on evaporative heat loss and whose

85 microhabitat use span terrestrial, aquatic, and arboreal environments. Because
86 microenvironmental features are essential for behavioural thermoregulation^{21,22}, modelling
87 microhabitats allow assessments of the effectiveness of different thermal refugia in buffering the
88 impacts of extreme heat events.

89 Here, we assess the global vulnerability of amphibians to extreme heat events in
90 different climatic scenarios and thermal refugia. By integrating predicted thermal limits for 60%
91 of amphibian species with daily operative body temperatures, our study offers the first
92 comprehensive evaluation of the impact of heat extremes on the physiological viability of
93 amphibians in nature.

94 ***Thermal limits and environmental exposure***

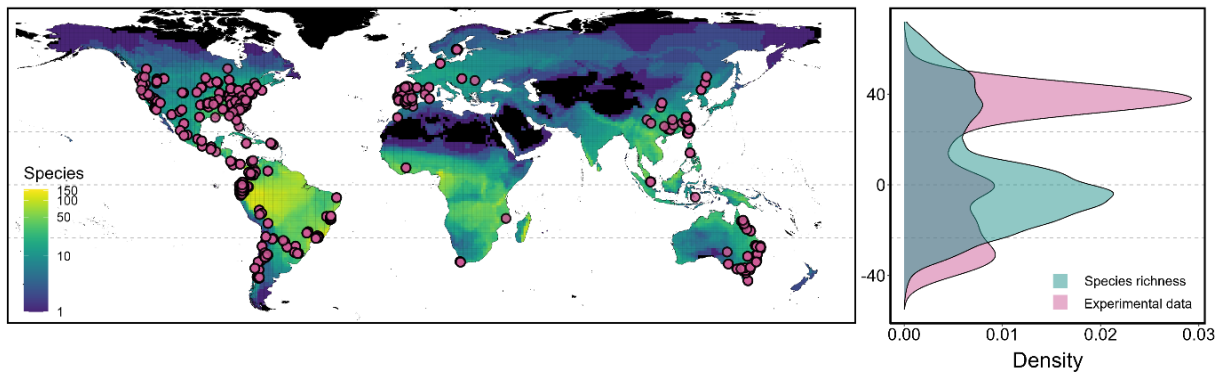
95 We first developed an approach to predict standardised thermal limits for 5,203 amphibian
96 species using data imputation based on phylogenetic niche clustering (Pagel's $\lambda = 0.95$ [0.91 –
97 0.98]) and known correlations between critical thermal limits (CT_{max}) and other variables ($n =$
98 2,661 estimates measured in 524 species; Fig. S2; Methods). Our phylogenetic model-based
99 imputation approach has expanded our understanding of amphibian thermal tolerance by
100 generating testable predictions for 4,679 unstudied species, particularly in biodiversity hotspots
101 (Fig. 1-2). We confirmed our imputation approach was accurate and unbiased by demonstrating
102 a strong congruence between experimental and imputed data in cross-validations (experimental
103 mean \pm standard deviation = 36.19 ± 2.67 ; imputed mean = 35.93 ± 2.54 ; $n = 375$; $r = 0.86$;
104 Extended Data Fig. 2a,b), though, as expected, the uncertainty in imputed predictions was
105 higher in understudied clades (Extended Data Fig. 2c).

106 We then integrated predicted thermal limits with daily maximum operative body
107 temperature fluctuations estimated from biophysical models to evaluate the sensitivity of
108 amphibians to extreme heat events in terrestrial, aquatic, and arboreal microhabitats (Extended
109 Data Fig. 1; Methods). Operative body temperatures are the steady-state body temperatures
110 that organisms would achieve in a given microenvironment, which can diverge significantly from
111 ambient air temperatures due to, for example, radiative and evaporative heat exchange

112 processes^{19,20}. For each microhabitat, we modelled daily operative body temperatures during
113 the warmest quarters of 2006-2015 and across the distribution range of each species
114 (Methods). We also used projected future climate data from TerraClimate²³ to generate
115 projections assuming 2°C or 4°C of global warming above pre-industrial levels. These
116 temperatures are within the range projected by the end of the century under low and
117 intermediate/high greenhouse gas emission scenarios, respectively²⁴. Notably, recent historical
118 CO₂ emissions most closely align with high warming scenarios²⁵ (i.e., 4.3°C of predicted
119 warming by 2100). All microenvironmental projections assumed access to 85% of shade and
120 sufficient humidity to maintain wet skin to simulate amphibians in thermal refugia (Methods).

121 We estimated the vulnerability of amphibians by estimating daily differences between
122 predicted thermal limits and maximum hourly operative body temperatures (Extended Data Fig.
123 1; Methods). We also adjusted daily thermal limits to assume that species were, on any given
124 day, acclimated to local mean weekly operative body temperatures, effectively accounting for
125 plasticity throughout species' distribution ranges (Methods). In total, we predicted vulnerability
126 metrics for 203,853 local species occurrences (individual species in 1° x 1° grid cells) in
127 terrestrial conditions (5,177 species), 204,808 local species occurrences in water bodies (5,203
128 species); and 56,210 local species occurrences (1,771 species) in above-ground vegetation, for
129 each warming scenario. The number of species examined in arboreal conditions was lower to
130 reflect morphological adaptations required for climbing in above-ground vegetation. These
131 estimates were then grouped into assemblages (all species occurring in 1° x 1° grid cells),
132 tallying 14,090 and 14,091 assemblages for terrestrial and aquatic species and 6,614
133 assemblages for arboreal species, respectively.

134

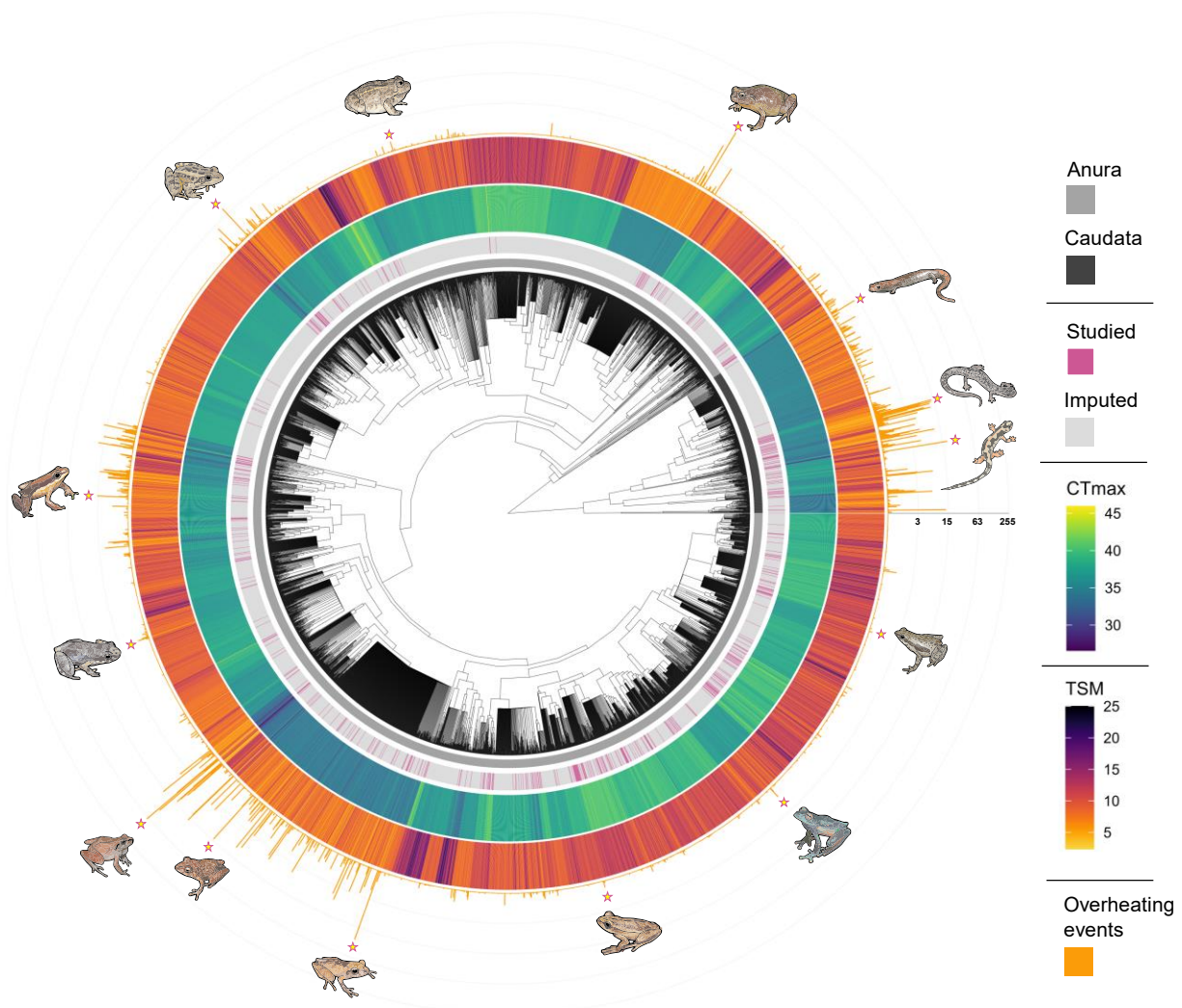


135

136 **Fig. 1 | Contrast between the geographical locations at which experimental data were**
 137 **collected and patterns in species richness.** Pink points denote experimental data (587
 138 species), while the colour gradients refer to species richness calculated in 1 x 1 ° grid cells in
 139 the imputed data (5,203 species). Density plots on the right panel represent the distribution of
 140 experimental data (pink) and the number of species inhabiting these areas (blue) across
 141 latitudes. Dashed lines represent the equator and tropics.

142

143



144
 145 **Fig. 2 | Phylogenetic coverage and taxonomic variation in climate vulnerability.** Heat
 146 maps show heat tolerance limits (CT_{max}) and thermal safety margins (TSM), while histograms
 147 show the number of overheating events (days) averaged across each species' distribution
 148 range ($n = 5,177$ species). Pink bars refer to species with prior knowledge ($n = 521$), while grey
 149 bars refer to entirely imputed species ($n = 4,656$). This figure was constructed assuming
 150 ground-level microclimates occurring under 4°C of global warming above pre-industrial levels.
 151 Phylogeny is based on the consensus of 10,000 trees sampled from a posterior distribution (see
 152 ²⁶ for details). Highlighted species starting from the right side, anti-clockwise: *Neurergus kaiseri*,
 153 *Plethodon kiamichi*, *Bolitoglossa altamazonica*, *Cophixalus aenigma*, *Tomaptera cryptotis*,
 154 *Lithobates palustris*, *Allobates subfolionidificans*, *Phyzelaphryne miriamae*, *Barycholos ternetzi*,
 155 *Pristimantis carvalhoi*, *Pristimantis ockendeni*, *Boana curupi*, *Teratohyla adenocheira*, *Atelopus*
 156 *spumarius*.

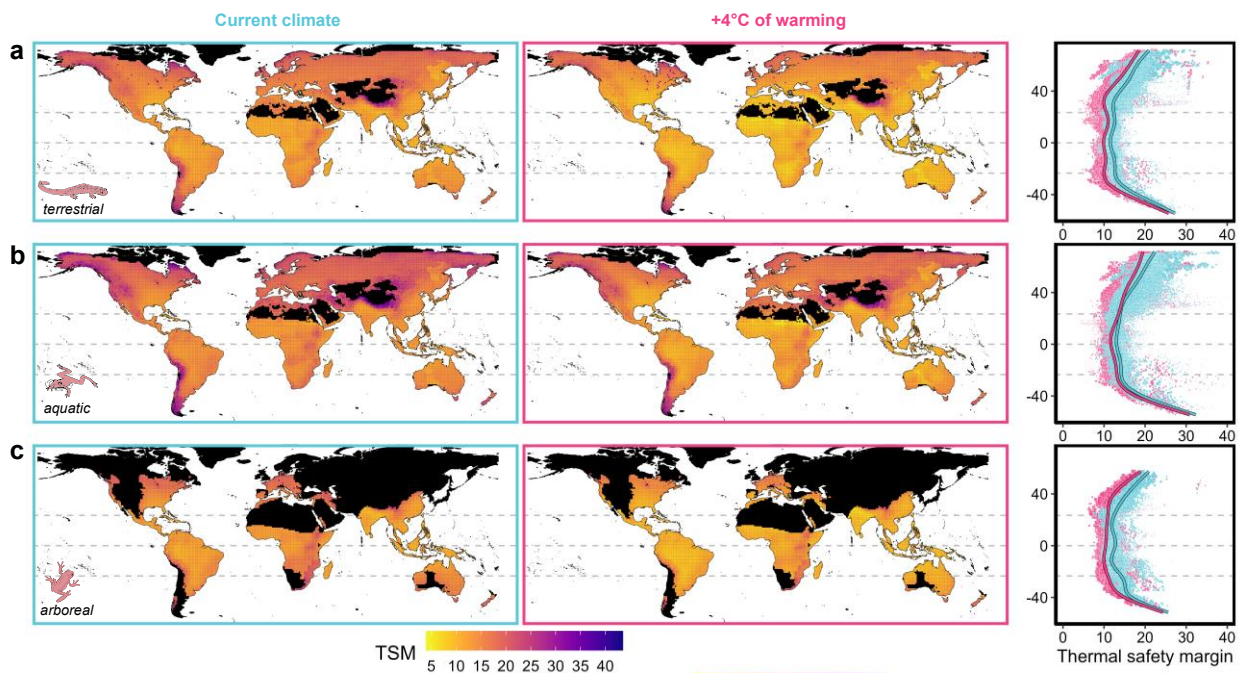
157

158

159 ***Vulnerability to historical and future heat***

160 We first calculated thermal safety margins (TSM, *sensu* ⁶) as the weighted mean difference
161 between heat tolerance limits (CT_{max}) and the maximum daily body temperatures of the warmest
162 quarters of 2006-2015 for each local species occurrence. Thermal safety margins averaged
163 from long-term climatology are routinely used in climate vulnerability analyses²⁷⁻²⁹. We found
164 evidence for a decline in TSM towards mid to low latitudes in all microhabitats, a pattern
165 maintained across warming scenarios (Fig. 3, Extended Data Fig. 3). However, warming
166 substantially reduce TSM at all latitudes (Fig. 3), likely reflecting the contrast between weak
167 plastic responses in CT_{max} across latitudes^{11,15} (Extended Data Fig. 3; Fig. S3) and large
168 variation in environmental temperatures (Extended Data Fig. 3). Across all conditions simulated,
169 TSM is always positive, even in the highest warming scenario (Fig. 3, Extended Data Fig. 3).
170 The mean TSM is lower for terrestrial (mean [95% confidence intervals]; current = 11.69 [8.86 –
171 14.43]; +4°C = 9.41 [6.53 – 12.09]) and arboreal conditions (current = 12.23 [9.40 – 14.96];
172 +4°C = 10.07 [7.23 – 12.80]) than for water bodies (current = 13.60 [10.71 – 16.28]; +4°C =
173 11.68 [8.80 – 14.36]; Fig. 3; Extended Data Table 1).

174



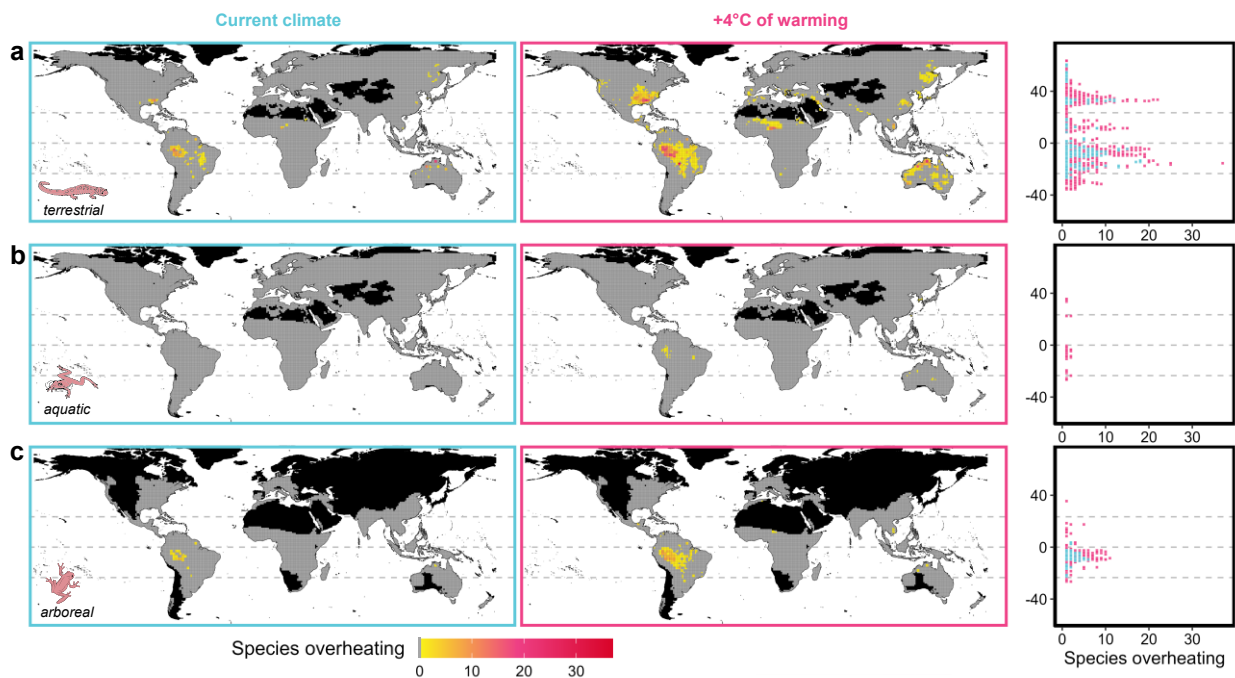
175
 176 **Fig. 3 | Assemblage-level patterns in thermal safety margin for amphibians in terrestrial**
 177 **(a), aquatic (b) or arboreal (c) microhabitats.** Thermal safety margins (TSM) were calculated
 178 as the weighted mean difference between CT_{max} and the predicted operative body temperature
 179 in full shade during the warmest quarters of 2006-2015 in each assemblage (1-degree grid cell).
 180 Black colour depicts areas with no data. The right panel depicts latitudinal patterns in TSM in
 181 current climates (blue) or assuming 4°C of global warming above pre-industrial levels (pink), as
 182 predicted from generalised additive mixed models. Point estimates are scaled by precision
 183 (1/s.e.). Dashed lines represent the equator and tropics.

184 Because extreme heat events are more likely to trigger overheating events than mean
 185 temperatures^{5,6,11}, we also calculated the binary probability (0/1) that operative body
 186 temperatures exceeded CT_{max} for at least one day across the warmest quarters of 2006-2015
 187 (i.e., overheating risk). Overall, overheating risk is low, although numerous species are
 188 predicted to face overheating events locally (Fig. 4, Extended Data Table 2). In terrestrial
 189 conditions, we predict that 104 species (836 local species occurrences from 253 assemblages)
 190 are likely to experience overheating events in current microclimates (Fig. 4-5). However, under
 191 4°C of warming, 391 species (4,248 local species occurrences from 1,328 assemblages) are
 192 expected to overheat, which represents nearly a four-fold increase relative to current conditions
 193 (Fig. 4-5; Extended Data Table 2-3). The number of species predicted to overheat in each grid
 194 cell also increases with warming; each assemblage comprises up to 18 vulnerable species in
 195 current climates (mean [95% confidence intervals] = 3.19 [0.60 – 6.88] species) and up to 37
 196 vulnerable species with 4°C of global warming (3.08 [0.62 – 6.56]; Fig. 4; Extended Data Table

197 3). In addition, the proportion of species predicted to experience overheating events in each
198 assemblage varies geographically and between warming scenarios (Extended Data Fig. 5;
199 Extended Data Table 4). The proportion of species at risk is high in some areas with high
200 species richness (e.g., Northern Australia, Southeastern United States) and not linearly
201 predicted by latitude (Extended Data Fig. 5).

202 In current conditions for species that can shelter in trees (arboreal), 74 assemblages
203 (comprising 1-6 species; 1.93 [0.05 – 5.05] species) are predicted to overheat, while 285
204 assemblages (comprising 1-11 species; 2.51 [0.31 – 5.69] species) are predicted to overheat
205 assuming 4°C of global warming (Fig. 4; Extended Data Table 3). While the overheating risk is
206 lower in arboreal conditions, considerably fewer species were examined than in terrestrial
207 conditions (1,771 vs. 5,177 species). In fact, comparing the responses of arboreal species in
208 different microhabitats revealed that occupying above-ground vegetation is only partially
209 beneficial (Extended Data Fig. 4). In current climates, up to 15 arboreal species (320 local
210 species occurrences) are predicted to experience overheating events in terrestrial conditions,
211 whereas 13 arboreal species (152 local species occurrences) are predicted to overheat in
212 above-ground vegetation (Extended Data Fig. 4). Furthermore, under 4°C of warming, 83
213 arboreal species (1,137 local species occurrences) are predicted to overheat in terrestrial
214 conditions, while retreating to above-ground vegetation only reduces the number of species
215 exposed to overheating events by 32.5% (56 species, 748 local species occurrences)
216 (Extended Data Fig. 4). Contrary to terrestrial and arboreal conditions, no amphibian
217 populations are predicted to overheat in water bodies in current or intermediate climate warming
218 scenarios due to the thermal buffering properties of water. However, assuming 4°C of climate
219 warming, we predict that 11 species (56 local species occurrences from 48 assemblages) will
220 exceed their physiological limits in aquatic microhabitats (Fig. 4).

221

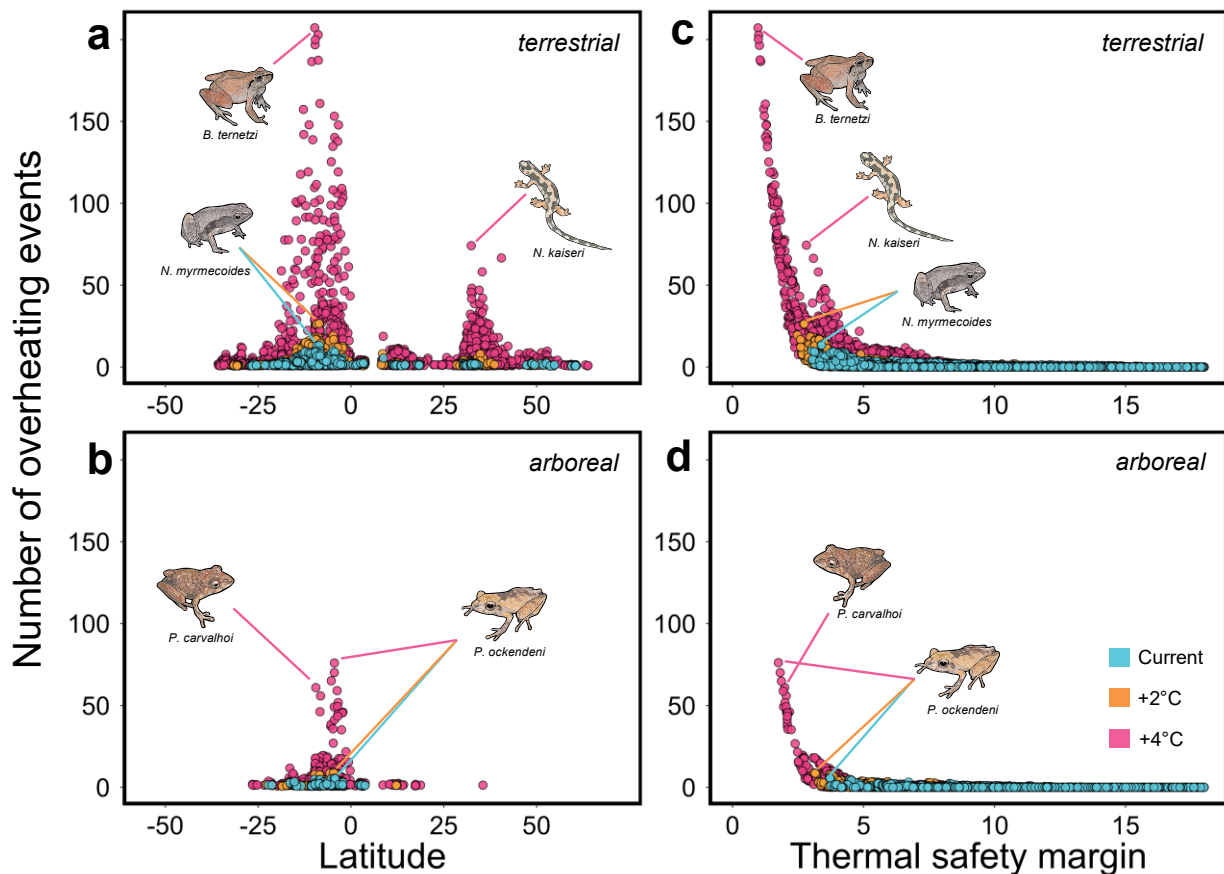


222
 223 **Fig. 4 | Number of species predicted to experience overheating events in terrestrial (a),**
 224 **aquatic (b), and arboreal (c) microhabitats.** The number of species overheating was
 225 assessed as the sum of species overheating for at least one day in the period surveyed
 226 (warmest quarters of 2006-2015) in each assemblage (1-degree grid cell). Black colour depicts
 227 areas with no data, and grey colour assemblage without species at risk of overheating. The right
 228 panel depicts latitudinal patterns in the number of species predicted to overheat in current
 229 climates (blue) or assuming 4°C of global warming above pre-industrial levels (pink). Dashed
 230 lines represent the equator and tropics.

231 Finally, we quantified the number of days (out of 910 simulated days across the warmest
 232 quarters of 2006-2015) each species was predicted to locally exceed their plasticity-adjusted
 233 heat tolerance limits. This metric fully integrates the frequency at which amphibians are
 234 predicted to experience temperatures beyond their thermal limits. For current climates, we
 235 found that species rarely experience overheating events in shaded terrestrial conditions (overall
 236 mean overheating days [95% confidence intervals] = 0.01 [0.01 – 0.08]; mean among
 237 overheating species = 2.15 [0.24 – 5.26] days); but these figures increase considerably with
 238 global warming (Fig. 5; Extended Data Table 2). Under 4°C of warming, species are predicted
 239 to overheat on as many as 207.18 [182.39 – 231.97] days, representing up to 22.8% of the
 240 warmest days of the year (overall mean = 0.15 [0.05 – 0.46] days; mean among overheating
 241 species = 6.75 [3.14 – 11.38] days; Fig. 5; Extended Data Table 2). This is noticeably more than
 242 what is predicted under 2°C of warming (overall mean = 0.02 [0.01 – 0.13] days; mean among
 243 overheating species = 2.58 [0.41 – 5.86] days; Fig. 5; Extended Data Table 2). In above-ground

244 vegetation, the frequency of overheating events is lower, as expected. Under current climates,
245 arboreal species are predicted to overheat on up to 5.65 [1.00 – 10.29] days in total (overall
246 mean = 0.01 [0.01 – 0.04] days; mean among overheating species = 1.62 [0.03 – 4.43] days;
247 Fig. 5; Tab. Extended Data Table 2). Under 4 degrees of warming, arboreal species are
248 predicted to overheat on up to 76.17 [59.79 – 92.54] days (overall mean = 0.08 [0.01 – 0.23]
249 days; mean among overheating species = 5.08 [1.81 – 9.39] days; Fig. 5; Extended Data Table
250 2). Arboreal species retreating to above-ground vegetation are predicted to experience fewer
251 overheating events than those in terrestrial conditions (Extended Data Fig. 4). Interestingly, we
252 found that species predicted to overheat locally have TSMs well above zero, although some are
253 living particularly close to their heat tolerance limits during the warmest months in both
254 terrestrial (mean [95% confidence intervals]; current = 8.20 [6.91 – 9.98], range: 3.02 – 12.19;
255 +4°C = 6.30 [5.02 – 8.09], range: 0.97 – 11.27) and above-ground conditions (current = 8.71
256 [7.20 – 10.28], range: 3.70 – 9.76; +4°C = 6.73 [5.44 – 8.48], range: 1.75 – 8.70; Fig. 5c,d).
257 Finally, we found a strong non-linear negative association between the number of overheating
258 events and the thermal safety margin, with stark contrasts between warming scenarios (Fig.
259 5c,d; Extended Data Table 5). In particular, overheating days increase rapidly as thermal safety
260 margins fall below 5°C (Figure 5c,d).

261
262



263
 264 **Fig. 5 | Latitudinal variation in the number of overheating events in terrestrial (a,c) and**
 265 **arboreal (b,d) microhabitats as a function of latitude (a,b) and thermal safety margin (c,d).**
 266 The number of overheating events (days) were calculated based on the mean probability that
 267 daily maximum temperatures exceeded CT_{max} during the warmest quarters of 2006-2015 for
 268 each species in each grid cell. Blue points depict the number of overheating events in current
 269 microclimates, while orange and pink points depict the number of overheating events assuming
 270 2°C and 4°C of global warming above pre-industrial levels, respectively. For clarity, only the
 271 species predicted to experience at least one overheating event are depicted across latitudes
 272 (a,b).

273

274 ***The mounting impacts of global warming***

275 Quantifying the resilience of biodiversity to a changing climate is one of the most pressing
 276 challenges for contemporary science^{7,8}. Here, we show that over a hundred species may
 277 already experience hourly temperatures that would likely result in death over minutes or hours
 278 of exposure in thermal refugia. This pattern is only predicted to worsen (Fig. 4-5). Assuming 4°C
 279 of global warming, the number of species and assemblages exposed to overheating events
 280 would be four to five times higher than currently, totalling 391 out of 5,203 species studied
 281 (7.5%; Fig. 4-5).

282 We also found striking disparities in overheating risk between the 2°C and 4°C warming
283 projections (Fig. 5; Extended Data Table 1), which are anticipated by the end of the century
284 under low and high greenhouse gas emission scenarios, respectively²⁴. The more extreme
285 warming scenario considerably increased the number of overheating events experienced by
286 amphibian populations (Fig. 5), highlighting the escalating and abrupt impacts of global
287 warming^{7,30}. Such an increase is attributable to the contrast between the rapid pace at which
288 temperatures are increasing and the low ability of amphibians to acclimate to new thermal
289 environments via plasticity (Extended Data Fig. 3; Fig. S3). Our study clearly demonstrates, as
290 others have suggested^{18,28,31,32}, that physiological plasticity is not a sufficient mechanism to
291 buffer many populations from the impacts of rapidly rising temperatures.

292 ***Extreme heat events drive vulnerability***

293 We found large spatial heterogeneity in the vulnerability of amphibians. In tropical areas, most
294 vulnerable species are concentrated in South America and Australia, whereas fewer species
295 are impacted in the African and Asian tropics (Fig. 4). Tropical species also experience
296 disproportionately more overheating events in the Southern Hemisphere, while non-tropical
297 species are more susceptible in the Northern Hemisphere (Fig. 5). Furthermore, the proportion
298 of species experiencing overheating events in each assemblage was not predicted by latitude
299 (Extended Data Fig. 5). Therefore, our findings are inconsistent with the expectation of a
300 general latitudinal gradient in overheating risk based on thermal safety margins^{4–6,13}. In fact, the
301 overheating risk does not increase linearly with TSM (Fig. 5c,d), and species with seemingly
302 comparable TSMs can have markedly different probabilities of overheating due to varying
303 exposure to daily temperature fluctuations (Fig. 5c,d). Therefore, TSMs alone hide critical
304 tipping points for thermal stress (Fig. 5c,d).

305 Our study questions the reliability of thermal safety margins and other climate
306 vulnerability metrics when averaged across large time scales (e.g., using the maximum
307 temperature of the warmest quarter) for detecting species most vulnerable to thermal extremes.
308 It also challenges the general notion that low-latitude species are uniformly most vulnerable to

309 warming^{4-6,13}, revealing a far more nuanced pattern of climate vulnerability across latitudes.
310 While the reliability of TSM-based assessments has been questioned in previous studies¹¹, our
311 work further emphasises the need to consider natural climatic variability and extreme hourly
312 temperatures^{4,16-18} when evaluating the vulnerability of ectotherms to global warming.
313 Considering alternative metrics, such as the number of predicted overheating events, may
314 prove particularly useful in identifying the most vulnerable species and populations.

315 ***The vital yet limited role of thermal retreats***

316 Our study⁴ highlights the critical yet sometimes insufficient role that thermal retreats play in
317 buffering the impacts of warming on amphibians. Most amphibian species are predicted not to
318 experience overheating events in full shade (Fig. 4), and the availability of water bodies allows
319 nearly all amphibians to maintain their body temperatures below critical levels, apart from 11
320 species in the most extreme warming scenario investigated. This is attributable to the higher
321 specific heat capacity of water relative to air, delaying rapid temperature rises and affording a
322 more stable environment during heat waves³³. Our findings add to the growing evidence that
323 finding access to cooler microhabitats is the main strategy amphibians and other ectotherms
324 can use to maintain sub-lethal body temperatures^{6,21,34}.

325 However, it is crucial to emphasise that vegetated terrestrial conditions in full shade offer
326 inadequate protection to 7.5% of species, and many arboreal species predicted to overheat at
327 ground level face similar risks in above-ground vegetation (Fig. 4-5, Extended Data Fig. 4). In
328 fact, although reducing the frequency of overheating events (Extended Data Fig. 4), access to
329 shaded above-ground vegetation only reduces the number of vulnerable species by 32.5%.
330 Moreover, although burrows offer cooler microclimates (see Fig. S9), the ability to use
331 underground spaces is not universal among amphibians and can greatly restrict activity,
332 reproduction, and foraging opportunities.

333 ***Warming impacts may exceed projections***

334 Our predictions are largely conservative, and likely overestimate the resilience of amphibians to
335 global warming in two main ways. First, we assume that microhabitats such as shaded ground-
336 level substrates, above-ground vegetation, and water bodies are available throughout a species'
337 range, and that amphibians can maintain wet skin. These assumptions will often be violated as
338 habitats are degraded. Deforestation and urbanization are diminishing vital shaded areas^{35,36},
339 while increased frequencies of droughts will cause water bodies to evaporate^{37,38}. These
340 changes compromise not only habitat integrity but also local humidity levels – key for effective
341 thermoregulation^{39,40}. Consequently, amphibians will likely experience higher body temperatures
342 and desiccation stress events than our models predict due to inconsistent access to cooler
343 microhabitats⁴¹, particularly in degraded systems.

344 Second, ectotherms can experience deleterious effects from heat stress before reaching
345 their heat tolerance limits. Prolonged exposure to sub-lethal temperatures can lead to altered
346 activity windows^{42,43}, disruptions to phenology^{44,45}, reduced reproductive fitness (fertility and
347 fecundity)^{29,46,47}, and death^{48,49}. Although comprehensive data on thermal incapacitation times
348 and fertility impacts are sparse in amphibians, integrating both the duration and intensity of
349 thermal stress^{49–51} will likely point to more extreme vulnerability estimates. This represents a
350 vital avenue for future research, albeit one requiring a large collection of empirical data.

351 Alternatively, species that can retreat underground during heat events are likely to
352 experience fewer overheating events than our models predict (see Fig. S9), and prolonged
353 exposure to high temperatures in the permissive range (*sensu*⁴⁸) can enhance performance
354 and fitness, thereby reducing the impacts of extreme heat on natural populations. In addition,
355 some species may adapt to changing temperatures. However, evidence for slow rates of
356 evolution and physiological constraints on thermal tolerance^{52,53} challenges the likelihood of
357 local adaptation to occur in rapidly warming climates.

358 ***The power of data imputation***

359 Our imputation approach has generated testable predictions of the thermal limits of 5,203
360 species, expanding the scope of previous research³ (Fig. 2). We also addressed geographical
361 biases by generating predictions in under-sampled but ecologically critical regions of Africa,
362 Asia, and South America (Fig. 2). We found that these understudied regions frequently harbor
363 species exhibiting the highest susceptibility to extreme heat events (Fig. 1,4-5), with 74% (288
364 out of 391) of vulnerable species remaining unstudied. Targeted research efforts in these
365 vulnerability hotspots are instrumental in validating our model predictions and advancing our
366 understanding of amphibian thermal physiology to inform their conservation. Though undeniable
367 logistical and financial challenges exist in accessing some of these remote locations,
368 collaboration with local scientists could expedite data collection and result in timely conservation
369 measures. Exemplary initiatives to sample numerous species in South America (e.g., ^{22,54,55}) are
370 promising steps in this direction, and we hope our findings will catalyse research activity in
371 these regions.

372 ***Amphibian biodiversity in a warming world***

373 Our study highlights the dire consequences of global warming on amphibians. Yet it is crucial to
374 differentiate between global extinction and local extirpations – the latter being confined
375 extinctions within specific geographic areas. Most species will not experience overheating
376 events throughout their entire range, and these overheating events may not occur
377 simultaneously. Hence, most species are likely to only experience local extirpation due to
378 overheating, according to our models. Nevertheless, local extirpations carry their own sets of
379 ecological repercussions, such as reshuffling community compositions and eroding genetic and
380 ecological diversity^{56,57}.

381 Some amphibian populations may also undergo range shifts, permanently or transiently
382 relocating to habitats with more hospitable weather patterns⁵⁸. However, this is only possible if
383 suitable habitats are available for establishment. Given the low dispersal rates of some
384 amphibians and their common reliance on water bodies for reproduction and thermoregulation,

385 opportunities for range shifts are likely to be rare for many species. Identifying which species at
386 high risk of overheating are simultaneously predicted to have limited ability to extend their range
387 is an interesting avenue for research. In addition, we stress that amphibians living close to their
388 physiological limits for extended times at the warm edge of their distribution are likely to
389 experience heat stress that could hamper activity, foraging opportunities, and reproductive
390 success, adding layers of complexity to their survival challenges and potentially leading to
391 population declines^{42,48}.

392 Overall, our study contributes to the evidence that climate change is a mounting threat to
393 amphibians^{2,10} and emphasises the importance of limiting global temperature rises below 2°C to
394 minimise the risk of overheating to amphibian populations. A 4°C temperature rise would not
395 just increase these risks but create a step-change in impact severity (e.g., Fig. 5c). The
396 mechanistic basis of our species- and habitat-specific predictions also leads to clear
397 management priorities. Particularly, our analyses revealed the critical importance of preserving
398 dense vegetation cover and water bodies. These microhabitats provide conditions with cooler
399 and more stable temperatures and increase the potential for amphibians and other ectothermic
400 species to disperse to more suitable microhabitats. Establishing protected areas and
401 undertaking habitat restoration initiatives may support amphibians in a changing climate and
402 buffer additional anthropogenic threats, in turn mitigating amphibian population declines^{2,10,59}.
403 These actions are critical for the amphibians at risk and the ecosystems they support⁶⁰ in a
404 planet undergoing perilous climatic changes.

405

406 **Main references**

- 407 1. Carey, C. & Alexander, M. A. Climate change and amphibian declines: is there a link?
408 *Divers. Distrib.* **9**, 111–121 (2003).
- 409 2. Luedtke, J. A. *et al.* Ongoing declines for the world’s amphibians in the face of emerging
410 threats. *Nature* **622**, 308–314 (2023).
- 411 3. Pottier, P. *et al.* A comprehensive database of amphibian heat tolerance. *Sci. Data* **9**, 600
412 (2022).
- 413 4. Pinsky, M. L., Eikeset, A. M., McCauley, D. J., Payne, J. L. & Sunday, J. M. Greater
414 vulnerability to warming of marine versus terrestrial ectotherms. *Nature* **569**, 108–111
415 (2019).
- 416 5. Deutsch, C. A. *et al.* Impacts of climate warming on terrestrial ectotherms across latitude.
417 *Proc. Natl. Acad. Sci. U.S.A.* **105**, 6668–6672 (2008).
- 418 6. Sunday, J. M. *et al.* Thermal-safety margins and the necessity of thermoregulatory
419 behavior across latitude and elevation. *Proc. Natl. Acad. Sci. U.S.A.* **111**, 5610–5615
420 (2014).
- 421 7. Urban, M. C. Accelerating extinction risk from climate change. *Science* **348**, 571–573
422 (2015).
- 423 8. Walther, G.-R. *et al.* Ecological responses to recent climate change. *Nature* **416**, 389–395
424 (2002).
- 425 9. Angilletta, M. J. Thermal adaptation: a theoretical and empirical synthesis. (Oxford
426 University Press, 2009).
- 427 10. Mi, C. *et al.* Global Protected Areas as refuges for amphibians and reptiles under climate
428 change. *Nat. Commun.* **14**, 1389 (2023).
- 429 11. Clusella-Trullas, S., Garcia, R. A., Terblanche, J. S. & Hoffmann, A. A. How useful are
430 thermal vulnerability indices? *Trends Ecol. Evol.* **36**, 1000–1010 (2021).
- 431 12. Huey, R. B. *et al.* Why tropical forest lizards are vulnerable to climate warming. *Proc. R.*
432 *Soc. B* **276**, 1939–1948 (2009).
- 433 13. Comte, L. & Olden, J. D. Climatic vulnerability of the world’s freshwater and marine fishes.
434 *Nat. Clim. Change* **7**, 718–722 (2017).
- 435 14. Carvalho, R. L. *et al.* Pervasive gaps in Amazonian ecological research. *Curr. Biol.* **33**,
436 3495-3504.e4 (2023).
- 437 15. Nesi, P., Luiselli, L. M. & Vignoli, L. “Heaven” of Data Deficient Species: The Conservation
438 Status of the Endemic Amphibian Fauna of Vietnam. *Diversity* **15**, 872 (2023).
- 439 16. Müller, J. *et al.* Weather explains the decline and rise of insect biomass over 34 years.
440 *Nature* **628**, 349–354 (2024).

- 441 17. Murali, G., Iwamura, T., Meiri, S. & Roll, U. Future temperature extremes threaten land
442 vertebrates. *Nature* **615**, 461–467 (2023).
- 443 18. Gunderson, A. R., Dillon, M. E. & Stillman, J. H. Estimating the benefits of plasticity in
444 ectotherm heat tolerance under natural thermal variability. *Funct. Ecol.* **31**, 1529–1539
445 (2017).
- 446 19. Anderson, R. O., White, C. R., Chapple, D. G. & Kearney, M. R. A hierarchical approach to
447 understanding physiological associations with climate. *Glob. Ecol. Biogeogr.* **31**, 332–346
448 (2022).
- 449 20. Briscoe, N. J. *et al.* Mechanistic forecasts of species responses to climate change: The
450 promise of biophysical ecology. *Glob. Change Biol.* **29**, 1451–1470 (2023).
- 451 21. Kearney, M., Shine, R. & Porter, W. P. The potential for behavioral thermoregulation to
452 buffer “cold-blooded” animals against climate warming. *Proc. Natl. Acad. Sci. U.S.A.* **106**,
453 3835–3840 (2009).
- 454 22. Duarte, H. *et al.* Can amphibians take the heat? Vulnerability to climate warming in
455 subtropical and temperate larval amphibian communities. *Glob. Change Biol.* **18**, 412–421
456 (2012).
- 457 23. Abatzoglou, J. T., Dobrowski, S. Z., Parks, S. A. & Hegewisch, K. C. TerraClimate, a high-
458 resolution global dataset of monthly climate and climatic water balance from 1958–2015.
459 *Sci. Data* **5**, 170191 (2018).
- 460 24. Masson-Delmotte, V. *et al.* Climate change 2021: the physical science basis. *Contribution*
461 *of working group I to the sixth assessment report of the intergovernmental panel on climate*
462 *change* **2**, (2021).
- 463 25. Schwalm, C. R., Glendon, S. & Duffy, P. B. RCP8.5 tracks cumulative CO2 emissions.
464 *Proc. Natl. Acad. Sci. U.S.A.* **117**, 19656–19657 (2020).
- 465 26. Jetz, W. & Pyron, R. A. The interplay of past diversification and evolutionary isolation with
466 present imperilment across the amphibian tree of life. *Nat Ecol Evol* **2**, 850–858 (2018).
- 467 27. Clusella-Trullas, S., Blackburn, T. M. & Chown, S. L. Climatic Predictors of Temperature
468 Performance Curve Parameters in Ectotherms Imply Complex Responses to Climate
469 Change. *Am. Nat.* **177**, 738–751 (2011).
- 470 28. Morley, S. A., Peck, L. S., Sunday, J. M., Heiser, S. & Bates, A. E. Physiological
471 acclimation and persistence of ectothermic species under extreme heat events. *Glob. Ecol.*
472 *Biogeogr.* **28**, 1018–1037 (2019).
- 473 29. van Heerwaarden, B. & Sgrò, C. M. Male fertility thermal limits predict vulnerability to
474 climate warming. *Nat. Commun.* **12**, 2214 (2021).
- 475 30. Trisos, C. H., Merow, C. & Pigot, A. L. The projected timing of abrupt ecological disruption
476 from climate change. *Nature* **580**, 496–501 (2020).

- 477 31. Gunderson, A. R. & Stillman, J. H. Plasticity in thermal tolerance has limited potential to
478 buffer ectotherms from global warming. *Proc. R. Soc. B* **282**, 20150401 (2015).
- 479 32. Pottier, P. *et al.* Developmental plasticity in thermal tolerance: Ontogenetic variation,
480 persistence, and future directions. *Ecol. Lett.* **25**, 2245–2268 (2022).
- 481 33. Denny, M. W. Thermal Properties: Body temperatures in Air and Water. in *Air and Water:*
482 *The biology and physics of life's media* 145–173 (Princeton University Press, Princeton,
483 New Jersey, USA, 1993).
- 484 34. Scheffers, B. R., Edwards, D. P., Diesmos, A., Williams, S. E. & Evans, T. A. Microhabitats
485 reduce animal's exposure to climate extremes. *Glob. Change Biol.* **20**, 495–503 (2014).
- 486 35. Stark, G., Ma, L., Zeng, Z.-G., Du, W.-G. & Levy, O. Cool shade and not-so-cool shade:
487 How habitat loss may accelerate thermal stress under current and future climate. *Glob.*
488 *Change Biol.* **29**, 6201–6216 (2023).
- 489 36. Nowakowski, A. J. *et al.* Tropical amphibians in shifting thermal landscapes under land-use
490 and climate change. *Conserv. Biol.* **31**, 96–105 (2017).
- 491 37. Dai, A. Increasing drought under global warming in observations and models. *Nat. Clim.*
492 *Change* **3**, 52–58 (2013).
- 493 38. McMenamin, S. K., Hadly, E. A. & Wright, C. K. Climatic change and wetland desiccation
494 cause amphibian decline in Yellowstone National Park. *Proc. Natl. Acad. Sci. U.S.A.* **105**,
495 16988–16993 (2008).
- 496 39. Greenberg, D. A. & Palen, W. J. Hydrothermal physiology and climate vulnerability in
497 amphibians. *Proc. R. Soc. B* **288**, 20202273 (2021).
- 498 40. Cheng, C.-T. *et al.* Open habitats increase vulnerability of amphibian tadpoles to climate
499 warming across latitude. *Glob. Ecol. Biogeogr.* **32**, 83–94 (2023).
- 500 41. Wu, N. C. *et al.* Global exposure risk of frogs to increasing environmental dryness. Preprint
501 at <https://doi.org/10.32942/X2ZG7S> (2024).
- 502 42. Kearney, M. R. Activity restriction and the mechanistic basis for extinctions under climate
503 warming. *Ecol. Lett.* **16**, 1470–1479 (2013).
- 504 43. Enriquez-Urzelai, U. *et al.* The roles of acclimation and behaviour in buffering climate
505 change impacts along elevational gradients. *J. Anim. Ecol.* **89**, 1722–1734 (2020).
- 506 44. Enriquez-Urzelai, U., Nicieza, A. G., Montori, A., Llorente, G. A. & Urrutia, M. B.
507 Physiology and acclimation potential are tuned with phenology in larvae of a prolonged
508 breeder amphibian. *Oikos* **2022**, e08566 (2022).
- 509 45. Parmesan, C. Ecological and Evolutionary Responses to Recent Climate Change. *Annu.*
510 *Rev. Ecol. Evol. Syst.* **37**, 637–669 (2006).
- 511 46. Wang, W. W.-Y. & Gunderson, A. R. The Physiological and Evolutionary Ecology of Sperm
512 Thermal Performance. *Front. Physiol.* **13**, (2022).

- 513 47. Walsh, B. S. *et al.* The Impact of Climate Change on Fertility. *Trends Ecol. Evol.* **34**, 249–
514 259 (2019).
- 515 48. Jørgensen, L. B., Ørsted, M., Malte, H., Wang, T. & Overgaard, J. Extreme escalation of
516 heat failure rates in ectotherms with global warming. *Nature* **611**, 93–98 (2022).
- 517 49. Rezende, E. L., Castañeda, L. E. & Santos, M. Tolerance landscapes in thermal ecology.
518 *Funct. Ecol.* **28**, 799–809 (2014).
- 519 50. Garcia, R. A., Allen, J. L. & Clusella-Trullas, S. Rethinking the scale and formulation of
520 indices assessing organism vulnerability to warmer habitats. *Ecography* **42**, 1024–1036
521 (2019).
- 522 51. Jørgensen, L. B., Malte, H., Ørsted, M., Klahn, N. A. & Overgaard, J. A unifying model to
523 estimate thermal tolerance limits in ectotherms across static, dynamic and fluctuating
524 exposures to thermal stress. *Sci. Rep.* **11**, 12840 (2021).
- 525 52. Bennett, J. M. *et al.* The evolution of critical thermal limits of life on Earth. *Nat. Commun.*
526 **12**, 1198 (2021).
- 527 53. Morgan, R., Finnøen, M. H., Jensen, H., Pélabon, C. & Jutfelt, F. Low potential for
528 evolutionary rescue from climate change in a tropical fish. *Proc. Natl. Acad. Sci. U.S.A.*
529 **117**, 33365–33372 (2020).
- 530 54. May, R. von *et al.* Thermal physiological traits in tropical lowland amphibians: Vulnerability
531 to climate warming and cooling. *PLOS One* **14**, e0219759 (2019).
- 532 55. Bovo, R. P. *et al.* Beyond Janzen's Hypothesis: How Amphibians That Climb Tropical
533 Mountains Respond to Climate Variation. *Integr. Org. Biol.* **5**, obad009 (2023).
- 534 56. Arenas, M., Ray, N., Currat, M. & Excoffier, L. Consequences of Range Contractions and
535 Range Shifts on Molecular Diversity. *Mol. Biol. Evol.* **29**, 207–218 (2012).
- 536 57. Rogan, J. E. *et al.* Genetic and demographic consequences of range contraction patterns
537 during biological annihilation. *Sci. Rep.* **13**, 1691 (2023).
- 538 58. Blaustein, A. R. *et al.* Direct and Indirect Effects of Climate Change on Amphibian
539 Populations. *Diversity* **2**, 281–313 (2010).
- 540 59. Nowakowski, J. A. *et al.* Protected areas slow declines unevenly across the tetrapod tree
541 of life. *Nature* **622**, 101–106 (2023).
- 542 60. Hocking, D. & Babbitt, K. Amphibian Contributions to Ecosystem Services. *Herpetol.*
543 *Conserv. Biol.* (2014).
- 544

545 **Methods**

546 ***Reporting***

547 We report author contributions using the CRediT (Contributor Roles Taxonomy) statement⁶¹ and
548 MeRIT (Method Reporting with Initials for Transparency) guidelines⁶². We also crafted the study
549 title, abstract and keywords to maximise indexing in search engines and databases⁶³. All
550 analyses were performed using R statistical software⁶⁴ (v. 4.3.0), and most computations used
551 the computational cluster Katana supported by Research Technology Services at UNSW
552 Sydney.

553 ***Amphibian heat tolerance limits***

554 We leveraged the most comprehensive compilation of amphibian heat tolerance limits³ for our
555 analyses (Extended Data Fig. 1). Briefly, these data were collated by systematically reviewing
556 the literature in five databases and seven languages, comprising 3,095 heat tolerance limits
557 from 616 amphibian species. To facilitate the comparability and analysis of heat tolerance limits,
558 we only included data matching four specific criteria. First, we only included heat tolerance limits
559 measured using a dynamic methodology (i.e., temperature at which animals lose their motor
560 coordination when exposed to ramping temperatures, critical thermal maximum CT_{max} ⁶⁵)
561 because it was the most used and comparable metric. Second, we only selected data for which
562 the laboratory acclimation temperature, or the field temperature during the month of capture,
563 was recorded. Third, we only included data from species listed in the phylogeny from ²⁶. Fourth,
564 we only included species for which their geographical range was reported in the International
565 Union for the Conservation of Nature red list⁶⁶ (accessed in January 2023).

566 These criteria were chosen to perform phylogenetically, climatically, and spatially informed
567 analyses. In total, we selected 2,661 heat tolerance limits estimates with metadata for 524
568 amphibian species (mean = 5.08; range = 1 - 146 estimates per species; 287 species with more
569 than one estimate). We also complemented this dataset with ecotypic data for each species.
570 Amphibians were grouped into six major ecotypes according to ⁴¹: ground-dwelling, fossorial,

571 aquatic, semi-aquatic, stream-dwelling and arboreal. Cave specialists were excluded because
572 they experience unique microclimatic conditions.

573 ***Data-deficient species***

574 Our objective was to assess the thermal tolerance of amphibians globally. However, the data
575 compiled in ³ are geographically and taxonomically biased. Therefore, we employed a data
576 imputation procedure to infer the thermal tolerance of data-deficient species, totalling 5,203
577 species at a broad geographical coverage (524 species + 4,679 data-deficient species; ~60% of
578 all described amphibian species, amphibiaweb.org; accessed in December 2023). We selected
579 data-deficient species from a species list that matched the phylogeny from ²⁶ (7,238 species),
580 was listed in the IUCN red list⁶⁶ along with geographic distribution data (5,792 species), and for
581 which ecotypes were known (6,245 species). We did not consider Caecilians (order
582 Gymnophiona) because, to our knowledge, heat tolerance limits are unknown for all Caecilian
583 species³. Of the 5,792 species for which we had distribution and phylogenetic data, 5,268 were
584 data-deficient for CT_{max}, of which 4,822 had a known ecotype. After removing Caecilians, we
585 were left with 4,679 species to impute. We also supplemented our dataset with published body
586 mass data retrieved from literature sources or estimated based on length-mass
587 allometries^{41,67,68}. We then estimated the geographical coordinates at which all extant species
588 occurred in their IUCN distribution range at a 1° x 1° resolution to use for biophysical modelling
589 (Extended Data Fig. 1).

590 ***Data imputation***

591 We developed a phylogenetic imputation procedure, here named Bayesian Augmentation with
592 Chained Equations (BACE). The BACE procedure combines the powers of Bayesian data
593 augmentation and multiple imputation with chain equations (MICE⁶⁹). Briefly, we ran multiple
594 iterative models using *MCMCglmm*⁷⁰ (v. 2.34) and supporting functions from the *hmi* package⁷¹.
595 In the first cycle, missing data was either taken as the arithmetic mean for continuous
596 predictors, or randomly sampled from existing values for (semi)categorical predictors. Predicted

597 (augmented) values from the models were then extracted from the response variables and used
598 as predictor variables in the next models to predict other response variables. Ultimately, heat
599 tolerance limits were predicted using augmented data from all predictors. We ran 5 cycles
600 where the data from one cycle was iteratively used in the next cycle, and estimations converged
601 after the first cycle (Fig. S1). Although the proportion of missing data was large (89.9%),
602 imputations based on large amounts of missing data are common^{13,72}, and although estimate
603 uncertainty increases with the proportion of missing data, as expected, simulation studies have
604 shown estimations remain unbiased^{73,74}. Note, however, that although our approach took the
605 uncertainty of missing data in the response or variable of interest (CT_{max}) into account, we used
606 the most likely values for the predictors. While such an approach could underestimate the
607 uncertainty in the response, point estimates should not be biased. In fact, our cross-validation
608 approach demonstrated the ability of our models to predict back known experimental estimates
609 with reasonable error (experimental mean \pm standard deviation = 36.19 ± 2.67 ; imputed mean =
610 35.93 ± 2.54 ; $r = 0.86$; Extended Data Fig. 2).

611 Heat tolerance limits were imputed based on the species' acclimation temperatures, the
612 duration of acclimation, the ramping rate and endpoint used in assays, the medium used for
613 measuring heat tolerance limits (i.e., ambient temperatures, water/body temperatures), and the
614 life stage of the animals (adults or larvae), and their ecotype. These variables were correlated
615 with amphibian heat tolerance limits (Fig. S2) and were fitted as covariates in Bayesian linear
616 mixed models. We also weighted heat tolerance estimates based on the inverse of their
617 sampling variance, accounted for phylogenetic non-independence using a correlation matrix of
618 phylogenetic relatedness, and fitted random intercepts for species-specific effects and
619 phylogenetic effects, as well as their correlation with acclimation temperatures (i.e., random
620 slopes). In other words, we modelled species-specific slopes (plasticity; see Fig. S2) and
621 partitioned the variance among phylogenetic and non-phylogenetic effects. We imputed data for
622 adult amphibians assuming they were acclimated to the median, 5th, or 95th percentile operative
623 body temperatures experienced across their geographical range (see *Microenvironmental data*

624 *and biophysical modelling*) for a duration of 10 days, tested using a ramping rate of 1°C/min in a
625 container filled with water, and for which thermal tolerance endpoint was recorded as the onset
626 of spasms. These methodological parameters were the median values in the experimental
627 dataset, or the most common values (mode). This allowed standardization of heat tolerance
628 limits for the comparative analysis⁷⁵⁻⁷⁷. In amphibians, the onset of spasms usually occurs after
629 the loss of righting response⁷⁸, meaning that our estimates are conservative. While we did
630 include data from larvae in the training data, we only imputed data for adults to increase the
631 comparability of our estimates.

632 For both known species and data-deficient species, we generated three ecologically relevant
633 and standardised heat tolerance estimates, and all analyses were built upon these standardised
634 imputed estimates. In total, we generated data for 5,203 species of amphibians (Extended Data
635 Fig. 1-2). Notably, our imputed estimates are accompanied by standard errors, which provide
636 estimates of uncertainty in the imputation, and errors were propagated throughout our analyses
637 (see *Climate vulnerability analysis*).

638 ***Microenvironmental data and biophysical modelling***

639 We used the package *NicheMapR*^{79,80} (v. 3.2.1) to estimate microenvironmental temperatures
640 and hourly operative body temperatures in current (2006-2015) and projected climatic
641 conditions (2°C or 4°C of global warming above pre-industrial levels). Operative body
642 temperatures are the steady-state body temperatures that organisms would achieve in a given
643 microenvironment, which can diverge significantly from ambient air temperatures due to, for
644 example, radiative and evaporative heat exchange processes^{19,20,81-86}.

645 For each geographic location, we generated microclimatic temperatures experienced by
646 amphibians on i) a vegetated ground-level substrate (i.e., terrestrial), ii) in above-ground
647 vegetation (i.e., arboreal), or iii) in a water body (i.e., aquatic) (Extended Data Fig. 1). For
648 terrestrial and aquatic species, we simulated microenvironmental temperatures 1 cm above the
649 surface. For arboreal species, we simulated microenvironmental temperatures 2 meters above

650 ground, applied a reduction of 80% in windspeed to account for reduced wind due to
651 vegetation⁸⁷, and assumed that 90% of the solar radiation was diffused due to canopy cover⁸⁸.
652 All microenvironmental projections were made using 85% shade to simulate animals in thermal
653 refugia, i.e., the microhabitats in which animals would retreat during the hottest times of the day.
654 We did not model temperatures in the sun because ectothermic species most likely
655 behaviourally thermoregulate by retreating to thermal refugia during extreme heat events²¹. Our
656 calculations thus represent conservative estimates of the vulnerability of amphibians to extreme
657 temperature events.

658 For microclimatic temperature estimates, we used the *micro_ncep* function from *NicheMapR*⁷⁹
659 (v. 3.2.1), which integrates 6-hourly macroclimatic data from the National Center for
660 Environmental Predictions (NCEP). This function also inputs from the *microclima* package⁸⁹ (v.
661 0.1.0) to predict microclimatic temperatures after accounting for variation in radiation, wind
662 speed, altitude, albedo, vegetation, and topography. These data are downscaled to an hourly
663 resolution, producing high-resolution microclimatic data. We used projected future monthly
664 climate data from TerraClimate²³ to generate hourly projections assuming 2°C or 4°C of global
665 warming above pre-industrial levels. These temperatures are within the range projected by the
666 end of the century under low (Shared Socioeconomic Pathway SSP 1-2.6 to SSP 2-4.5) and
667 high (SSP 3-7.0 to SSP 5-8.5) greenhouse gas emission scenarios, respectively²⁴. TerraClimate
668 projections use monthly data on precipitation, minimum temperature, maximum temperature,
669 wind speed, vapor pressure deficit, soil moisture, and downward surface shortwave radiation.
670 These projections impose monthly climate projections from 23 CMIP5 global circulation models,
671 as described in ⁹⁰. The *micro_ncep* function then downscales monthly TerraClimate inputs to
672 hourly by imposing a diurnal cycle to the data and imposes TerraClimate offsets onto the
673 climatic data from NCEP. Because the TerraClimate data is already bias-corrected, adding
674 future climate projections onto the NCEP data did not require further bias correction. We ran all
675 microclimatic estimations between 2005 and 2015 to match the range of pseudo-years available
676 for TerraClimate future climate projections. We did not use a larger range of historical records

677 and only used climate projections available in TerraClimate (i.e., 2°C and 4°C) to reduce
678 computational demands.

679 We then used microclimate estimates to generate hourly operative body temperatures using the
680 *ectotherm* function in *NicheMapR*⁸⁰. This modelling system has been extensively validated with
681 field observations^{91–93} (see also Fig. S12). We modelled an adult amphibian in the shape of the
682 leopard frog *Lithobates pipiens*, positioned 1 cm above ground (or 2 m for arboreal species),
683 and assumed that 80% of the skin acted as a free water surface (wet skin). Estimating body
684 mass-specific operative body temperatures for each grid cell, species, and microhabitat was too
685 computationally extensive, given the geographic and taxonomic scale of our study (464,871
686 local species occurrences). Therefore, we ran the ectotherm models using the median body
687 mass of the species assemblage in each geographical coordinate. When body mass was
688 unknown, we ran models assuming a body mass of 8.4 grams, the median assemblage-level
689 body mass. Given that most amphibians in our dataset are small (median = 1.4 g, mean = 27.5
690 g), body temperatures equilibrate quickly with the environment, and operative body
691 temperatures are likely representative of core body temperatures.

692 To model operative body temperatures in water bodies (e.g., ponds or wetlands), we used the
693 container model from *NicheMapR*. Unlike previously mentioned calculations predicting steady-
694 state temperatures, this approach accounts for transient temperature changes, capturing lags
695 due to thermal inertia (i.e., transient heat budget model^{94,95}). For pond simulations, we modelled
696 a container permanently filled with water (12 m width and 1.5 m-depth) and decreased direct
697 solar radiation to zero to simulate full shade. This modelling approach serves as a proxy for
698 estimating the body temperature of ectotherms submerged in water bodies such as ponds or
699 wetlands, which was validated with field measurements (e.g.,^{40,92}). Ground-level and water
700 temperatures were modelled for all species regardless of their ecotype (apart from
701 paedomorphic salamanders that were only assessed in aquatic environments) because
702 arboreal and terrestrial species may retreat on land or in water occasionally. Temperatures in
703 above-ground vegetation were only estimated for arboreal and semi-arboreal species as

704 reaching 2 meters height in vegetation requires a morphology adapted to climbing. Our
705 biophysical models assume that shaded microhabitats are available to species throughout their
706 range. While this may not hold true, fine-scaled distribution of these microenvironments are not
707 available at global scales. Moreover, assuming that these microenvironments are available
708 serves a functional role; it provides a best-case scenario that is useful for comparative analyses
709 and offers actionable insights for conservation. For instance, reduced exposure to overheating
710 events in aquatic relative to terrestrial environments would suggest that preserving ponds and
711 wetlands may be critical in buffering the impacts of climate change on amphibians.

712 We then estimated, for each geographical coordinate, the maximum daily body temperature and
713 the mean and maximum weekly maximum body temperature experienced in the 7 days prior to
714 each given day to account for acclimation responses and to assess climate vulnerability
715 metrics¹⁸ (see *Climate vulnerability analyses*). We only used data for the 91 warmest days (i.e.,
716 warmest quarter) of each year, as we were interested in the responses of amphibians to
717 extreme heat events¹⁸. Note that data from the year 2005 was excluded *a posteriori* as a burn-in
718 to remove the effects of initial conditions on soil temperature, soil moisture, and pond
719 calculations. Therefore, our analyses are based on 910 days (91 days per year in the range
720 2006-2015) for each climatic scenario (current climate, 2°C above pre-industrial levels, 4°C
721 above pre-industrial levels).

722 We also used maximum daily body temperatures on terrestrial conditions to calculate the
723 median, 5th percentile and 95th percentile maximum body temperature experienced by each
724 species across their range of distribution. These values were used as acclimation temperatures
725 in the training data to calibrate the data imputation with ecologically-relevant environmental
726 temperatures (see *Data imputation*); while maximizing the range of temperatures used to infer
727 the plasticity of heat tolerance limits (see *Climate vulnerability analysis*).

728 ***Climate vulnerability analysis***

729 Using the imputed data, we fitted an individual meta-analytic model for each species to estimate
730 the plasticity of imputed heat tolerance limits (CT_{max}) to changes in operative body temperatures
731 using the *metafor* package⁹⁶ (v. 4.2-0). CT_{max} was used as the response variable, acclimation
732 temperature (i.e., median, 5th percentile, or 95th percentile daily maximum body temperature
733 experienced by a species across its distribution range) was used as the predictor variable, and
734 imputed estimates were weighted based on their standard error. From these models, we used
735 out-of-sample model predictions (using the *predict* function) to estimate the CT_{max} of each
736 species in each 1° x 1° grid cell across their distribution range in different warming scenarios,
737 based on predicted mean weekly body temperatures. Specifically, we assumed that species
738 were, on any given day, acclimated to the mean daily body temperature experienced in the 7
739 days prior¹⁸. Therefore, CT_{max} was simulated as a plastic trait, which varied daily, as animals
740 acclimate to new environmental conditions (Extended Data Fig. 1). While evidence in small
741 amphibians suggests the full acclimation potential is reached within 3-4 days⁹⁷⁻⁹⁹, other
742 evidence points to some variation after longer periods¹⁰⁰. Therefore, we chose 7 days to reflect
743 that some amphibians may require longer to acclimate. Because we used out-of-sample model
744 predictions, we propagated errors from the imputation when estimating the predicted CT_{max}
745 across geographical coordinates. Predicted CT_{max} values and their associated standard errors
746 thus reflect variation in both the imputation procedure and the estimation of plastic responses.
747 Our approach to accounting for plasticity assumes that plasticity is homogeneous within species
748 and ignores the possible influence of local adaptation. However, given the low variability in
749 plasticity among species (Fig. S2-3), lack of evidence for latitudinal variation in plasticity
750 (^{28,31,101}), high phylogenetic signal in thermal tolerance (Pagel's $\lambda^{102} = 0.95 [0.91 - 0.98]$; see
751 *Sensitivity Analyses*), and evidence for slow rates of evolution and physiological constraints on
752 CT_{max} ^{52,53}, geographic variation in thermal tolerance and plasticity is unlikely to have a major
753 influence on our results.

754 We then estimated the vulnerability of amphibians to global warming using three metrics
755 (Extended Data Fig. 1). First, we calculated the difference between CT_{max} and the maximum
756 daily body temperature, i.e., the thermal safety margin (i.e., TSM, *sensu* ⁶). We calculated
757 weighted means and standard errors (*sensu* ¹⁰³) of thermal safety margins across years to
758 estimate the mean difference between CT_{max} and the maximum temperature during the warmest
759 quarters. Using TSM averaged from the maximum temperature of the warmest quarter is
760 common in the literature^{27–29}. Second, we calculated the number of days the maximum daily
761 operative body temperature exceeded CT_{max} across the warmest quarters of 2006-2015, i.e.,
762 the number of overheating events. To propagate the uncertainty, we calculated the mean
763 probability that daily operative body temperatures exceeded the predicted distribution of CT_{max}
764 (using the *dnorm* function). Note that the standard error (standard deviation of estimates) of
765 simulated CT_{max} distributions were restricted to one (i.e., simulating distributions within $\sim 3^{\circ}C$ of
766 the mean) to avoid inflating overheating probabilities due to large imputation uncertainty (*cf* ⁷²;
767 see also *Sensitivity analyses*; Fig. S8). We then multiplied the mean overheating probability by
768 the total number of simulated days (910) to estimate the number of overheating events and their
769 associated standard error using properties of the binomial distribution. Third, we calculated the
770 binary probability (0/1) that species overheat for at least one day across the 910 days surveyed
771 (warmest quarters of 2006-2015). The latter two metrics provide a finer resolution than TSMs,
772 as they capture daily temperature fluctuations and potential overheating events¹⁸.

773 ***Macroecological patterns***

774 The objective of this study was to characterise the vulnerability of amphibians to global
775 warming. We investigated patterns at the level of local species occurrences (presence of a
776 given species in a $1^{\circ} \times 1^{\circ}$ grid cell based on IUCN data), allowing one to identify specific
777 populations and species that may be more susceptible to heat stress and direct targeted
778 research efforts. We also analysed data at the assemblage level, the species composition within
779 a grid cell. In such case, we calculated the weighted mean and standard error of TSM (*sensu*
780 ¹⁰³) across species in each grid cell. Assemblage-level analyses allow one to identify areas

781 containing a higher number of vulnerable species, offering actionable insights for broader-scale
782 conservation initiatives.

783 We used the *gamm4* package¹⁰⁴ to fit generalised additive mixed models (GAMM) against
784 latitude. For local species occurrences, we fitted latitude as a fixed factor, and nested genus
785 and species identity as random terms to account for phylogenetic non-independence. Note that
786 we did not include family as a random term because models failed at estimating higher
787 taxonomic variation. While better methods exist to model phylogenetic patterns, generalised
788 additive linear models do not allow for phylogenetic correlation matrices, and other functions
789 such as *brms*¹⁰⁵ surpassed our computational time and memory limits. Nevertheless, imputed
790 estimates already reflect variation due to phylogeny (see *Data imputation*), and phylogeny was
791 further modelled when deriving mean estimates in each microhabitat and climatic scenario (see
792 below). We fitted models using the three metrics as response variables independently: the
793 thermal safety margin, overheating risk, and number of overheating events. The former was
794 modelled using a Gaussian distribution of residuals, overheating risk was modelled using a
795 binomial error structure, and the latter using a Poisson error structure. Note that overheating
796 risks were rounded to integer values to fit a Poisson distribution. Thermal safety margin
797 estimates were weighted by the inverse of their sampling variance to account for the uncertainty
798 in the imputation and predictions across geographical coordinates. We fitted separate models
799 for each climatic scenario (current climate, 2°C above preindustrial levels, 4°C above
800 preindustrial levels) and microhabitat (terrestrial, aquatic, arboreal).

801 To investigate the mean TSM in each microhabitat and climatic scenario, we fitted models with
802 the interaction between microhabitat and climatic scenario as a fixed effect using *MCMCglmm*⁷⁰
803 (v. 2.34) and flat, parameter-expanded priors. In these models, we weighted estimates based
804 on the inverse of their sampling variance, species identity was fitted as a random effect, and we
805 accounted for phylogenetic non-independence using a variance-covariance matrix of
806 phylogenetic relatedness (calculated from the consensus tree of ²⁶). To investigate the overall
807 overheating risk and number of overheating events in each condition, we attempted to fit

808 models in *MCMCglmm* but these models failed to converge. Therefore, we fitted Poisson and
809 binomial models using *lme4*¹⁰⁶ (v. 1.1-33) and nested genus, species, and observation as
810 random terms. We used similar Poisson models to investigate the relationship between the
811 number of overheating events and thermal safety margins. While the mean estimates from
812 these simpler models should be unbiased, estimate uncertainty is likely underestimated¹⁰⁷.

813 We also investigated patterns of climate vulnerability at the assemblage level. We calculated
814 the weighted average of TSM and overheating risk in each 1-degree grid cell (14,091; 14,090;
815 or 6,614 grid cells for terrestrial, aquatic, and arboreal species, respectively), and mapped
816 patterns geographically. Averaging overheating risk effectively returned the proportion of
817 species overheating in each coordinate; and we also calculated the number of species
818 overheating in each grid cell. For assemblage-level models, we fitted Gaussian, binomial or
819 Poisson models as described above, but without taxon-level random effects because these
820 cannot be modelled at the assemblage level. All models were fitted without a contrast structure
821 to estimate mean effects in each microhabitat and climatic scenario, and with two-sided
822 contrasts to draw comparisons with current terrestrial conditions.

823 ***Cross-validation and sensitivity analyses***

824 We assessed the accuracy of the data imputation procedure using a cross-validation approach.
825 Specifically, we removed heat tolerance estimates for 5% of the species in the experimental
826 data and 5% of the data-deficient species (maintaining the same proportion of missing data)
827 and assessed how well experimental values could be predicted from the models. Of relevance,
828 we only removed data that were comparable to the data that were imputed. That is, data from
829 adult animals tested using a ramping rate of 1°C/min, and where thermal limits were recorded
830 as the onset of spasms. While we could have trimmed any data entry in the experimental data,
831 validation of the imputation performance can only be achieved by comparing comparable
832 entries, and imputing data from species tested in unusual settings would naturally result in large
833 errors. In total, we cross-validated experimental estimates for 77 species.

834 We investigated alternative ways to i) calculate thermal safety margins, ii) account for
835 acclimation responses, and iii) control for prediction uncertainty (see *Supplementary methods*;
836 Fig. S6-8) and investigated the influence of different parameters of our biophysical models (i.e.,
837 shade and burrow availability, plant height, solar radiation, wind speed, pond depth) on
838 predicted vulnerability risks (see *Supplementary methods*; Fig. S9-11). Our results were
839 generally robust to changes in model parameters, although amphibians are likely to experience
840 more overheating events in open habitats^{6,42} (Fig. S9) and shallow ponds (Fig. S10), and lower
841 risks in underground conditions¹⁰⁸ (Fig. S9). We also confirmed that predicted operative body
842 temperatures were comparable to field body temperatures measured in some wild frogs (see
843 *Supplementary methods*; Fig. S12).

844 Finally, we confirmed the presence of a phylogenetic signal in the experimental dataset by fitting
845 a Bayesian linear mixed model using all complete (no missing data) predictors (i.e., acclimation
846 temperature, endpoint, acclimation status, life stage, and ecotype) in *MCMCglmm*. We
847 accounted for phylogenetic non-independence using a correlation matrix of phylogenetic
848 relatedness and fitted random intercepts for non-phylogenetic species effects. The phylogenetic
849 signal (Pagel's λ ¹⁰², which is equivalent to phylogenetic heritability^{109,110}) was calculated as the
850 proportion of variance explained by phylogenetic effects relative to the total non-residual
851 variance.

852 Results from all statistical models and additional data visualizations are available at [https://p-](https://p-pottier.github.io/Vulnerability_amphibians_global_warming/)
853 [pottier.github.io/Vulnerability_amphibians_global_warming/](https://p-pottier.github.io/Vulnerability_amphibians_global_warming/).

854 ***Data availability***

855 Raw and processed data are available at [https://github.com/p-](https://github.com/p-pottier/Vulnerability_amphibians_global_warming)
856 [pottier/Vulnerability_amphibians_global_warming](https://github.com/p-pottier/Vulnerability_amphibians_global_warming). Note, however, that some intermediate data
857 files were too large to be shared online. These files are available upon request and will be
858 uploaded to a permanent repository upon acceptance. TerraClimate data is available from
859 <https://www.climatologylab.org/terraclimate.html> and NCEP data is available from
860 https://psl.noaa.gov/thredds/catalog/Datasets/ncep.reanalysis2/gaussian_grid/catalog.html.

861 ***Code availability***

862 All code needed to reproduce the analyses is available at <https://github.com/p->

863 [pottier/Vulnerability_amphibians_global_warming](https://github.com/p-pottier/Vulnerability_amphibians_global_warming).

864

865 **Methods references**

- 866 61. McNutt, M. K. *et al.* Transparency in authors' contributions and responsibilities to promote
867 integrity in scientific publication. *Proc. Natl. Acad. Sci. U.S.A.* **115**, 2557–2560 (2018).
- 868 62. Nakagawa, S. *et al.* Method Reporting with Initials for Transparency (MeRIT) promotes
869 more granularity and accountability for author contributions. *Nat. Commun.* **14**, 1788
870 (2023).
- 871 63. Pottier, P. *et al.* Title, abstract and keywords: a practical guide to maximise the visibility
872 and impact of academic papers. *Proc. R. Soc. B* **291**, 2023.10.02.559861 (2024).
- 873 64. R Core Team. R: A language and environment for statistical computing. R Foundation for
874 Statistical Computing (2019).
- 875 65. Lutterschmidt, W. I. & Hutchison, V. H. The critical thermal maximum: history and critique.
876 *Can. J. Zool.* **75**, 1561–1574 (1997).
- 877 66. IUCN. *The IUCN Red List of Threatened Species*. <https://www.iucnredlist.org> (2021).
- 878 67. Johnson, J. V. *et al.* What drives the evolution of body size in ectotherms? A global
879 analysis across the amphibian tree of life. *Glob. Ecol. Biogeogr.* **32**, 1311–1322 (2023).
- 880 68. Santini, L., Benítez-López, A., Ficetola, G. F. & Huijbregts, M. A. J. Length–mass
881 allometries in amphibians. *Integr. Zool.* **13**, 36–45 (2018).
- 882 69. Buuren, S. van & Groothuis-Oudshoorn, K. mice: Multivariate Imputation by Chained
883 Equations in R. *J. Stat. Softw.* **45**, 1–67 (2011).
- 884 70. Hadfield, J. D. MCMC Methods for Multi-Response Generalized Linear Mixed Models: The
885 MCMCglmm R Package. *J. Stat. Softw.* **33**, 1–22 (2010).
- 886 71. Speidel, M., Drechsler, J. & Jolani, S. *R Package Hmi: A Convenient Tool for Hierarchical*
887 *Multiple Imputation and Beyond*. <https://www.econstor.eu/handle/10419/182156> (2018).
- 888 72. Callaghan, C. T., Nakagawa, S. & Cornwell, W. K. Global abundance estimates for 9,700
889 bird species. *Proc. Natl. Acad. Sci. U.S.A.* **118**, e2023170118 (2021).
- 890 73. Austin, P. C. & van Buuren, S. The effect of high prevalence of missing data on estimation
891 of the coefficients of a logistic regression model when using multiple imputation. *BMC*
892 *Med. Res. Methodol.* **22**, 196 (2022).
- 893 74. Madley-Dowd, P., Hughes, R., Tilling, K. & Heron, J. The proportion of missing data should
894 not be used to guide decisions on multiple imputation. *J. Clin. Epidemiol.* **110**, 63–73
895 (2019).
- 896 75. Lutterschmidt, W. I. & Hutchison, V. H. The critical thermal maximum: data to support the
897 onset of spasms as the definitive end point. *Can. J. Zool.* **75**, 1553–1560 (1997).
- 898 76. Camacho, A. & Rusch, T. W. Methods and pitfalls of measuring thermal preference and
899 tolerance in lizards. *J. Therm. Biol.* **68**, 63–72 (2017).

- 900 77. Hoffmann, A. A. & Sgrò, C. M. Comparative studies of critical physiological limits and
901 vulnerability to environmental extremes in small ectotherms: How much environmental
902 control is needed? *Integr. Zool.* **13**, 355–371 (2018).
- 903 78. Lutterschmidt, W. I. & Hutchison, V. H. The critical thermal maximum: data to support the
904 onset of spasms as the definitive end point. *Can. J. Zool.* **75**, 1553–1560 (1997).
- 905 79. Kearney, M. R. & Porter, W. P. NicheMapR – an R package for biophysical modelling: the
906 microclimate model. *Ecography* **40**, 664–674 (2017).
- 907 80. Kearney, M. R. & Porter, W. P. NicheMapR – an R package for biophysical modelling: the
908 ectotherm and Dynamic Energy Budget models. *Ecography* **43**, 85–96 (2020).
- 909 81. Pincebourde, S. & Suppo, C. The Vulnerability of Tropical Ectotherms to Warming Is
910 Modulated by the Microclimatic Heterogeneity. *Integr. Comp. Biol.* **56**, 85–97 (2016).
- 911 82. Tracy, C. R., Christian, K. A. & Tracy, C. R. Not just small, wet, and cold: effects of body
912 size and skin resistance on thermoregulation and arboreality of frogs. *Ecology* **91**, 1477–
913 1484 (2010).
- 914 83. Köhler, A. *et al.* Staying warm or moist? Operative temperature and thermal preferences of
915 common frogs (*Rana temporaria*), and effects on locomotion. *Herpetol. J.* **21**, 17–26
916 (2011).
- 917 84. Navas, C. A., Carvajalino-Fernández, J. M., Saboyá-Acosta, L. P., Rueda-Solano, L. A. &
918 Carvajalino-Fernández, M. A. The body temperature of active amphibians along a tropical
919 elevation gradient: patterns of mean and variance and inference from environmental data.
920 *Funct. Ecol.* **27**, 1145–1154 (2013).
- 921 85. Barton, M. G., Clusella-Trullas, S. & Terblanche, J. S. Spatial scale, topography and
922 thermoregulatory behaviour interact when modelling species' thermal niches. *Ecography*
923 **42**, 376–389 (2019).
- 924 86. García-García, A. *et al.* Soil heat extremes can outpace air temperature extremes. *Nat.*
925 *Clim. Change* **13**, 1237–1241 (2023).
- 926 87. Davies-Colley, R. J., Payne, G. W. & van Elswijk, M. Microclimate gradients across a
927 forest edge. *N. Z. J. Ecol.* **24**, 111–121 (2000).
- 928 88. Campbell, G. S. & Norman, J. M. *An Introduction to Environmental Biophysics*. (Springer
929 Science & Business Media, 2000).
- 930 89. Maclean, I. M. D., Mosedale, J. R. & Bennie, J. J. Microclima: An r package for modelling
931 meso- and microclimate. *Methods Ecol. Evol.* **10**, 280–290 (2019).
- 932 90. Qin, Y. *et al.* Agricultural risks from changing snowmelt. *Nat. Clim. Change* **10**, 459–465
933 (2020).
- 934 91. Tracy, C. R. A Model of the Dynamic Exchanges of Water and Energy between a
935 Terrestrial Amphibian and Its Environment. *Ecol. Monogr.* **46**, 293–326 (1976).

- 936 92. Enriquez-Urzelai, U., Kearney, M. R., Nicieza, A. G. & Tingley, R. Integrating mechanistic
937 and correlative niche models to unravel range-limiting processes in a temperate
938 amphibian. *Glob. Change Biol.* **25**, 2633–2647 (2019).
- 939 93. Kearney, M. R., Munns, S. L., Moore, D., Malishev, M. & Bull, C. M. Field tests of a general
940 ectotherm niche model show how water can limit lizard activity and distribution. *Ecol.*
941 *Monogr.* **88**, 672–693 (2018).
- 942 94. Kearney, M. R., Porter, W. P. & Huey, R. B. Modelling the joint effects of body size and
943 microclimate on heat budgets and foraging opportunities of ectotherms. *Methods Ecol.*
944 *Evol.* **12**, 458–467 (2021).
- 945 95. Kearney, M. *et al.* Modelling species distributions without using species distributions: the
946 cane toad in Australia under current and future climates. *Ecography* **31**, 423–434 (2008).
- 947 96. Viechtbauer, W. Conducting meta-analyses in R with the metafor package. *J. Stat. Softw.*
948 **36**, 1–48 (2010).
- 949 97. Brattstrom, B. H. & Lawrence, P. The Rate of Thermal Acclimation in Anuran Amphibians.
950 *Physiol. Zool.* **35**, 148–156 (1962).
- 951 98. Layne, J. R. & Claussen, D. L. The time courses of CTMax and CTMin acclimation in the
952 salamander *Desmognathus fuscus*. *J. Therm. Biol.* **7**, 139–141 (1982).
- 953 99. Turriago, J. L., Tejedro, M., Hoyos, J. M., Camacho, A. & Bernal, M. H. The time course of
954 acclimation of critical thermal maxima is modulated by the magnitude of temperature
955 change and thermal daily fluctuations. *J. Therm. Biol.* **114**, 103545 (2023).
- 956 100. Dallas, J. & Warne, R. W. Heat hardening of a larval amphibian is dependent on
957 acclimation period and temperature. *J. Exp. Zool. Part A* **339**, 339–345 (2023).
- 958 101. Ruthsatz, K. *et al.* Acclimation capacity to global warming of amphibians and freshwater
959 fishes: Drivers, patterns, and data limitations. *Glob. Change Biol.* **30**, e17318 (2024).
- 960 103. Higgins, J. P. T. & Thompson, S. G. Quantifying heterogeneity in a meta-analysis. *Stat.*
961 *Med.* **21**, 1539–1558 (2002).
- 962 104. Wood, S. & Scheipl, F. gamm4: Generalized additive mixed models using mgcv and lme4.
963 (2014).
- 964 105. Bürkner, P.-C. brms: An R Package for Bayesian Multilevel Models Using Stan. *J. Stat.*
965 *Softw.* **80**, 1–28 (2017).
- 966 106. Bates, D., Mächler, M., Bolker, B. & Walker, S. Fitting Linear Mixed-Effects Models using
967 lme4. Preprint at <https://doi.org/10.48550/arXiv.1406.5823> (2014).
- 968 107. Cinar, O., Nakagawa, S. & Viechtbauer, W. Phylogenetic multilevel meta-analysis: A
969 simulation study on the importance of modelling the phylogeny. *Methods Ecol. Evol.* **13**,
970 383–395 (2022).

- 971 108. Carlo, M. A., Riddell, E. A., Levy, O. & Sears, M. W. Recurrent sublethal warming reduces
972 embryonic survival, inhibits juvenile growth, and alters species distribution projections
973 under climate change. *Ecol. Lett.* **21**, 104–116 (2018).
- 974 109. Hadfield, J. D. & Nakagawa, S. General quantitative genetic methods for comparative
975 biology: phylogenies, taxonomies and multi-trait models for continuous and categorical
976 characters. *J. Evol. Biol.* **23**, 494–508 (2010).
- 977 110. Lynch, M. Methods for the Analysis of Comparative Data in Evolutionary Biology. *Evolution*
978 **45**, 1065–1080 (1991).
- 979 111. Ivimey-Cook, E. R. *et al.* Implementing code review in the scientific workflow: Insights from
980 ecology and evolutionary biology. *J. Evol. Biol.* **36**, 1347–1356 (2023).
- 981

982 **Acknowledgements**

983 This study was funded by UNSW Scientia Doctoral Scholarships awarded to PPottier, SB, and
984 PPollo. SN was supported by the Australian Research Council (ARC) Discovery Project
985 (DP210100812). SMD was supported by the ARC Discovery Early Career Award
986 (DE180100202). We thank the authors of the original studies who provided the groundwork for
987 our analyses. We pay our respects to the Bedegal people, the traditional custodians of the land
988 on which this work was primarily conducted.

989 **Authors' contributions**

990 This study was conceptualized by PPottier, MRK, SB, SMD, and SN. All data manipulation and
991 analyses were performed by PPottier (with conceptual and technical input from SMD and SN for
992 the imputation methods and statistical analyses, MRK, ARG, JER, and NCW for the biophysical
993 modelling and climate vulnerability analyses). All code was reviewed by NCW, ARG, and JER
994 following the recommendations of ¹¹¹. Ecotype information was collected by NCW, PPollo, and
995 ANRV. PPottier, NCW, and SMD contributed to data visualization. PPottier wrote the initial draft,
996 and all authors were involved in the review and editing. PPottier oversaw the project
997 administration, while SMD and SN were in charge of the supervision.

998 **Inclusion & ethics statement**

999 This study did not involve researchers who collected the original data. All data used for the
1000 analyses were taken from a previous data compilation, and original references are listed in
1001 Supplementary Information (*Data sources*).

1002 **Competing interest declaration**

1003 The authors declare no conflict or competing interests.

1004

1005 **Additional information**

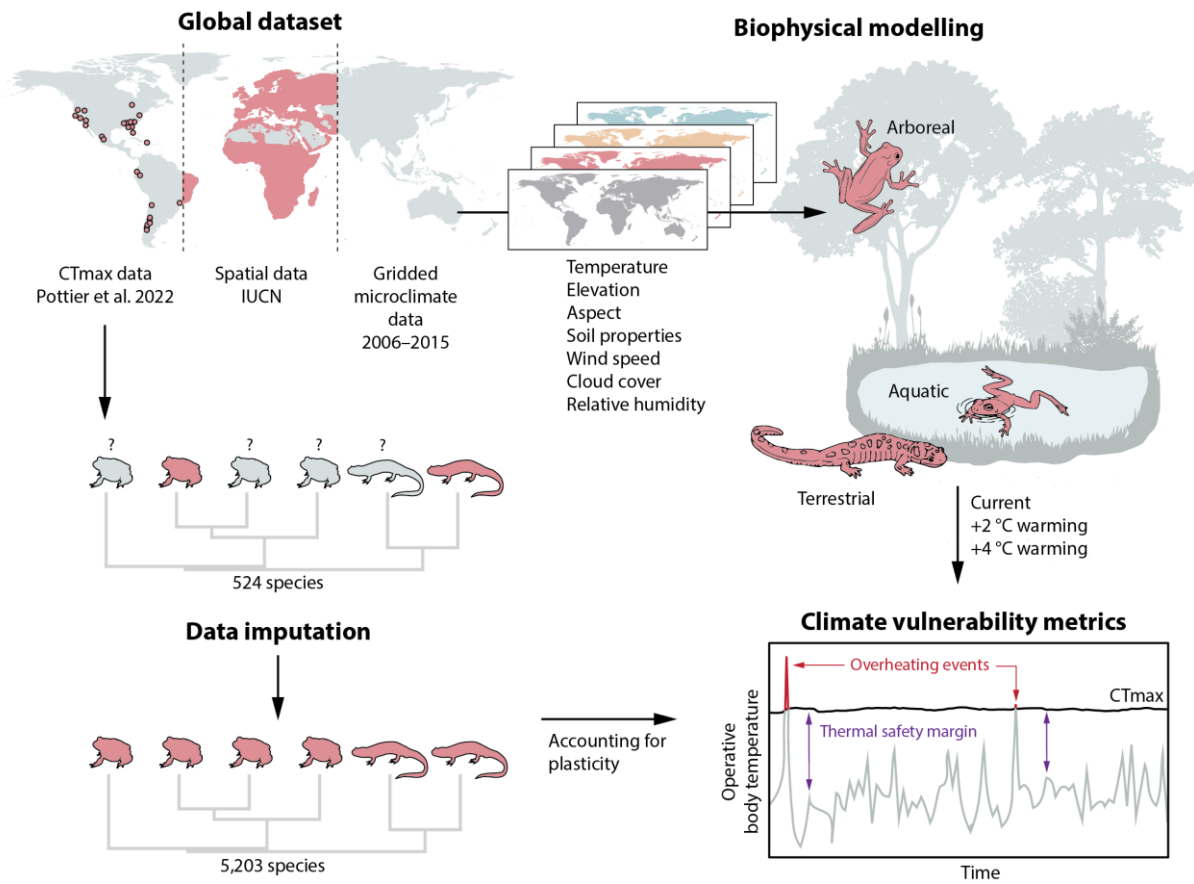
1006 Supplementary Information is available for this paper.

1007 Correspondence and requests for materials should be addressed to Patrice Pottier.

1008 Reprints and permissions information is available at www.nature.com/reprints.

1009 **Extended data**

1010



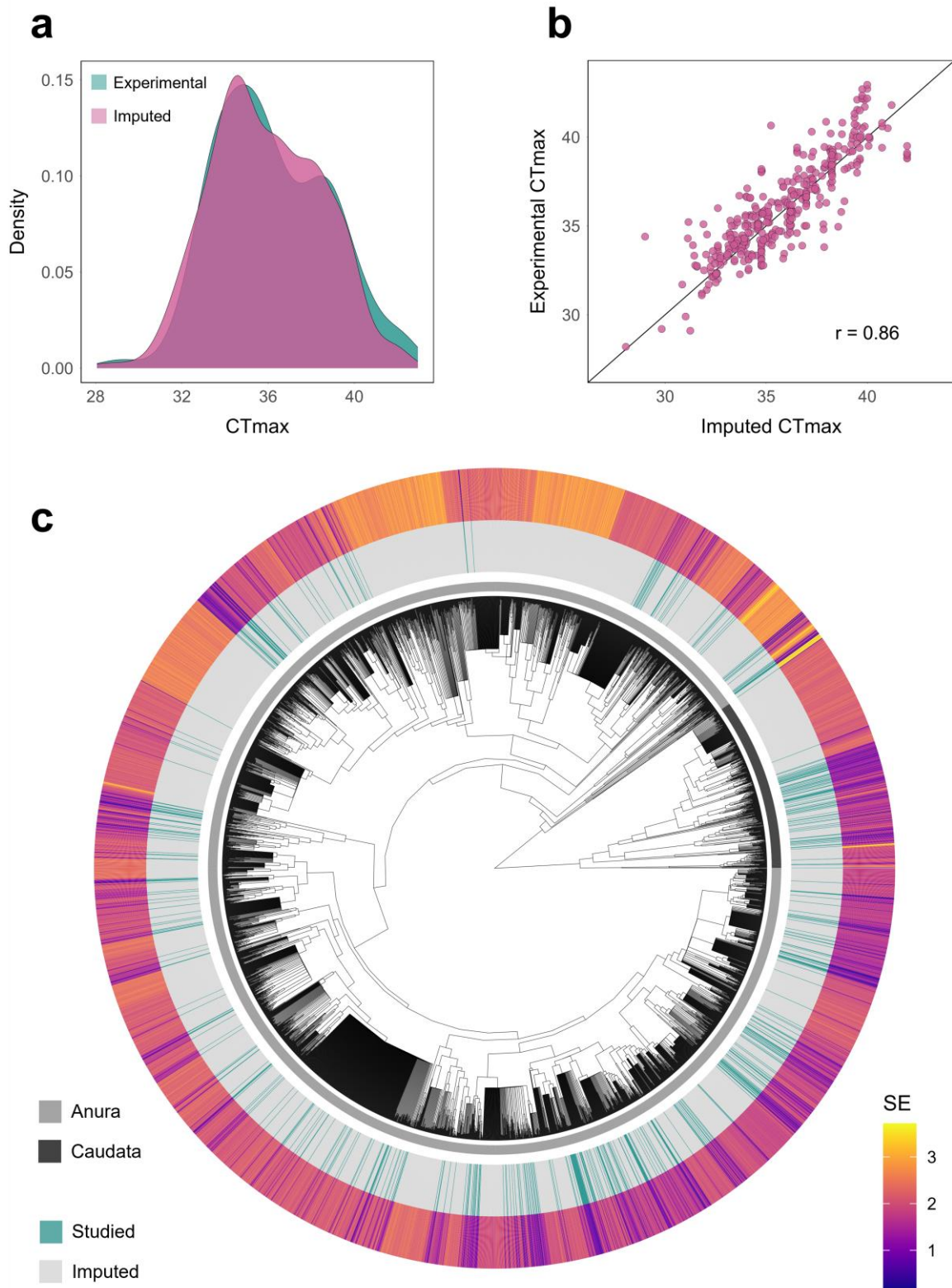
1011

1012 **Extended Data Fig. 1 | Conceptual overview of the methods employed to assess the**
1013 **vulnerability of amphibians to global warming.**

1014

1015

1016

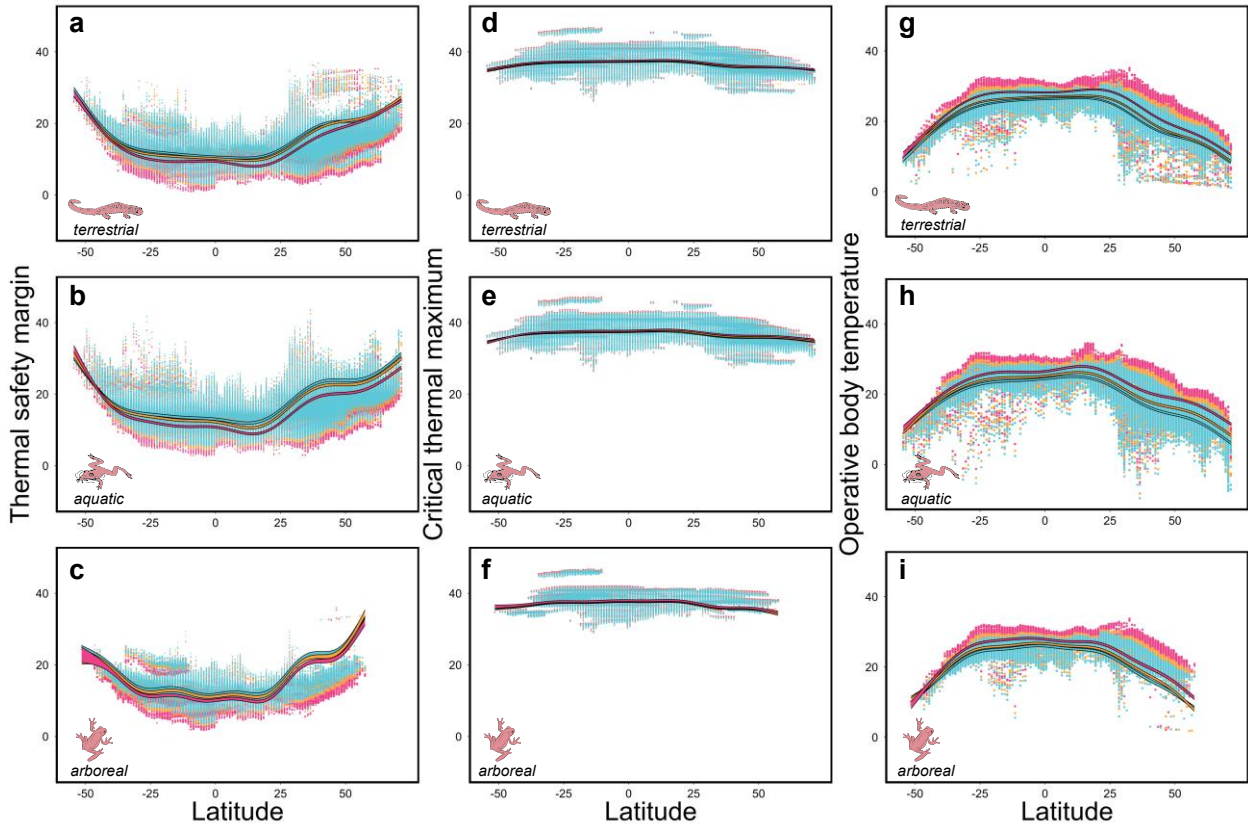


1017

1018 **Extended Data Fig. 2 | Accuracy of the data imputation procedure.** a) Probability density
 1019 distributions ($n = 375$ observations, 77 species) of experimental CT_{max} (blue) and CT_{max} cross-
 1020 validated using our data imputation procedure (pink). b) Correlation between experimental and
 1021 imputed CT_{max} values. c) Variation in the uncertainty (standard error, SE) of imputed CT_{max}
 1022 predictions (outer heat map) across studied (blue; $n = 524$) and imputed (grey; $n = 4,679$)
 1023 species.

1024

1025



1026

1027

1028

1029

1030

1031

1032

1033

1034

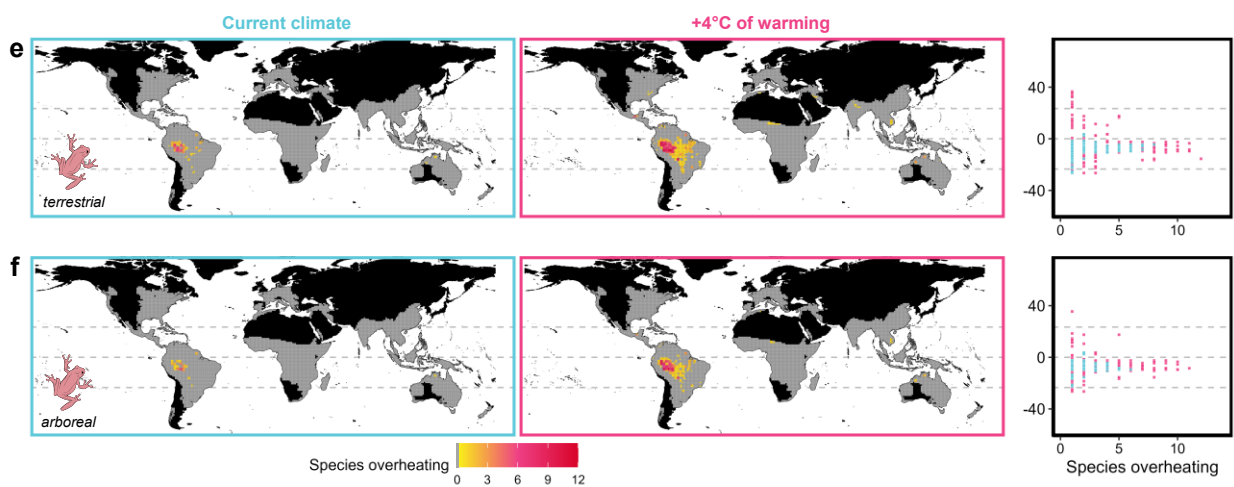
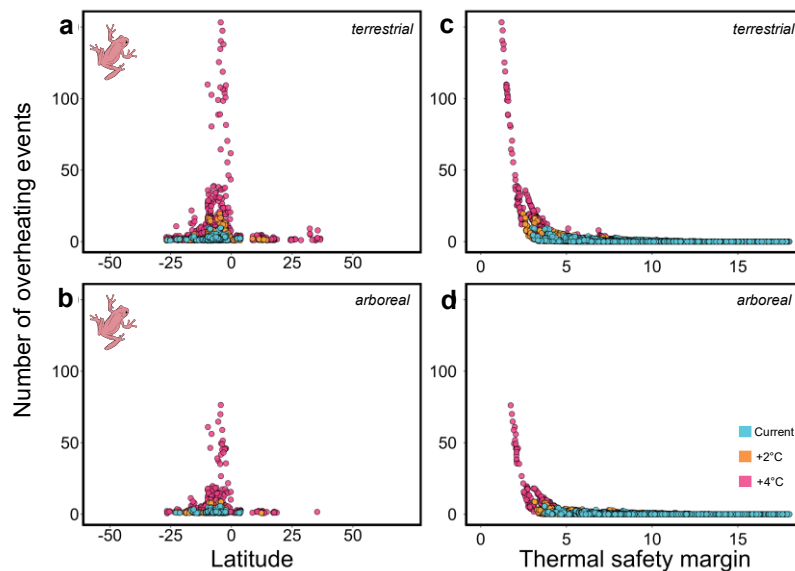
1035

1036

1037

1038

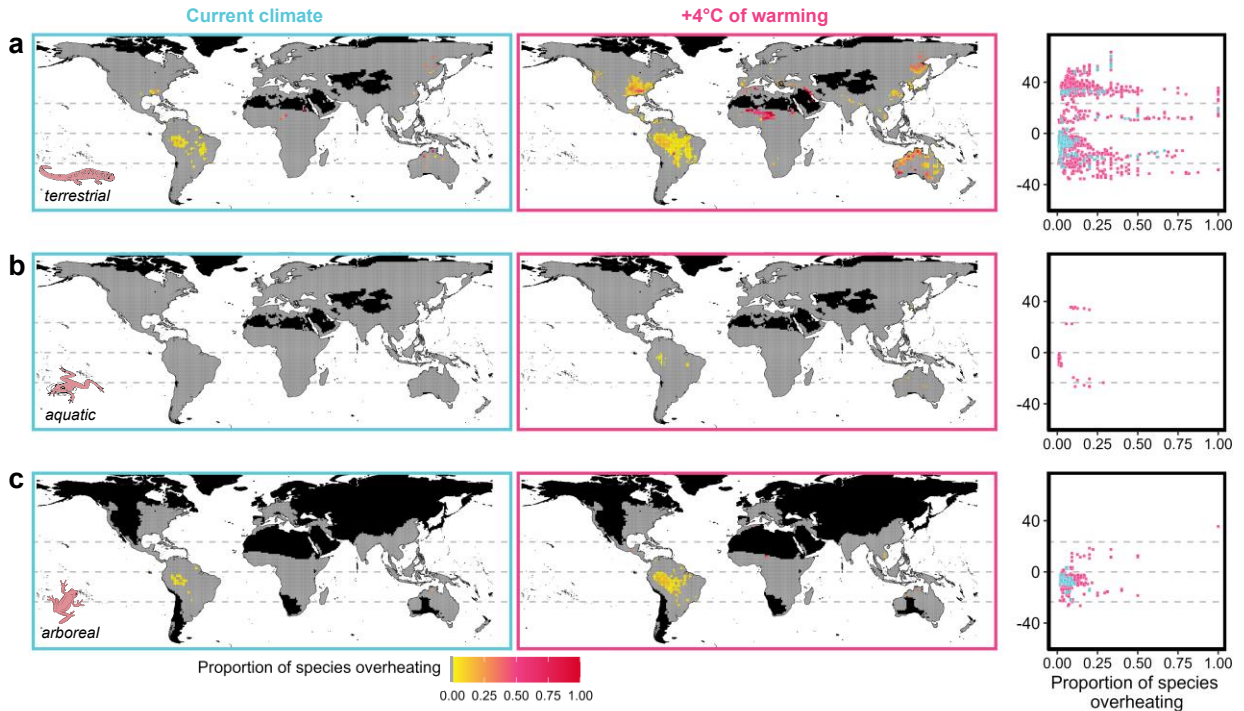
Extended Data Fig. 3 | Thermal safety margin, critical thermal maximum, and operative body temperatures in different microhabitats and climatic scenarios. Weighted mean thermal safety margins (TSM; a-c), critical thermal maximum (CT_{max} ; d-f) and operative body temperatures (g-i) in terrestrial (a,d,g), aquatic (b,e,h) and arboreal (c,f,i) microhabitats are depicted in current microclimates (blue data points), or assuming 2°C and 4°C of global warming above pre-industrial levels (orange, and pink data points, respectively) across latitudes. Lines represent 95% confidence intervals of model predictions from generalised additive mixed models. CT_{max} and TSM estimates are scaled by precision ($1/s.e.$). Each point represents a species in a given grid cell.



1039
1040
1041
1042
1043
1044
1045
1046
1047
1048
1049
1050
1051
1052
1053
1054
1055
1056
1057
1058

Extended Data Fig. 4 | Vulnerability of arboreal amphibians in terrestrial and arboreal microhabitats.

Depicted are the number of overheating events experienced by arboreal species across latitudes (a-b) and in relation to thermal safety margins (c-d) in terrestrial (a-c) and arboreal microhabitats (b-d). The number of overheating events were calculated based on the mean probability that daily maximum temperatures exceeded CT_{max} during the warmest quarters of 2006-2015 for each species in each grid cell. Blue points depict the number of overheating events in historical microclimates, while orange and pink points depict the number of overheating events assuming 2°C and 4°C of global warming above pre-industrial levels, respectively. In panel a) and b), only the species predicted to overheat for at least one day are displayed. The number of arboreal species predicted to experience overheating events in terrestrial (e) and arboreal (f) microhabitats in each assemblage is also depicted. The number of species overheating was assessed as the sum of species overheating for at least one day in the period surveyed (warmest quarters of 2006-2015) in each assemblage (1-degree grid cell). Black colour depicts areas with no data, and grey colour assemblages without species at risk. The right panel depicts latitudinal patterns in the number of species predicted to overheat in current climates (blue) or assuming 4°C of global warming above pre-industrial levels (pink). Dashed lines represent the equator and tropics. Few species ($n = 11$) were predicted to experience overheating events in water bodies, and hence are not displayed.



1060
 1061
 1062
 1063
 1064
 1065
 1066
 1067
 1068
 1069

Extended Data Fig. 5 | Proportion of species predicted to experience overheating events in terrestrial (a), aquatic (b), and arboreal (c) microhabitats. The proportion of species overheating was assessed as the sum of species overheating for at least one day in the period surveyed (warmest quarters of 2006-2015) divided by the number of species in each assemblage (1-degree grid cell). Black colour depicts areas with no data, and grey colour assemblages without species at risk. The right panel depicts latitudinal patterns in the proportion of species predicted to overheat in current climates (blue) or assuming 4°C of global warming above pre-industrial levels (pink). Dashed lines represent the equator and tropics.

1070

1071 **Extended Data Table 1 | Statistical model estimates for thermal safety margins calculated**
 1072 **for local species occurrences and assemblages**

1073 Model estimates for each microhabitat
 1074 (terrestrial, arboreal, aquatic) and each climatic scenario (current, +2°C, or +4°C of global
 1075 warming above pre-industrial levels) are depicted. mean: mean model estimate; Cl.lb: lower
 1076 bound of the 95% confidence interval; Cl.ub: upper bound of the 95% confidence interval; k_{sp} :
 1077 number of species; k_{obs} : number of observations; Var_{sp} : variance explained by differences
 1078 between species; Var_{phy} : variance explained by shared evolutionary history; Var_{obs} : residual
 variance.

<i>Local species patterns in thermal safety margin</i>								
	mean	Cl.lb	Cl.ub	k_{sp}	k_{obs}	Var_{sp}	Var_{phy}	Var_{obs}
Terrestrial (current)	11.694	8.856	14.428	5177	203853			
Terrestrial (+2°C)	10.914	8.025	13.594	5177	203853			
Terrestrial (+4°C)	9.409	6.530	12.090	5177	203853			
Arboreal (current)	12.235	9.402	14.960	1771	56210			
Arboreal (+2°C)	11.517	8.660	14.236	1771	56210	1.295	11.960	1.828
Arboreal (+4°C)	10.073	7.229	12.797	1771	56210			
Aquatic (current)	13.598	10.708	16.276	5203	204808			
Aquatic (+2°C)	12.827	8.796	14.361	5203	204808			
Aquatic (+4°C)	11.682	8.796	14.361	5203	204808			

<i>Assemblage-level patterns in thermal safety margin</i>					
	mean	Cl.lb	Cl.ub	k_{obs}	Var_{obs}
Terrestrial (current)	15.279	15.208	15.330	14090	
Terrestrial (+2°C)	14.328	14.279	14.396	14090	
Terrestrial (+4°C)	12.602	12.542	12.657	14090	
Arboreal (current)	14.279	14.191	14.381	6614	11.06
Arboreal (+2°C)	13.393	13.298	13.478	6614	
Arboreal (+4°C)	11.746	11.666	11.830	6614	
Aquatic (current)	17.408	17.352	17.471	14091	
Aquatic (+2°C)	16.528	16.468	16.581	14091	
Aquatic (+4°C)	15.287	15.225	15.346	14091	

1079

1080

1081

1082 **Extended Data Table 2 | Statistical model estimates for overheating risk and the number**
 1083 **of overheating events.** Model estimates for each microhabitat (terrestrial, arboreal) and each
 1084 climatic scenario (current, +2°C, or +4°C of global warming above pre-industrial levels) are
 1085 depicted. The estimated number of overheating events in species predicted to experience at
 1086 least one overheating event (i.e., overheating species) are also depicted. Model estimates for
 1087 aquatic microhabitats are not displayed because no species was predicted to experience
 1088 overheating events in this microhabitat. mean: mean model estimate; CI.lb: lower bound of the
 1089 95% confidence interval; CI.ub: upper bound of the 95% confidence interval; k_{sp} : number of
 1090 genera; k_{sp} : number of species; k_{obs} : number of observations; Var_{genus} : variance explained by
 1091 differences between genera; Var_{sp} : variance explained by differences between species; Var_{obs} :
 1092 residual variance.

<i>Overheating risk</i>									
	mean	CI.lb	CI.ub	k_{genus}	k_{sp}	k_{obs}	Var_{genus}	Var_{sp}	
Terrestrial (current)	9.98×10^{-7}	5.60×10^{-7}	1.78×10^{-6}	464	5177	203853			
Terrestrial (+2°C)	1.93×10^{-6}	1.09×10^{-6}	3.43×10^{-6}	464	5177	203853			
Terrestrial (+4°C)	9.09×10^{-6}	5.13×10^{-6}	1.61×10^{-5}	464	5177	203853	0.306	69.653	
Arboreal (current)	4.77×10^{-7}	2.58×10^{-7}	8.80×10^{-7}	174	1771	56210			
Arboreal (+2°C)	9.78×10^{-7}	5.45×10^{-7}	1.75×10^{-6}	174	1771	56210			
Arboreal (+4°C)	3.72×10^{-6}	2.08×10^{-6}	6.67×10^{-6}	174	1771	56210			
<i>Number of overheating events (all species)</i>									
	mean	CI.lb	CI.ub	k_{genus}	k_{sp}	k_{obs}	Var_{genus}	Var_{sp}	
Terrestrial (current)	0.014	0.001	0.080	464	5177	203853			
Terrestrial (+2°C)	0.025	0.002	0.127	464	5177	203853			
Terrestrial (+4°C)	0.153	0.046	0.460	464	5177	203853	0.110	52.500	
Arboreal (current)	0.008	0.001	0.043	174	1771	56210			
Arboreal (+2°C)	0.015	0.001	0.083	174	1771	56210			
Arboreal (+4°C)	0.076	0.012	0.230	174	1771	56210			
<i>Number of overheating events (among overheating species)</i>									
	mean	CI.lb	CI.ub	k_{genus}	k_{sp}	k_{obs}	Var_{genus}	Var_{sp}	Var_{obs}
Terrestrial (current)	2.155	0.239	5.264	38	104	836			
Terrestrial (+2°C)	2.576	0.410	5.857	61	168	1424			
Terrestrial (+4°C)	6.747	3.136	11.385	118	391	4248	0.253	0.187	0.310
Arboreal (current)	1.621	0.026	4.429	4	13	152			
Arboreal (+2°C)	1.956	0.113	4.973	5	16	283			
Arboreal (+4°C)	5.084	1.806	9.387	17	56	748			

1093

1094 **Extended Data Table 3 | Statistical model estimates for the number of species predicted**
 1095 **to experience overheating events.** Model estimates for each microhabitat (terrestrial,
 1096 arboreal) and each climatic scenario (current, +2°C, or +4°C of global warming above pre-
 1097 industrial levels) are depicted. The estimated number of species overheating in assemblages
 1098 containing at least one species predicted to experience at least one overheating event (i.e.,
 1099 overheating assemblages) are also depicted. Model estimates for aquatic microhabitats are not
 1100 displayed because no species was predicted to experience overheating events in this
 1101 microhabitat. mean: mean model estimate; Cl.lb: lower bound of the 95% confidence interval;
 1102 Cl.ub: upper bound of the 95% confidence interval; k_{obs} : number of observations; Var_{obs} :
 1103 residual variance.

<i>Number of species overheating (all assemblages)</i>					
	mean	Cl.lb	Cl.ub	k_{obs}	Var_{obs}
Terrestrial (current)	0.056	0.016	0.118	14090	
Terrestrial (+2°C)	0.096	0.029	0.199	14090	
Terrestrial (+4°C)	0.288	0.083	0.604	14090	
Arboreal (current)	0.021	0.002	0.054	6614	55.47
Arboreal (+2°C)	0.040	0.006	0.094	6614	
Arboreal (+4°C)	0.107	0.021	0.243	6614	
<i>Number of species overheating (among overheating assemblages)</i>					
	mean	Cl.lb	Cl.ub	k_{obs}	Var_{obs}
Terrestrial (current)	3.185	0.601	6.883	253	
Terrestrial (+2°C)	3.228	0.678	6.810	426	
Terrestrial (+4°C)	3.084	0.617	6.557	1328	
Arboreal (current)	1.930	0.054	5.054	74	0.601
Arboreal (+2°C)	2.445	0.189	5.649	111	
Arboreal (+4°C)	2.509	0.312	5.692	285	

1104

1105

1106

1107 **Extended Data Table 4 | Statistical model estimates for the proportion of species**
 1108 **predicted to experience overheating events.** Model estimates for each microhabitat
 1109 (terrestrial, arboreal) and each climatic scenario (current, +2°C, or +4°C of global warming
 1110 above pre-industrial levels) are depicted. The estimated proportion of species overheating in
 1111 assemblages containing at least one species predicted to experience at least one overheating
 1112 event (i.e., overheating assemblages) are also depicted. Model estimates for aquatic
 1113 microhabitats are not displayed because no species was predicted to experience overheating
 1114 events in this microhabitat. mean: mean model estimate; CI.lb: lower bound of the 95%
 1115 confidence interval; CI.ub: upper bound of the 95% confidence interval; k_{obs} : number of
 1116 observations; Var_{obs} : residual variance.

<i>Proportion of species overheating (all assemblages)</i>					
	mean	CI.lb	CI.ub	k_{obs}	Var_{obs}
Terrestrial (current)	1.22×10^{-5}	8.96×10^{-6}	1.66×10^{-5}	14090	
Terrestrial (+2°C)	2.09×10^{-5}	1.60×10^{-5}	2.72×10^{-5}	14090	
Terrestrial (+4°C)	8.13×10^{-5}	6.60×10^{-5}	1.00×10^{-4}	14090	
Arboreal (current)	1.19×10^{-5}	7.07×10^{-6}	2.02×10^{-5}	6614	42.26
Arboreal (+2°C)	1.86×10^{-5}	1.19×10^{-5}	2.89×10^{-5}	6614	
Arboreal (+4°C)	4.99×10^{-5}	3.62×10^{-5}	6.87×10^{-5}	6614	

<i>Proportion of species overheating (among overheating assemblages)</i>					
	mean	CI.lb	CI.ub	k_{obs}	Var_{obs}
Terrestrial (current)	0.053	0.046	0.061	253	
Terrestrial (+2°C)	0.058	0.052	0.065	426	
Terrestrial (+4°C)	0.094	0.088	0.100	1328	
Arboreal (current)	0.038	0.029	0.050	74	1.019
Arboreal (+2°C)	0.054	0.043	0.067	111	
Arboreal (+4°C)	0.061	0.053	0.070	285	

1117

1118

1119

1120 **Extended Data Table 5 | Statistical model estimates for the association between the**
 1121 **number of overheating events and thermal safety margins.** Model estimates for each
 1122 microhabitat (terrestrial, arboreal) and each climatic scenario (current, +2°C, or +4°C of global
 1123 warming above pre-industrial levels) are depicted. Model estimates for aquatic microhabitats
 1124 are not displayed because no species was predicted to experience overheating events in this
 1125 microhabitat. All model estimates are on the log scale. mean: mean model estimate; se:
 1126 standard error; k_{sp} : number of genera; k_{sp} : number of species; k_{obs} : number of observations;
 1127 Var_{genus} : variance explained by differences between genera; Var_{sp} : variance explained by
 1128 differences between species; Var_{obs} : residual variance.

	mean	se	p	k_{genus}	k_{sp}	k_{obs}	Var_{genus}	Var_{sp}	Var_{obs}
<i>Terrestrial (current)</i>									
Intercept	3.723	0.390	<0.001	464	5177	203853	5.850	3.346	0.116
Slope (TSM)	-1.201	0.031	<0.001						
<i>Terrestrial (+2°C)</i>									
Intercept	6.318	0.310	<0.001	464	5177	203853	5.272	2.380	0.078
Slope (TSM)	-1.452	0.027	<0.001						
<i>Terrestrial (+4°C)</i>									
Intercept	7.611	0.171	<0.001	464	5177	203853	2.954	1.025	0.248
Slope (TSM)	-1.616	0.015	<0.001						
<i>Arboreal (current)</i>									
Intercept	4.929	1.091	<0.001	174	1771	56210	0.001	15.190	0.001
Slope (TSM)	-1.511	0.094	<0.001						
<i>Arboreal (+2°C)</i>									
Intercept	7.836	0.836	<0.001	174	1771	56210	4.359	2.358	0.001
Slope (TSM)	-1.739	0.080	<0.001						
<i>Arboreal (+4°C)</i>									
Intercept	10.093	0.587	<0.001	174	1771	56210	8.789	0.917	0.001
Slope (TSM)	-2.085	0.039	<0.001						

1129

1130

26	Table of contents	
27		
28	Supplementary Methods.....	3
29	Supplementary Figures	5
30	Figure S1.....	5
31	Figure S2.....	6
32	Figure S3.....	7
33	Figure S4.....	8
34	Figure S5.....	9
35	Figure S6.....	10
36	Figure S7.....	11
37	Figure S8.....	12
38	Figure S9.....	13
39	Figure S10.....	14
40	Figure S11.....	15
41	Figure S12.....	16
42	Supplementary References	17
43	Data sources.....	18
44		
45		

46 **Supplementary methods**

47

48 *Sensitivity analyses*

49 In this study, we projected CT_{max} estimates assuming animals were acclimated to the mean
50 weekly temperature experienced prior to each day. We also assessed the climate vulnerability
51 of amphibians assuming they were acclimated to weekly maximum body temperatures (*cf.* ¹),
52 which reflects more conservative estimates (Fig. S7).

53 We also calculated thermal safety margins as the difference between the maximum (or 95th
54 percentile, *cf.* ²) hourly body temperature experienced by each population and their predicted
55 CT_{max} to investigate the consequences of averaging temperatures when calculating TSMs
56 (Fig. S6). To increase the comparability of our estimations with similar studies (e.g., ²), we also
57 calculated climate vulnerability metrics more conservatively. Specifically, we excluded
58 temperature data falling below the 5th percentile and above the 95th percentile body
59 temperature for each population to mitigate the impact of outliers (Fig. S6). However, extreme
60 weather events, which are typically captured by these outlier values, are the very phenomena
61 most likely to precipitate mortality events^{3,4}. Omitting these outliers could therefore obscure
62 the ecological significance of extreme temperatures, thereby underestimating true overheating
63 risks.

64 To estimate overheating probabilities, we calculated the mean daily probability that operative
65 body temperatures exceeded the predicted distribution of CT_{max} and restricted the standard
66 deviation of simulated distributions to one (i.e., within ~3°C of the mean) to avoid inflating
67 overheating probability for observations with large uncertainty. We also provided alternative
68 results (Fig. S8) where the standard deviation of CT_{max} was restricted to the “*biological range*”,
69 i.e., the standard deviation of the distribution of all CT_{max} estimates across species (range =
70 1.84 – 2.17). We also provide a sensitivity analysis where overheating risk was positive only
71 when the 95% confidence intervals of predicted overheating days did not overlap with zero
72 (Fig. S8).

73 We also investigated the influence of different parameters of our biophysical models (i.e.,
74 shade and burrow availability, height in above-ground vegetation, solar radiation, wind speed,
75 pond depth) on predicted vulnerability risks (Fig. S9-11). Specifically, we modelled the
76 responses of the species at highest risk in terrestrial and aquatic conditions, *Noblella*
77 *myrmecoides*, in its most vulnerable location (latitude, longitude = -9.5, -69.5). For terrestrial
78 conditions, we modelled the response of amphibians with different body sizes (0.5, 4.28, or
79 50 grams), and with different levels of exposure to open habitat conditions. Specifically, we

80 modelled an amphibian exposed to 50% of shade to simulate an open habitat lightly covered
81 by vegetation, and inferred temperatures at different soil depths (2.5, 5, 10, 15, or 20 cm
82 underground). For aquatic conditions, we adjusted pond depths to simulate a very shallow
83 pond (50 cm) and compared it to deeper ponds (1.5- or 3-meters depth). For arboreal
84 conditions, we modelled the responses of *Pristimantis ockendeni*, in its most vulnerable
85 location (-4.5, -71.5), and adjusted the height in above-ground vegetation (0.5, 2, or 5 meters),
86 the percentage of radiation diffused by vegetation (50%, 75%, or 90% of radiation diffused),
87 and the percentage of wind speed reduced by vegetation (0%, 50%, or 80% of wind speed
88 reduced by vegetation). We did not estimate the influence of these parameters on all species
89 and at all locations because of the scale of our study, but these results should provide insight
90 into how varying microenvironmental features and biological characteristics may impact our
91 general conclusions.

92 Finally, we compared our predictions of operative body temperatures with field body
93 temperature measurements. We extracted night-time (18:00 – 00:30) field body temperatures
94 measured for 11 species of frogs in Mexico (21.48° N, -104.85° W; and 21.45° N, -105.03° W)
95 between June and October of 2013 and 2015 from Table 1 of ⁵. We chose this study because
96 it provided the data and location of body temperature measurements, covered multiple species
97 from different sites, and matched our study timeframe (2006-2015). We then compare these
98 estimates with hourly operative body temperatures predicted in shaded terrestrial conditions
99 at the same dates and time windows (Fig. S12).

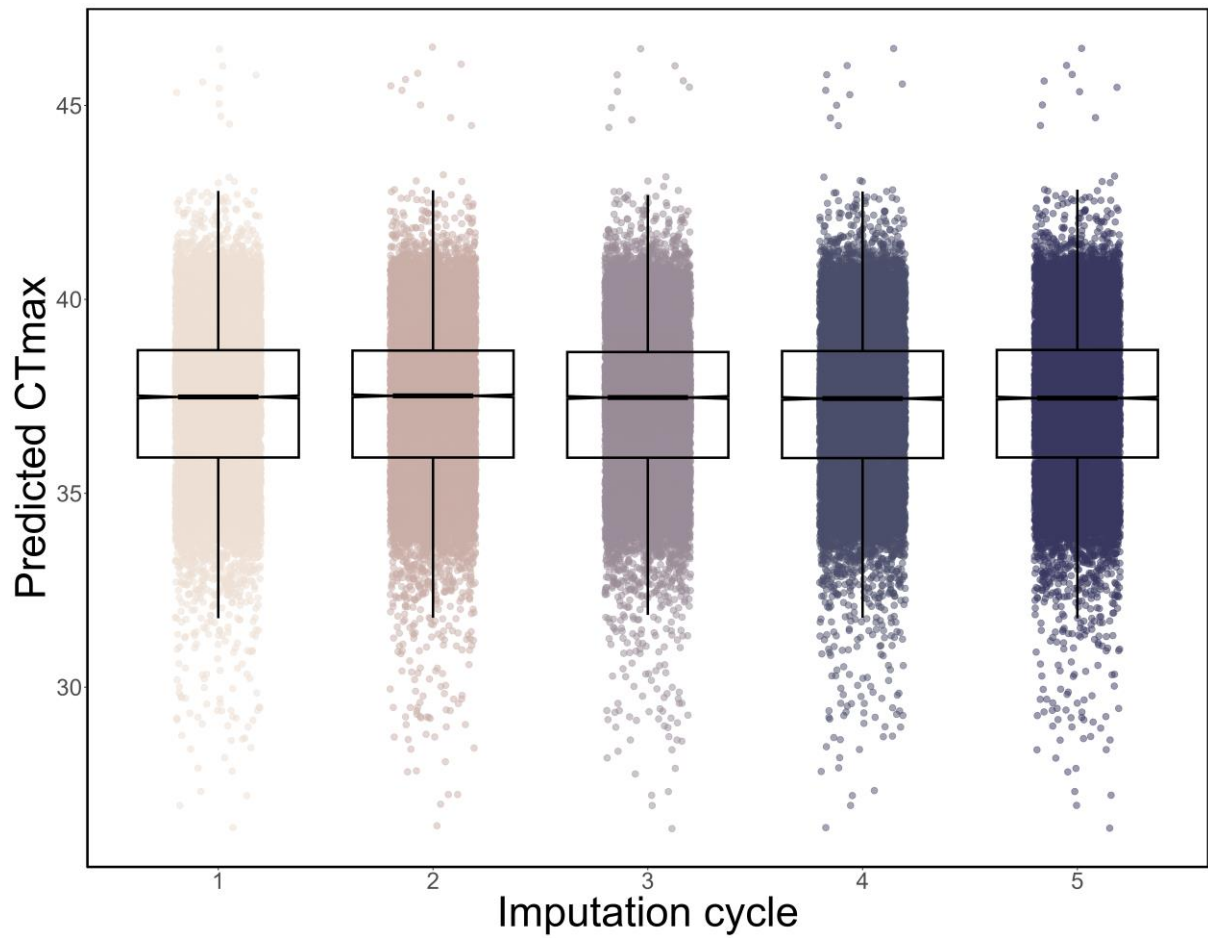
100 Results from all statistical models and additional data visualizations are available at [https://p-](https://p-pottier.github.io/Vulnerability_amphibians_global_warming/)
101 [pottier.github.io/Vulnerability_amphibians_global_warming/](https://p-pottier.github.io/Vulnerability_amphibians_global_warming/).

102 Original studies on which our analyses are built upon are listed in *Data sources*^{6–218}.

103

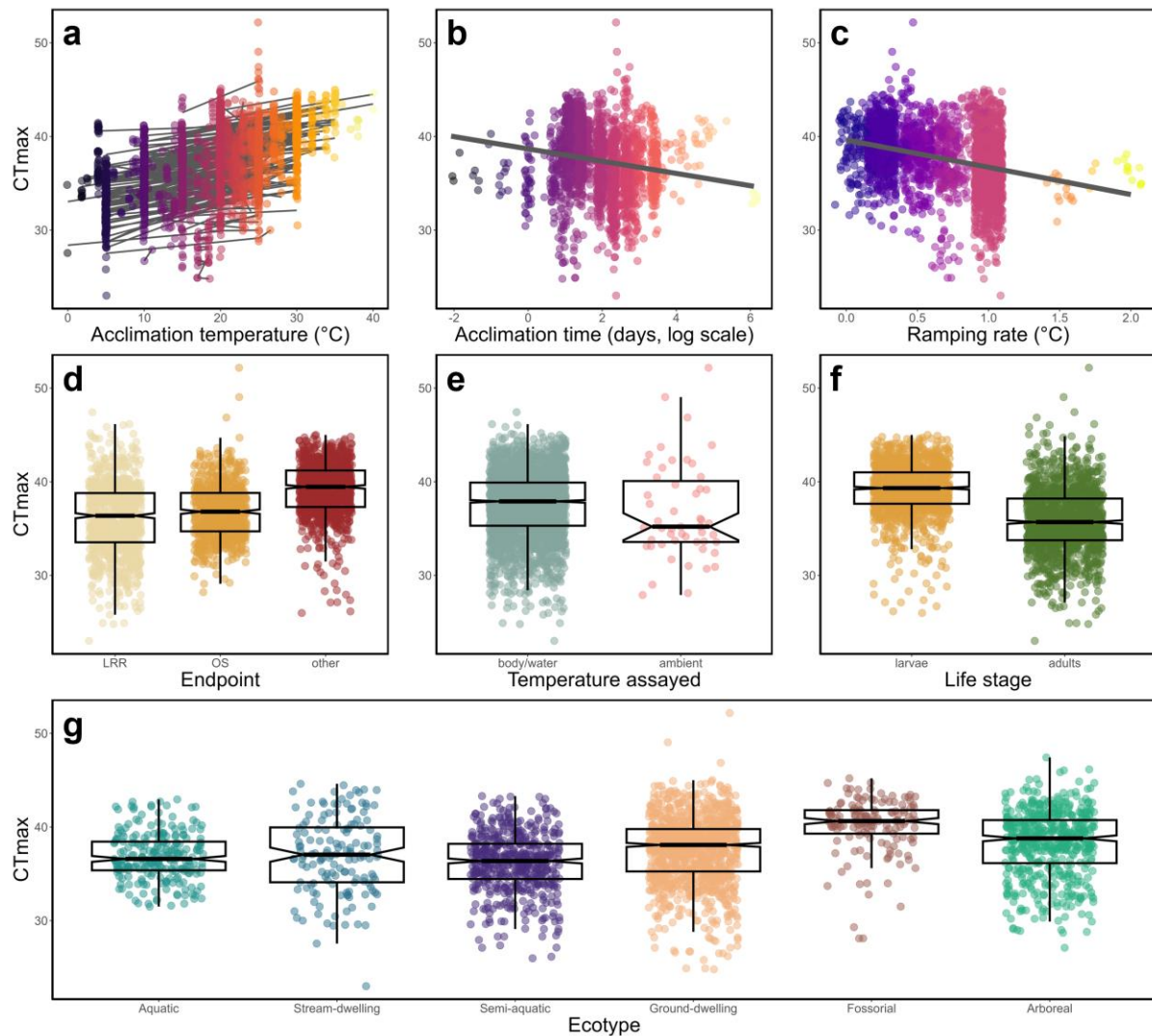
104

105 **Supplementary figures**



107 **Fig. S1 | Predicted critical thermal maximum (CT_{max}) across imputation cycles.**
108 Boxplots depict median (horizontal line), interquartile ranges (boxes), and whiskers
109 extend to 1.5 times the interquartile range.

110



111

112

113

114

115

116

117

118

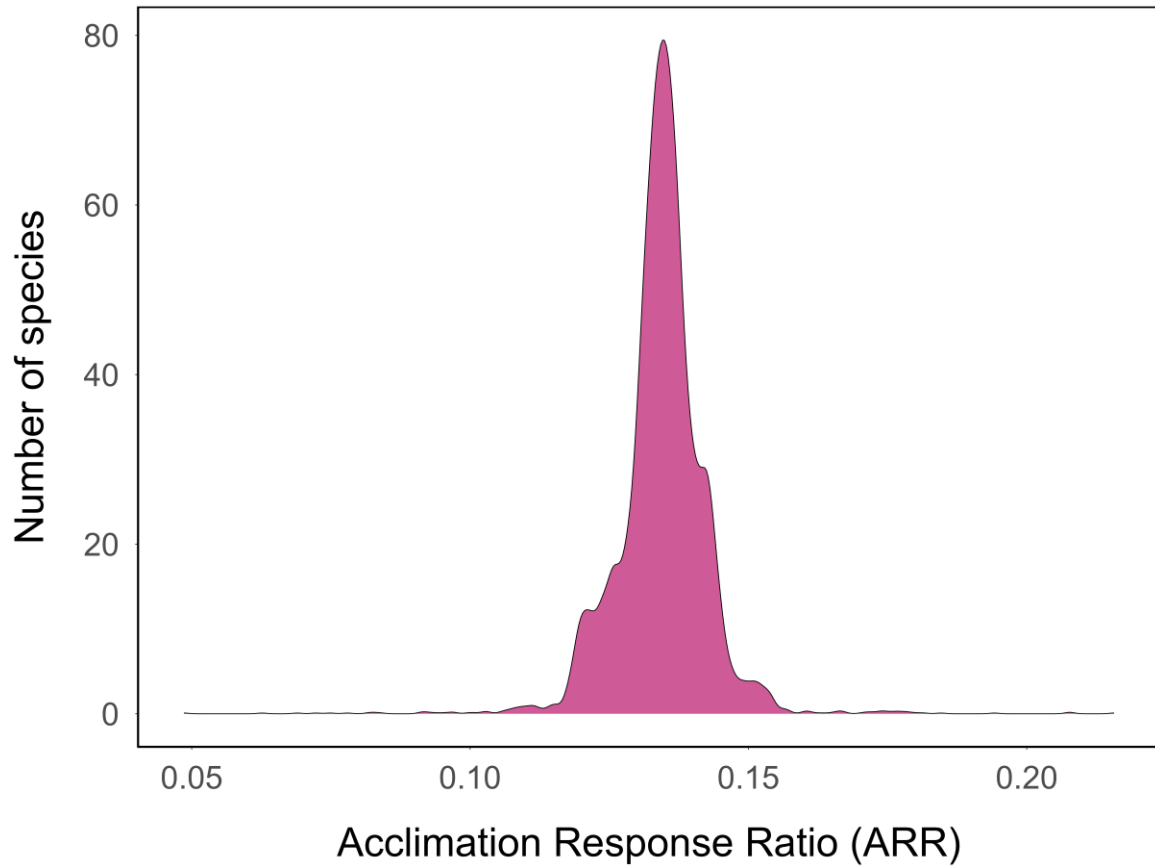
119

120

121

122

Fig. S2 | Correlations between critical thermal maximum (CT_{max}) and predictors used for the imputation. CT_{max} from the experimental dataset was plotted against acclimation temperature (a), acclimation time (b, log scale), ramping rate (c). Colours are proportional to the values of the continuous predictors and the line refers to predictions from a simple linear regression between CT_{max} and the predictors. Individual slopes for each species are depicted for species when CT_{max} was estimated at different acclimation temperatures (a). Depicted is also the variation in CT_{max} with different endpoints (d), media used to infer body temperature (e), life stages (f), and ecotypes (g). Boxplots depict median (horizontal line), interquartile ranges (boxes), and whiskers extend to 1.5 times the interquartile range. LRR: loss of righting response. OS: onset of spasms.



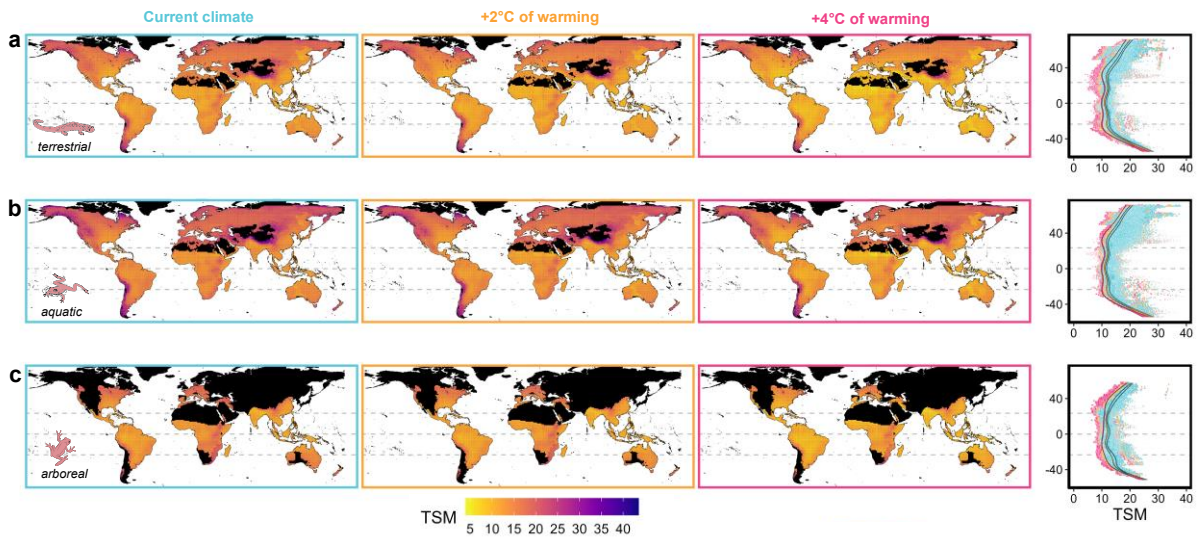
123

124 **Fig. S3 | Variation in plastic responses across species.** The acclimation response
125 ratio (ARR) represents the magnitude change in heat tolerance limits for each degree
126 change in environmental temperature. We found limited variation in ARR (mean \pm
127 standard deviation = 0.134 ± 0.008 ; range = $0.049 - 0.216$; $n = 5203$).

128

129

130



131

132

133

134

135

136

137

138

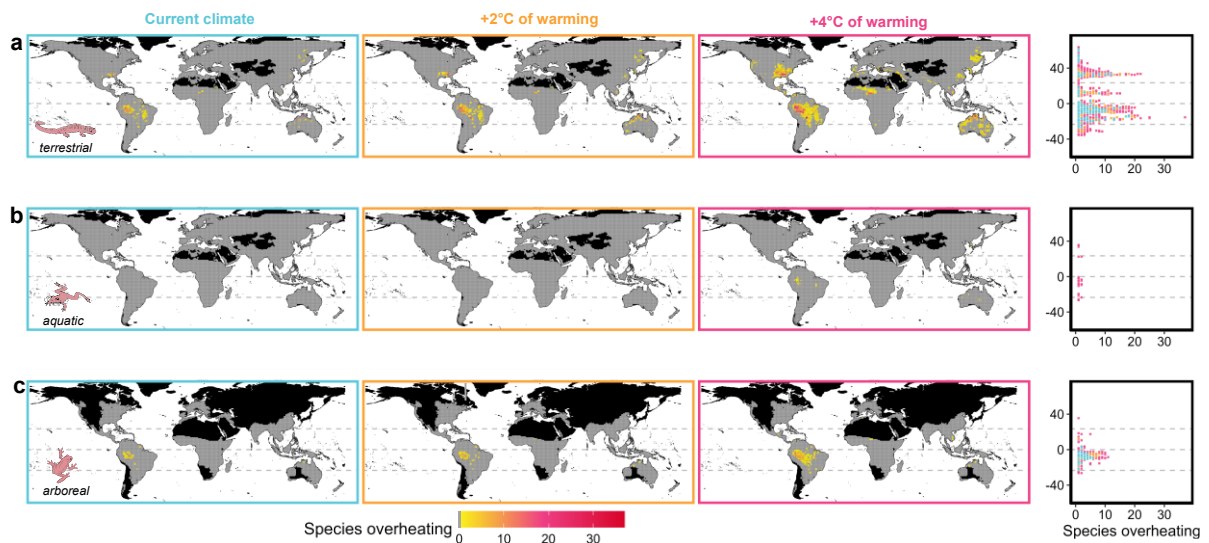
139

140

141

Fig. S4 | Assemblage-level patterns in thermal safety margin for amphibians on terrestrial (a), aquatic (b), or arboreal (c) microhabitats. Thermal safety margins (TSM) were calculated as the mean difference between CT_{max} and the predicted operative body temperature in full shade during the warmest quarters of 2006-2015 in each assemblage (1-degree grid cell). Black colour depicts areas with no data. The right panel depicts latitudinal patterns in TSM in current climates (blue) or assuming 2°C (orange) or 4°C of global warming above pre-industrial levels (pink), as predicted from generalized additive mixed models. Point estimates are scaled by precision (1/s.e.). Dashed lines represent the equator and tropics.

142



143

144

145

146

147

148

149

150

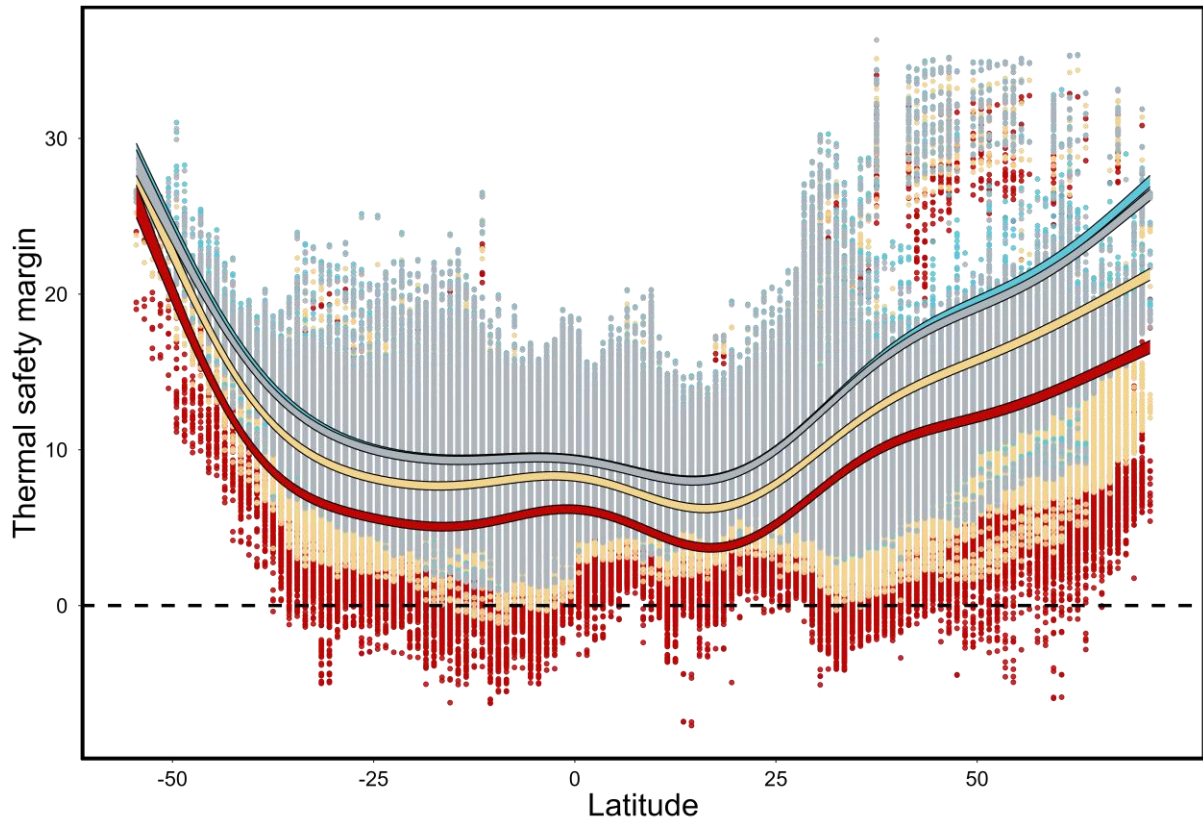
151

152

153

154

Fig. S5 | Number of species predicted to experience overheating events in terrestrial (a), aquatic (b), and arboreal (c) microhabitats. The number of species overheating was assessed as the sum of species overheating for least one day in the period surveyed (warmest quarters of 2006-2015) in each assemblage (1-degree grid cell). Black colour depicts areas with no data and grey colour assemblages without species at risk. The right panel depicts latitudinal patterns in the number of species predicted to overheat in current climates (blue) or assuming 2°C (orange) or 4°C of global warming above pre-industrial levels (pink). Dashed lines represent the equator and tropics. No species were predicted to experience overheating events in water bodies, and hence are not displayed.



155

156

157

158

159

160

161

162

163

164

165

166

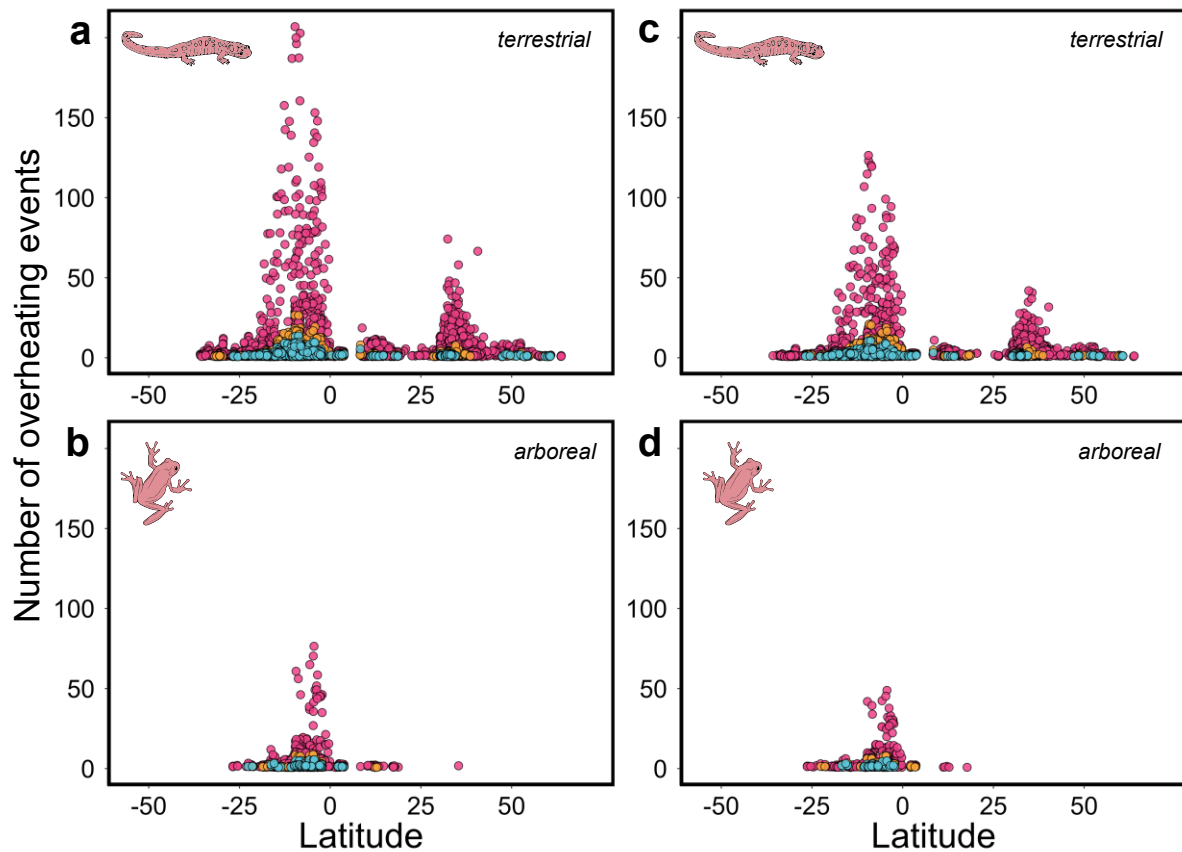
167

168

Fig. S6 | Variation in thermal safety margins calculated using different assumptions. Thermal safety margins (TSM) were calculated as the mean difference between CT_{max} and the predicted operative body temperature in full shade during the warmest quarters of 2006-2015 (grey), as the mean difference between CT_{max} and the predicted operative body temperature in full shade during the warmest quarters of 2006-2015 excluding body temperatures falling outside the 5% and 95% percentile temperatures (blue), as the difference between the 95% percentile operative body temperature and the corresponding CT_{max} (yellow), or as the difference between the maximum operative body temperature and the corresponding CT_{max} (red). Lines represented 95% confidence interval ranges predicted from generalized additive mixed models. This figure was constructed assuming ground-level microclimates occurring under 4°C of global warming above pre-industrial levels.

168

169



170

171

172

173

174

175

176

177

178

179

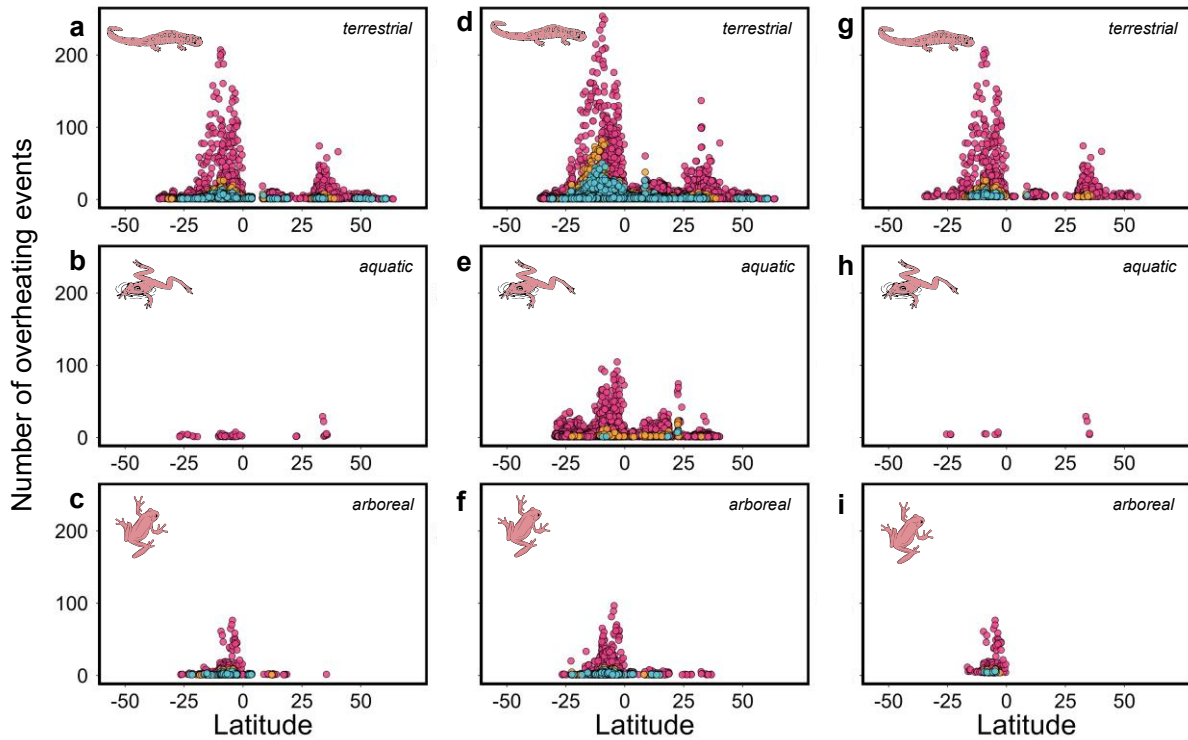
180

Fig. S7 | Latitudinal variation in the number of overheating events when animals are acclimated to the mean (a,b) or maximum (c,d) weekly body temperature experienced in the seven days prior in terrestrial (a,c) and arboreal (b,d) microhabitats. The number of overheating events (days) were calculated based on the mean probability that daily maximum temperatures exceeded CT_{max} during the warmest quarters of 2006-2015 for each species in each grid cell. Blue points depict the number of overheating events in historical microclimates, while orange and pink points depict the number of overheating events assuming 2°C and 4°C of global warming above pre-industrial levels, respectively. For clarity, only the species predicted to experience overheating events across latitudes are depicted.

181

182

183



184

185

186

187

188

189

190

191

192

193

194

195

196

197

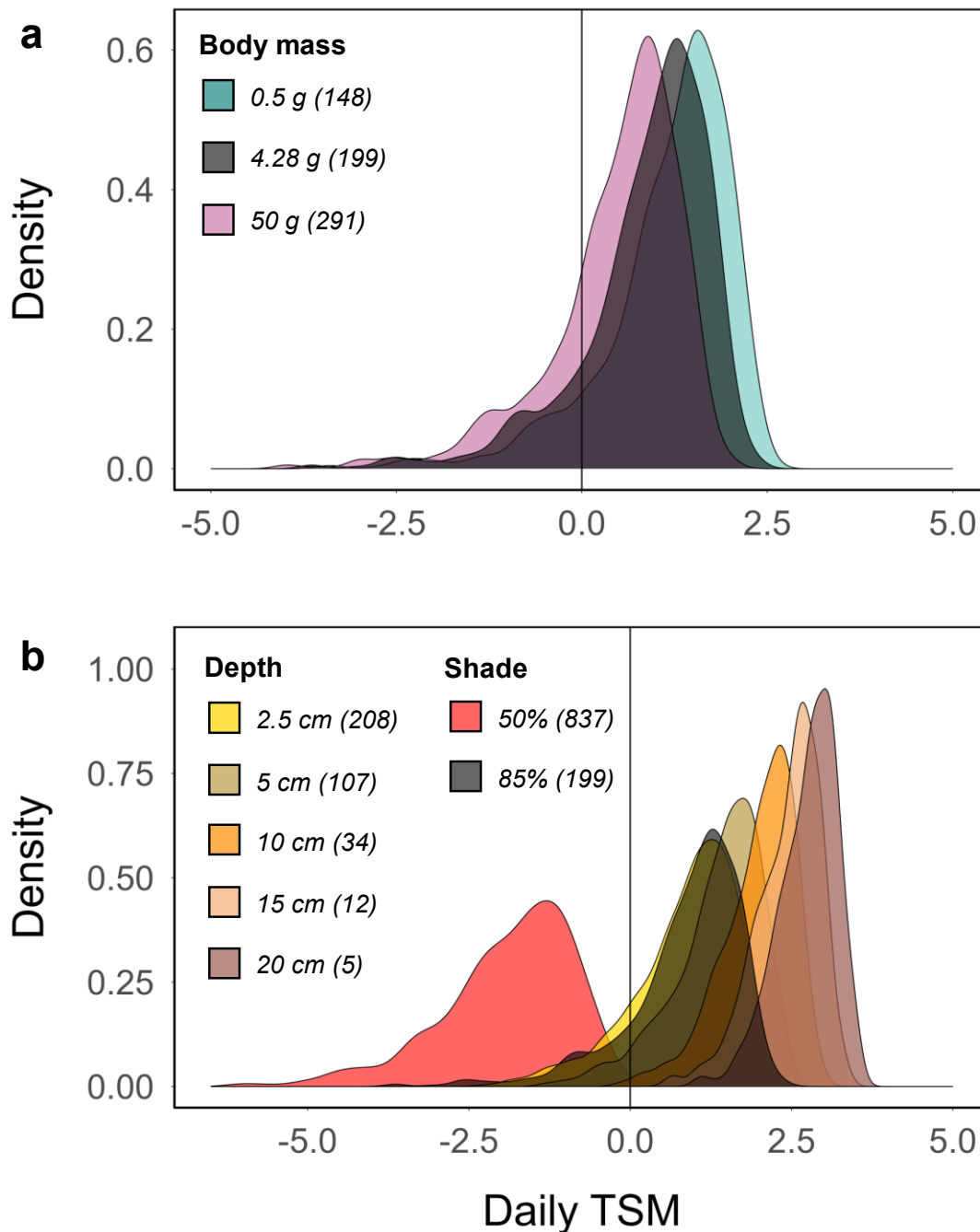
198

199

200

Fig. S8 | Latitudinal variation in the number of overheating events using regular (a,b,c), uncertain (d,e,f), or conservative estimates (g,h,i) in terrestrial (a,d,g), aquatic (b,e,h) and arboreal (c,f,i) microhabitats. The number of overheating events (days) were calculated based on the mean probability that daily maximum temperatures exceeded CT_{max} during the warmest quarters of 2006-2015 for each species in each grid cell. Uncertain estimates are those where daily overheating probabilities were calculated based on broad predicted distributions of CT_{max} (i.e., simulated over the whole “*biological range*”), likely inflating overheating probabilities for observations with large uncertainty. Conservative estimates are those when overheating risk was considered only when the 95% confidence intervals of the predicted number of overheating events did not overlap with zero (e,f). Blue points depict the number of overheating events in historical microclimates, while orange and pink points depict the number of overheating events assuming 2°C and 4°C of global warming above pre-industrial levels, respectively. For clarity, only the species predicted to experience overheating events across latitudes are depicted.

201

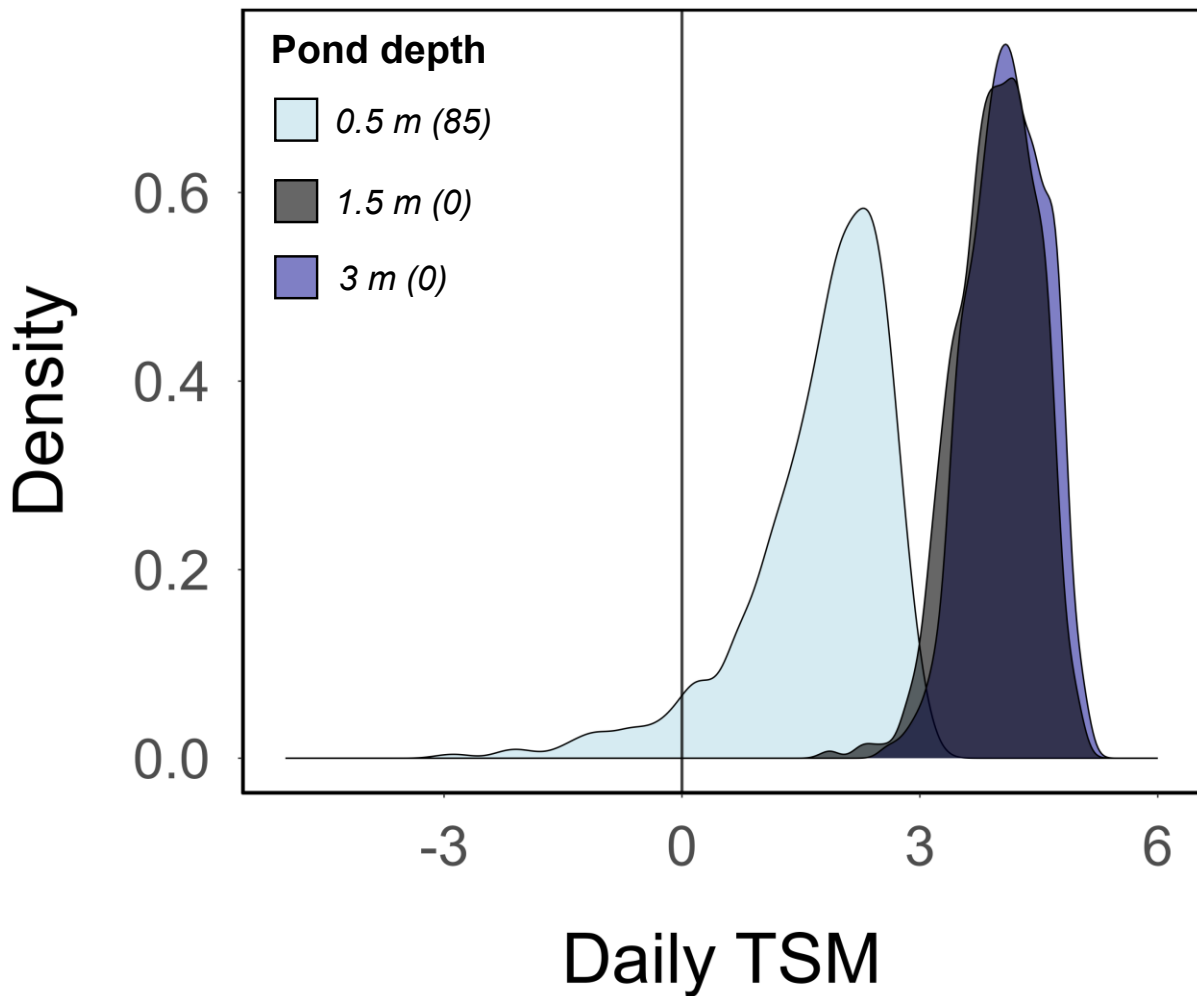


202

203 **Fig. S9 | Influence of biophysical model parameters on the estimation of**
 204 **terrestrial thermal safety margins.** Depicted is the variation in daily thermal safety
 205 margins (TSM) as density distributions according to body mass (a), shade availability
 206 and soil depth (b). All simulations were performed assuming 4°C of global warming
 207 above pre-industrial levels in a specific grid cell (latitude, longitude = -9.5, -69.5; where
 208 the highest number of overheating events was predicted), for the most vulnerable
 209 species (*Noblella myrmecoides*). Negative daily TSMs were recorded as overheating
 210 events, and conditions depicted in dark grey reflect the results presented in the
 211 manuscript. The number of predicted overheating events is indicated in brackets for
 212 each condition.

213

214



215

216

217

218

219

220

221

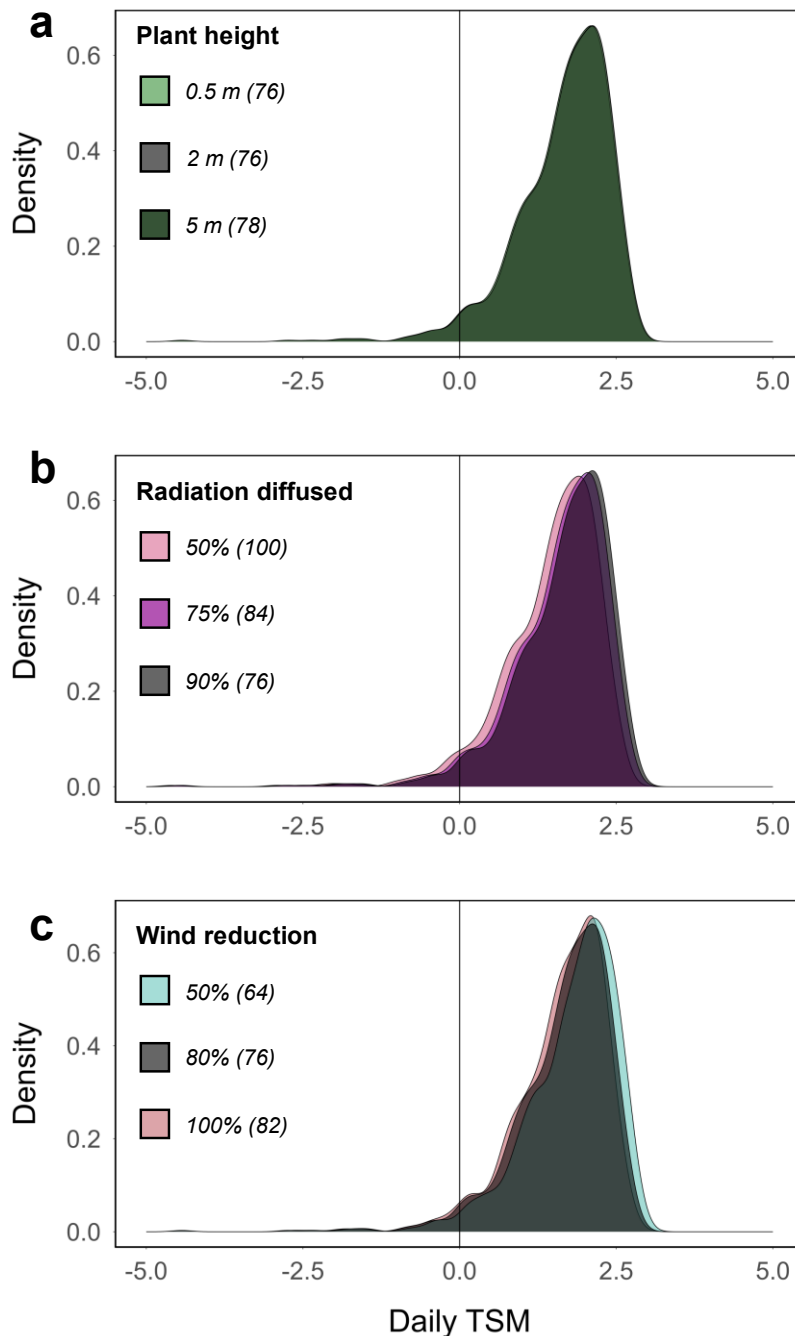
222

223

224

225

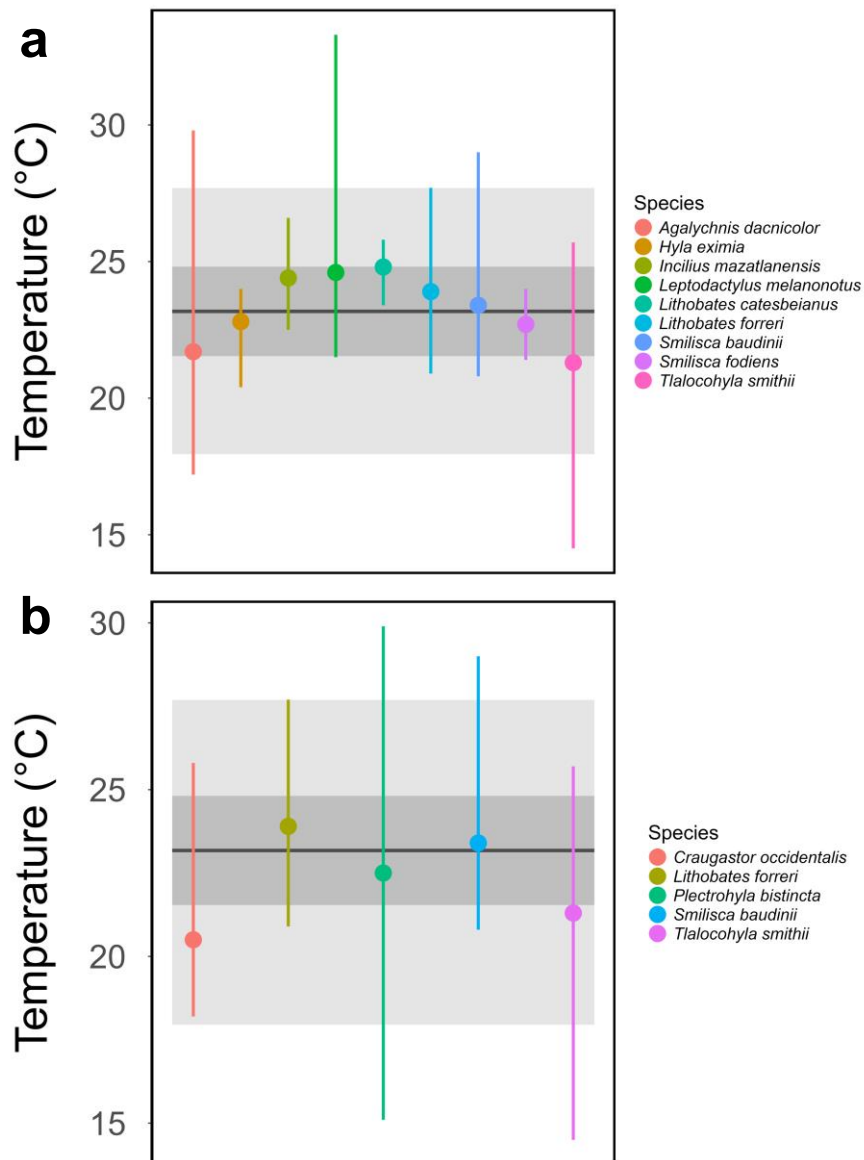
Fig. S10 | Influence of pond depth on the estimation of aquatic thermal safety margins. All simulations were performed assuming 4°C of global warming above pre-industrial levels in a specific grid cell (latitude, longitude = -9.5, -69.5; where the highest number of overheating events was predicted), for the most vulnerable species (*Noblella myrmecoides*). Depicted is the variation in daily thermal safety margins (TSM) as density distributions. Negative daily TSMs were recorded as overheating events, and conditions depicted in dark grey reflect the results presented in the manuscript. The number of predicted overheating events is indicated in brackets for each condition.



226

227 **Fig. S11 | Influence of biophysical parameters on the estimation of aquatic**
 228 **arboreal safety margins.** All simulations were performed assuming 4°C of global
 229 warming above pre-industrial levels in a specific grid cell (latitude, longitude = -9.5, -
 230 69.5; where the highest number of overheating events was predicted), for the most
 231 vulnerable arboreal species (*Pristimantis ockendeni*). Depicted is the variation in daily
 232 thermal safety margins (TSM) as density distributions according to height of the animal
 233 in above-ground vegetation (a), the percentage of solar radiation diffused by
 234 vegetation (b) and the percentage of wind reduced by vegetation (c). Negative daily
 235 TSMs were recorded as overheating events, and conditions depicted in dark grey
 236 reflect the results presented in the manuscript. The number of predicted overheating
 237 events is indicated in brackets for each condition.

238



239

240 **Fig. S12 | Validation of operative body temperature estimations.** Terrestrial
 241 operative body temperatures estimated from biophysical models were compared to
 242 field body temperatures recorded around Tepic (21.48° N, -104.85° W; panel a) and
 243 El Cuarenteño (21.45° N, -105.03° W; panel b) between June and October of
 244 2013/2015, for 11 species of frogs⁵. The mean hourly operative body temperatures
 245 predicted from our models for the same date and time windows (18:00 – 01:00)
 246 are represented by the black horizontal line, along with their standard deviation (dark grey
 247 box), and range (light grey box). The mean (point) and range (bars) of field body
 248 temperatures recorded for each species are presented in colour. Note that our
 249 analyses were based on the maximum daily temperature recorded at each site during
 250 the warmest quarters of 2006-2015, which may not match the times and dates at which
 251 field body temperatures were recorded. Nevertheless, congruence between night-time
 252 predicted and field body temperatures suggests our models are likely to capture true
 253 biological variation in operative body temperatures throughout the day.

254 **Supplementary references**

- 255 1. Gunderson, A. R., Dillon, M. E. & Stillman, J. H. Estimating the benefits of plasticity in
256 ectotherm heat tolerance under natural thermal variability. *Functional Ecology* **31**, 1529–
257 1539 (2017).
- 258 2. Pinsky, M. L., Eikeset, A. M., McCauley, D. J., Payne, J. L. & Sunday, J. M. Greater
259 vulnerability to warming of marine versus terrestrial ectotherms. *Nature* **569**, 108–111
260 (2019).
- 261 3. Müller, J. et al. Weather explains the decline and rise of insect biomass over 34 years.
262 *Nature* 1–6 (2023).
- 263 4. Murali, G., Iwamura, T., Meiri, S. & Roll, U. Future temperature extremes threaten land
264 vertebrates. *Nature* **615**, 461–467 (2023).
- 265 5. Lara-Resendiz, R. A., & Luja, V. H. Body temperatures of some amphibians from Nayarit,
266 Mexico. *Revista mexicana de biodiversidad* **89**, 577-581 (2018).
- 267
- 268

269 **Data sources**

- 270 6. Agudelo-Cantero, G. A. & Navas, C. A. Interactive effects of experimental heating
271 rates, ontogeny and body mass on the upper thermal limits of anuran larvae. *Journal of*
272 *Thermal Biology* **82**, 43–51 (2019).
- 273 7. Alveal Riquelme, N. Relaciones entre la fisiología térmica y las características
274 bioclimáticas de *Rhinella spinulosa* (Anura: Bufonidae) en Chile a través del enlace
275 mecanicista de nicho térmico (Universidad de Concepción, 2015).
- 276 8. Alves, M. Tolerância térmica em espécies de anuros neotropicais do gênero
277 *Dendropsophus* Fitzinger, 1843 e efeito da temperatura na resposta à predação.
278 (Universidade Estadual de Santa Cruz, 2016).
- 279 9. Anderson, R. C. O. & Andrade, D. V. Trading heat and hops for water: Dehydration
280 effects on locomotor performance, thermal limits, and thermoregulatory behavior of a
281 terrestrial toad. *Ecology and Evolution* **7**, 9066–9075 (2017).
- 282 10. Aponte Gutiérrez, A. Endurecimiento térmico en *Pristimantis medemi* (Anura:
283 Craugastoridae), en coberturas boscosas del Municipio de Villavicencio (Meta).
284 (Universidad Nacional de Colombia, 2020).
- 285 11. Arrigada García, K. Conductas térmica en dos poblaciones de *Batrachyla taeniata*
286 provenientes de la localidad de Ucúquer en la región de O'Higgins y de la localidad de
287 Hualpén en la región del Bío-Bío (Universidad de Concepción, 2019).
- 288 12. Azambuja, G., Martins, I. K., Franco, J. L. & Santos, T. G. dos. Effects of mancozeb
289 on heat Shock protein 70 (HSP70) and its relationship with the thermal physiology of
290 *Physalaemus henselii* (Peters, 1872) tadpoles (Anura: Leptodactylidae). *Journal of*
291 *Thermal Biology* **98**, 102911 (2021).
- 292 13. Bacigalupe, L. D. *et al.* Natural selection on plasticity of thermal traits in a highly
293 seasonal environment. *Evolutionary Applications* **11**, 2004–2013 (2018).
- 294 14. Barria, A. M. & Bacigalupe, L. D. Intraspecific geographic variation in thermal limits
295 and acclimatory capacity in a wide distributed endemic frog. *Journal of Thermal Biology*
296 **69**, 254–260 (2017).
- 297 15. Beltrán, I., Ramírez-Castañeda, V., Rodríguez-López, C., Lasso, E. & Amézquita, A.
298 Dealing with hot rocky environments: critical thermal maxima and locomotor performance
299 in *Leptodactylus lithonaetes* (anura: Leptodactylidae). *Herpetological Journal* **29**, 155–161
300 (2019).
- 301 16. Berkhouse, C. & Fries, J. Critical thermal maxima of juvenile and adult San Marcos
302 salamanders (*Eurycea nana*). *Southwestern Naturalist* **40**, 430–434 (1995).

- 303 17. Blem, C. R., Ragan, C. A. & Scott, L. S. The thermal physiology of two sympatric
304 treefrogs *Hyla cinerea* and *Hyla chrysoscelis* (Anura; Hylidae). *Comparative Biochemistry*
305 *and Physiology -- Part A: Physiology* **85**, 563–570 (1986).
- 306 18. Bonino, M. F., Cruz, F. B. & Perotti, M. G. Does temperature at local scale explain
307 thermal biology patterns of temperate tadpoles? *Journal of Thermal Biology* **94**, (2020).
- 308 19. Bovo, R. P. Fisiologia térmica e balanço hídrico em anfíbios anuros. (Universidade
309 Estadual Paulista, 2015).
- 310 20. Brattstrom, B. H. Thermal acclimation in Australian amphibians. *Comparative*
311 *Biochemistry And Physiology* **35**, 69–103 (1970).
- 312 21. Brattstrom, B. H. & Regal, P. Rate of thermal acclimation in the Mexican salamander
313 *Chiropterotriton*. *Copeia* **1965**, 514–515 (1965).
- 314 22. Brattstrom, B. H. A Preliminary Review of the Thermal Requirements of Amphibians.
315 *Ecology* **44**, 238–255 (1963).
- 316 23. Brattstrom, B. H. Thermal acclimation in Anuran amphibians as a function of latitude
317 and altitude. *Comparative Biochemistry and Physiology* **24**, 93–111 (1968).
- 318 24. Brattstrom, B. H. & Lawrence, P. The Rate of Thermal Acclimation in Anuran
319 Amphibians. *Physiological Zoology* **35**, 148–156 (1962).
- 320 25. Brown, H. A. The heat resistance of some anuran tadpoles (Hylidae and
321 Pelobatidae). *Copeia* **1969**, 138 (1969).
- 322 26. Burke, E. M. & Pough, F. H. The role of fatigue in temperature resistance of
323 salamanders. *Journal of Thermal Biology* **1**, 163–167 (1976).
- 324 27. Burrowes, P. A., Navas, C. A., Jiménez-Robles, O., Delgado, P. & De La Riva, I.
325 Climatic heterogeneity in the bolivian andes: Are frogs trapped? *South American Journal*
326 *of Herpetology* **18**, 1–12 (2020).
- 327 28. Bury, R. B. Low thermal tolerances of stream amphibians in the Pacific Northwest:
328 Implications for riparian and forest management. *Applied Herpetology* **5**, 63–74 (2008).
- 329 29. Castellanos García, L. A. Days of futures past : integrating physiology,
330 microenvironments, and biogeographic history to predict response of frogs in neotropical
331 dry-forest to global warming. (Universidad de los Andes, 2017).
- 332 30. Castro, B. Influence of environment on thermal ecology of direct-developing frogs
333 (Anura: craugastoridae: pristimantis) in the eastern Andes of Colombia. (Universidad de
334 los Andes, 2019).
- 335 31. Catenazzi, A., Lehr, E. & Vredenburg, V. T. Thermal physiology, disease, and
336 amphibian declines on the eastern slopes of the andes. *Conservation Biology* **28**, 509–
337 517 (2014).
- 338 32. Chang, L.-W. Heat tolerance and its plasticity in larval *Bufo bankorensis* from
339 different altitudes. (National Cheng Kung University, 2002).

- 340 33. Chavez Landi, P. A. Fisiología térmica de un depredador *Dasythemis* sp. (Odonata:
341 Libellulidae) y su presa *Hypsiboas pellucens* (Anura: Hylidae) y sus posibles
342 implicaciones frente al cambio climático (Pontificia Universidad Católica Del Ecuador,
343 2017).
- 344 34. Chen, T.-C., Kam, Y.-C. & Lin, Y.-S. Thermal physiology and reproductive phenology
345 of *Buergeria japonica* (rhacophoridae) breeding in a stream and a geothermal hot spring in
346 Taiwan. *Zoological Science* **18**, 591–596 (2001).
- 347 35. Cheng, C.-B. A study of warming tolerance and thermal acclimation capacity of
348 tadpoles in Taiwan. (Tunghai University, 2017).
- 349 36. Cheng, Y.-J. Effect of salinity on the critical thermal maximum of tadpoles living in
350 brackish water. (Tunghai University, 2017).
- 351 37. Christian, K. A., Nunez, F., Clos, L. & Diaz, L. Thermal relations of some tropical
352 frogs along an altitudinal gradient. *Biotropica* **20**, 236–239 (1988).
- 353 38. Claussen, D. L. The thermal relations of the tailed frog, *Ascaphus truei*, and the
354 pacific treefrog, *Hyla regilla*. *Comparative Biochemistry and Physiology -- Part A:
355 Physiology* **44**, 137–153 (1973).
- 356 39. Claussen, D. L. Thermal acclimation in ambystomatid salamanders. *Comparative
357 Biochemistry and Physiology -- Part A: Physiology* **58**, 333–340 (1977).
- 358 40. Contreras Cisneros, J. Temperatura crítica máxima, tolerancia al frío y
359 termopreferendum del tritón del Montseny (*Calotriton arnoldii*). (Universitat de Barcelona,
360 2019).
- 361 41. Contreras Oñate, S. Posible efecto de las temperaturas de aclimatación sobre las
362 respuestas térmicas en temperaturas críticas máximas (TC_{más}) y mínimas (TC_{mín}) de
363 una población de *Batrachyla taeniata* (Girard, 1955) (Universidad de Concepción, 2016).
- 364 42. Cooper, R. D. & Shaffer, H. B. Allele-specific expression and gene regulation help
365 explain transgressive thermal tolerance in non-native hybrids of the endangered California
366 tiger salamander (*Ambystoma californiense*). *Molecular Ecology* **30**, 987–1004 (2021).
- 367 43. Crow, J. C., Forstner, M. R. J., Ostr, K.G. & Tomasso, J. R. The role of temperature
368 on survival and growth of the barton springs salamander (*Eurycea sosorum*).
369 *Herpetological Conservation and Biology* **11**, 328–334 (2016).
- 370 44. Cupp, P. V. Thermal Tolerance of Five Salientian Amphibians during Development
371 and Metamorphosis. *Herpetologica* **36**, 234–244 (1980).
- 372 45. Dabruzzi, T. F., Wygoda, M. L. & Bennett, W. A. Some Like it Hot: Heat Tolerance of
373 the Crab-Eating Frog, *Fejervarya cancrivora*. *Micronesica* **43**, 101–106 (2012).
- 374 46. Dainton, B. H. Heat tolerance and thyroid activity in developing tadpoles and juvenile
375 adults of *Xenopus laevis* (Daudin). *Journal of Thermal Biology* **16**, 273–276 (1991).

- 376 47. Daniel, N. J. J. Impact of climate change on Singapore amphibians. (National
377 University of Singapore, 2013).
- 378 48. Davies, S. J., McGeoch, M. A. & Clusella-Trullas, S. Plasticity of thermal tolerance
379 and metabolism but not water loss in an invasive reed frog. *Comparative Biochemistry
380 and Physiology -Part A : Molecular and Integrative Physiology* **189**, 11–20 (2015).
- 381 49. de Oliveira Anderson, R. C., Bovo, R. P. & Andrade, D. V. Seasonal variation in the
382 thermal biology of a terrestrial toad, *Rhinella icterica* (Bufonidae), from the Brazilian
383 Atlantic Forest. *Journal of Thermal Biology* **74**, 77–83 (2018).
- 384 50. de Vlaming, V. L. & Bury, R. B. Thermal Selection in Tadpoles of the Tailed-Frog,
385 *Ascaphus truei*. *Journal of Herpetology* **4**, 179–189 (1970).
- 386 51. Delson, J. & Whitford, W. G. Critical Thermal Maxima in Several Life History Stages
387 in Desert and Montane Populations of *Ambystoma tigrinum*. *Herpetologica* **29**, 352–355
388 (1973).
- 389 52. Duarte, H. et al. Can amphibians take the heat? Vulnerability to climate warming in
390 subtropical and temperate larval amphibian communities. *Global Change Biology* **18**,
391 412–421 (2012).
- 392 53. Duarte, H. S. A comparative study of the thermal tolerance of tadpoles of iberian
393 anurans. (Universidade de Lisboa, 2011).
- 394 54. Dunlap, D. Evidence for a daily rhythm of heat resistance in cricket frogs, *Acris
395 crepitans*. *Copeia* 852- (1969).
- 396 55. Dunlap, D. G. Critical Thermal Maximum as a Function of Temperature of
397 Acclimation in Two Species of Hylid Frogs. *Physiological Zoology* **41**, 432–439 (1968).
- 398 56. Elwood, J. R. L. Variation in hsp70 levels and thermotolerance among terrestrial
399 salamanders of the *Plethodon glutinosus* complex. (Drexel University, 2003).
- 400 57. Enriquez-Urzelai, U. et al. Ontogenetic reduction in thermal tolerance is not alleviated
401 by earlier developmental acclimation in *Rana temporaria*. *Oecologia* **189**, 385–394
402 (2019).
- 403 58. Enriquez-Urzelai, U. et al. The roles of acclimation and behaviour in buffering climate
404 change impacts along elevational gradients. *Journal of Animal Ecology* **89**, 1722–1734
405 (2020).
- 406 59. Erskine, D. J. & Hutchison, V. H. Reduced thermal tolerance in an amphibian treated
407 with melatonin. *Journal of Thermal Biology* **7**, 121–123 (1982).
- 408 60. Escobar Serrano, D. Acclimation scope of the critical thermal limits in *Agalychnis
409 spurrelli* (Hylidae) and *Gastrotheca pseustes* (Hemiphractidae) and their implications
410 under climate change scenarios. (Pontificia Universidad Católica Del Ecuador, 2016).

- 411 61. Fan, X., Lei, H. & Lin, Z. Ontogenetic shifts in selected body temperature and thermal
412 tolerance of the tiger frog, *Hoplobatrachus chinensis*. *Acta Ecologica Sinica* **32**, 5574–
413 5580 (2012).
- 414 62. Fan, X. L., Lin, Z. H. & Scheffers, B. R. Physiological, developmental, and behavioral
415 plasticity in response to thermal acclimation. *Journal of Thermal Biology* **97**, (2021).
- 416 63. Fernández-Loras, A. et al. Infection with *Batrachochytrium dendrobatidis* lowers heat
417 tolerance of tadpole hosts and cannot be cleared by brief exposure to CTmax. *PLoS ONE*
418 **14**, (2019).
- 419 64. Floyd, R. B. Ontogenetic change in the temperature tolerance of larval *Bufo marinus*
420 (Anura: bufonidae). *Comparative Biochemistry and Physiology -- Part A: Physiology* **75**,
421 267–271 (1983).
- 422 65. Floyd, R. B. Effects of Photoperiod and Starvation on the Temperature Tolerance of
423 Larvae of the Giant Toad, *Bufo marinus*. *Copeia* **1985**, 625–631 (1985).
- 424 66. Fong, S.-T. Thermal tolerance of adult Asiatic painted frog *Kaloula pulchra* from
425 different populations. (National University of Tainan, 2014).
- 426 67. Frishkoff, L. O., Hadly, E. A. & Daily, G. C. Thermal niche predicts tolerance to
427 habitat conversion in tropical amphibians and reptiles. *Global Change Biology* **21**, 3901–
428 3916 (2015).
- 429 68. Frost, J. S. & Martin, E. W. A Comparison of Distribution and High Temperature
430 Tolerance in *Bufo americanus* and *Bufo woodhousii fowleri*. *Copeia* **1971**, 750 (1971).
- 431 69. Gatz, A. J. Critical Thermal Maxima of *Ambystoma maculatum* (Shaw) and
432 *Ambystoma jeffersonianum* (Green) in Relation to Time of Breeding. *Herpetologica* **27**,
433 157–160 (1971).
- 434 70. Gatz, A. J. Intraspecific Variations in Critical Thermal Maxima of *Ambystoma*
435 *maculatum*. *Herpetologica* **29**, 264–268 (1973).
- 436 71. Geise, W. & Linsenmair, K. E. Adaptations of the reed frog *Hyperolius viridiflavus*
437 (Amphibia, Anura, Hyperoliidae) to its arid environment - IV. Ecological significance of
438 water economy with comments on thermoregulation and energy allocation. *Oecologia* **77**,
439 327–338 (1988).
- 440 72. González-del-Pliego, P. et al. Thermal tolerance and the importance of microhabitats
441 for Andean frogs in the context of land use and climate change. *Journal of Animal*
442 *Ecology* **89**, 2451–2460 (2020).
- 443 73. Gouveia, S. F. et al. Climatic niche at physiological and macroecological scales: The
444 thermal tolerance-geographical range interface and niche dimensionality. *Global Ecology*
445 *and Biogeography* **23**, 446–456 (2014).

- 446 74. Gray, R. Lack of physiological differentiation in three color morphs of the cricket frog
447 (Acris crepitans) in Illinois. *Transactions of the Illinois State Academy of Science* **70**, 73–
448 79 (1977).
- 449 75. Greenspan, S. E. et al. Infection increases vulnerability to climate change via effects
450 on host thermal tolerance. *Scientific Reports* **7**, (2017).
- 451 76. Guevara-Molina, E. C., Gomes, F. R. & Camacho, A. Effects of dehydration on
452 thermoregulatory behavior and thermal tolerance limits of *Rana catesbeiana* (Shaw,
453 1802). *Journal of Thermal Biology* **93**, (2020).
- 454 77. Gutiérrez Pesquera, L. Una valoración macrofisiológica de la vulnerabilidad al
455 calentamiento global. Análisis de los límites de tolerancia térmica en comunidades de
456 anfibios en gradientes latitudinales y altitudinales. (Pontificia Universidad Católica Del
457 Ecuador, 2015).
- 458 78. Gutiérrez Pesquera, M. Thermal tolerance across latitudinal and altitudinal gradients
459 in tadpoles. (Universidad de Sevilla, 2016).
- 460 79. Gutiérrez-Pesquera, L. M. et al. Testing the climate variability hypothesis in thermal
461 tolerance limits of tropical and temperate tadpoles. *Journal of Biogeography* **43**, 1166–
462 1178 (2016).
- 463 80. Gvoždík, L., Puky, M. & Šugerková, M. Acclimation is beneficial at extreme test
464 temperatures in the Danube crested newt, *Triturus dobrogicus* (Caudata, Salamandridae).
465 *Biological Journal of the Linnean Society* **90**, 627–636 (2007).
- 466 81. Heatwole, H., De Austin, S. B. & Herrero, R. Heat tolerances of tadpoles of two
467 species of tropical anurans. *Comparative Biochemistry And Physiology* **27**, 807–815
468 (1968).
- 469 82. Heatwole, H., Mercado, N. & Ortiz, E. Comparison of Critical Thermal Maxima of Two
470 Species of Puerto Rican Frogs of the Genus *Eleutherodactylus*. *Physiological Zoology* **38**,
471 1–8 (1965).
- 472 83. Holzman, N. & McManus, J. J. Effects of acclimation on metabolic rate and thermal
473 tolerance in the carpenter frog, *Rana vergatipes*. *Comparative Biochemistry and*
474 *Physiology -- Part A: Physiology* **45**, 833–842 (1973).
- 475 84. Hoppe, D. M. Thermal Tolerance in Tadpoles of the Chorus Frog *Pseudacris*
476 *triseriata*. *Herpetologica* **34**, 318–321 (1978).
- 477 85. Hou, P.-C. Thermal tolerance and preference in the adult amphibians from different
478 altitudinal LTER sites. (National Cheng Kung University, 2003).
- 479 86. Howard, J. H., Wallace, R. L. & Stauffer Jr, J. R. Critical thermal maxima in
480 populations of *Ambystoma macrodactylum* from different elevations. *Journal of*
481 *Herpetology* **17**, 400–402 (1983).

- 482 87. Hutchison, V. H. & Ritchart, J. P. Annual cycle of thermal tolerance in the
483 salamander, *Necturus maculosus*. *Journal of Herpetology* **23**, 73–76 (1989).
- 484 88. Hutchison, V. H. The Distribution and Ecology of the Cave Salamander, *Eurycea*
485 *lucifuga*. *Ecological Monographs* **28**, 2–20 (1958).
- 486 89. Hutchison, V. H. Critical Thermal Maxima in Salamanders. *Physiological Zoology* **34**,
487 92–125 (1961).
- 488 90. Hutchison, V. H., Engbretson, G. & Turney, D. Thermal Acclimation and Tolerance in
489 the Hellbender, *Cryptobranchus alleganiensis*. *Copeia* **1973**, 805–807 (1973).
- 490 91. Hutchison, V. H. & Rowlan, S. D. Thermal Acclimation and Tolerance in the
491 Mudpuppy, *Necturus maculosus*. *Journal of Herpetology* **9**, 367–368 (1975).
- 492 92. Jiang, S., Yu, P. & Hu, Q. A study on the critical thermal maxima of five species of
493 salamanders of China. *Acta Herpetologica Sinica* **6**, 56–62 (1987).
- 494 93. John-Alder, H. B., Morin, P. J. & Lawler, S. Thermal Physiology, Phenology, and
495 Distribution of Tree Frogs. *The American Naturalist* **132**, 506–520 (1988).
- 496 94. Johnson, C. R. Daily variation in the thermal tolerance of *Litoria caerulea* (Anura:
497 Hylidae). *Comparative Biochemistry and Physiology -- Part A: Physiology* **40**, 1109–1111
498 (1971).
- 499 95. Johnson, C. R. Thermal relations and water balance in the day frog, *Taudactylus*
500 *diurnus*, from an Australian rain forest. *Australian Journal of Zoology* **19**, 35–39 (1971).
- 501 96. Johnson, C. R. Diel variation in the thermal tolerance of *Litoria gracilentata* (Anura:
502 Hylidae). *Comparative Biochemistry and Physiology -- Part A: Physiology* **41**, 727–730
503 (1972).
- 504 97. Johnson, C. R. & Prine, J. E. The effects of sublethal concentrations of
505 organophosphorus insecticides and an insect growth regulator on temperature tolerance
506 in hydrated and dehydrated juvenile western toads, *Bufo boreas*. *Comparative*
507 *Biochemistry and Physiology -- Part A: Physiology* **53**, 147–149 (1976).
- 508 98. Johnson, C. R. Observations on body temperatures, critical thermal maxima and
509 tolerance to water loss in the Australian hylid, *Hyla caerulea* (White). *Proceedings of the*
510 *Royal Society of Queensland* **82**, 47–50 (1970).
- 511 99. Johnson, C. R. Thermal Relations and Daily Variation in the Thermal Tolerance in
512 *Bufo marinus*. *Journal of Herpetology* **6**, 35 (1972).
- 513 100. Johnson, C. Thermal relations in some southern and eastern Australian anurans.
514 *Proceedings of the Royal Society of Queensland* **82**, 87–94 (1971).
- 515 101. Johnson, C. The effects of five organophosphorus insecticides on thermal stress in
516 tadpoles of the Pacific tree frog, *Hyla regilla*. *Zoological Journal of the Linnean Society* **69**,
517 143–147 (1980).

- 518 102. Katzenberger, M., Duarte, H., Relyea, R., Beltrán, J. F. & Tejedo, M. Variation in
519 upper thermal tolerance among 19 species from temperate wetlands. *Journal of Thermal*
520 *Biology* **96**, (2021).
- 521 103. Katzenberger, M. et al. Swimming with predators and pesticides: How environmental
522 stressors affect the thermal physiology of tadpoles. *PLoS ONE* **9**, (2014).
- 523 104. Katzenberger, M., Hammond, J., Tejedo, M. & Relyea, R. Source of environmental
524 data and warming tolerance estimation in six species of North American larval anurans.
525 *Journal of Thermal Biology* **76**, 171–178 (2018).
- 526 105. Katzenberger, M. Thermal tolerance and sensitivity of amphibian larvae from
527 Palearctic and Neotropical communities. (Universidade de Lisboa, 2013).
- 528 106. Katzenberger, M. Impact of global warming in holarctic and neotropical communities
529 of amphibians. (Universidad de Sevilla, 2014).
- 530 107. Kern, P., Cramp, R. L. & Franklin, C. E. Temperature and UV-B-insensitive
531 performance in tadpoles of the ornate burrowing frog: An ephemeral pond specialist.
532 *Journal of Experimental Biology* **217**, 1246–1252 (2014).
- 533 108. Kern, P., Cramp, R. L., Seebacher, F., Ghanizadeh Kazerouni, E. & Franklin, C. E.
534 Plasticity of protective mechanisms only partially explains interactive effects of
535 temperature and UVR on upper thermal limits. *Comparative Biochemistry and Physiology*
536 *-Part A : Molecular and Integrative Physiology* **190**, 75–82 (2015).
- 537 109. Kern, P., Cramp, R. L. & Franklin, C. E. Physiological responses of ectotherms to
538 daily temperature variation. *Journal of Experimental Biology* **218**, 3068–3076 (2015).
- 539 110. Komaki, S., Igawa, T., Lin, S.-M. & Sumida, M. Salinity and thermal tolerance of
540 Japanese stream tree frog (*Buergeria japonica*) tadpoles from island populations.
541 *Herpetological Journal* **26**, 207–211 (2016).
- 542 111. Komaki, S., Lau, Q. & Igawa, T. Living in a Japanese onsen: Field observations and
543 physiological measurements of hot spring amphibian tadpoles, *Buergeria japonica*.
544 *Amphibia Reptilia* **37**, 311–314 (2016).
- 545 112. Krakauer, T. Tolerance limits of the toad, *Bufo marinus*, in South Florida.
546 *Comparative Biochemistry And Physiology* **33**, 15–26 (1970).
- 547 113. Kurabayashi, A. et al. Improved transport of the model amphibian, *Xenopus*
548 *tropicalis*, and its viable temperature for transport. *Current Herpetology* **33**, 75–87 (2014).
- 549 114. Lau, E. T. C., Leung, K. M. Y. & Karraker, N. E. Native amphibian larvae exhibit
550 higher upper thermal limits but lower performance than their introduced predator
551 *Gambusia affinis*. *Journal of Thermal Biology* **81**, 154–161 (2019).
- 552 115. Layne, J. R. & Claussen, D. L. Seasonal variation in the thermal acclimation of critical
553 thermal maxima (CTMax) and minima (CTMin) in the salamander *Eurycea bislineata*.
554 *Journal of Thermal Biology* **7**, 29–33 (1982).

- 555 116. Layne, J. R. & Claussen, D. L. The time courses of CTMax and CTMin acclimation in
556 the salamander *Desmognathus fuscus*. *Journal of Thermal Biology* **7**, 139–141 (1982).
- 557 117. Lee, P.-T. Acidic effect on tadpoles living in container habitats. (Tunghai University,
558 2019).
- 559 118. Longhini, L. S., De Almeida Prado, C. P., Bicego, K. C., Zena, L. A. & Gargaglioni, L.
560 H. Measuring cardiorespiratory variables on small tadpoles using a non-invasive
561 methodology. *Revista Cubana de Investigaciones Biomedicas* **38**, (2019).
- 562 119. López Rosero, A. C. Ontogenetic variation of thermal tolerance in two anuran
563 species of Ecuador: *Gastrotheca pseustes* (Hemiphractidae) and *Smilisca phaeota*
564 (Hylidae) and their relative vulnerability to environmental temperature change. (Pontificia
565 Universidad Católica Del Ecuador, 2015).
- 566 120. Lotshaw, D. P. Temperature adaptation and effects of thermal acclimation in *Rana*
567 *sylvatica* and *Rana catesbeiana*. *Comparative Biochemistry and Physiology -- Part A:*
568 *Physiology* **56**, 287–294 (1977).
- 569 121. Lu, H.-L., Wu, Q., Geng, J. & Dang, W. Swimming performance and thermal
570 resistance of juvenile and adult newts acclimated to different temperatures. *Acta*
571 *Herpetologica* **11**, 189–195 (2016).
- 572 122. Lu, H. L., Geng, J., Xu, W., Ping, J. & Zhang, Y. P. Physiological response and
573 changes in swimming performance after thermal acclimation in juvenile chinese fire-belly
574 newts, *Cynops orientalis*. *Acta Ecologica Sinica* **37**, 1603–1610 (2017).
- 575 123. Lutterschmidt, W. I. & Hutchison, V. H. The critical thermal maximum: Data to
576 support the onset of spasms as the definitive end point. *Canadian Journal of Zoology* **75**,
577 1553–1560 (1997).
- 578 124. Madalozzo, B. Variação latitudinal nos limites de tolerância e plasticidade térmica em
579 anfíbios em um cenário de mudanças climáticas: efeito dos micro-habitats, sazonalidade
580 e filogenia. (Universidade Federal de Santa Maria, 2018).
- 581 125. Mahoney, J. J. & Hutchison, V. H. Photoperiod acclimation and 24-hour variations in
582 the critical thermal maxima of a tropical and a temperate frog. *Oecologia* **2**, 143–161
583 (1969).
- 584 126. Maness, J. D. & Hutchison, V. H. Acute adjustment of thermal tolerance in vertebrate
585 ectotherms following exposure to critical thermal maxima. *Journal of Thermal Biology* **5**,
586 225–233 (1980).
- 587 127. Manis, M. L. & Claussen, D. L. Environmental and genetic influences on the thermal
588 physiology of *Rana sylvatica*. *Journal of Thermal Biology* **11**, 31–36 (1986).
- 589 128. Markle, T. M. & Kozak, K. H. Low acclimation capacity of narrow-ranging thermal
590 specialists exposes susceptibility to global climate change. *Ecology and Evolution* **8**,
591 4644–4656 (2018).

- 592 129. Marshall, E. & Grigg, G. C. Acclimation of CTM, LD50, and Rapid Loss of Acclimation
593 of Thermal Preferendum in Tadpoles of *Limnodynastes peronii* (Anura, Myobatrachidae).
594 *The Australian Zoologist* **20**, 447–456 (1980).
- 595 130. Mathias, J. H. The Comparative Ecologies of Two Species of Amphibia (*B. bufo* and
596 *B. calamita*) on the Ainsdale Sand Dunes National Nature Reserve. (The University of
597 Manchester, 1971).
- 598 131. McManus, J. J. & Nellis, D. W. The critical thermal maximum of the marine toad, *Bufo*
599 *marinus*. *Caribbean Journal of Science* **15**, 67–70 (1975).
- 600 132. Menke, M. E. & Claussen, D. L. Thermal acclimation and hardening in tadpoles of the
601 bullfrog, *Rana catesbeiana*. *Journal of Thermal Biology* **7**, 215–219 (1982).
- 602 133. Merino-Viteri, A. R. The vulnerability of microhylid frogs, *Cophixalus* spp., to climate
603 change in the Australian Wet Tropics. (James Cook University, 2018).
- 604 134. Messerman, A. F. Tales of an 'Invisible' Life Stage: Survival and Physiology Among
605 Terrestrial Juvenile Ambystomatid Salamanders. (University of Missouri, 2019).
- 606 135. Meza-Parral, Y., García-Robledo, C., Pineda, E., Escobar, F. & Donnelly, M. A.
607 Standardized ethograms and a device for assessing amphibian thermal responses in a
608 warming world. *Journal of Thermal Biology* **89**, (2020).
- 609 136. Miller, K. & Packard, G. C. Critical thermal maximum: Ecotypic variation between
610 montane and piedmont chorus frogs (*Pseudacris triseriata*, Hylidae). *Experientia* **30**, 355–
611 356 (1974).
- 612 137. Miller, K. & Packard, G. C. An Altitudinal Cline in Critical Thermal Maxima of Chorus
613 Frogs (*Pseudacris triseriata*). *The American Naturalist* **111**, 267–277 (1977).
- 614 138. Mueller, C. A., Bucsky, J., Korito, L. & Manzanares, S. Immediate and persistent
615 effects of temperature on oxygen consumption and thermal tolerance in embryos and
616 larvae of the baja California chorus frog, *pseudacris hypochondriaca*. *Frontiers in*
617 *Physiology* **10**, (2019).
- 618 139. Navas, C. A., Antoniazzi, M. M., Carvalho, J. E., Suzuki, H. & Jared, C. Physiological
619 basis for diurnal activity in dispersing juvenile *Bufo granulosus* in the Caatinga, a Brazilian
620 semi-arid environment. *Comparative Biochemistry and Physiology - A Molecular and*
621 *Integrative Physiology* **147**, 647–657 (2007).
- 622 140. Navas, C. A., Úbeda, C. A., Logares, R. & Jara, F. G. Thermal Tolerances in
623 Tadpoles of Three Species of Patagonian Anurans. *South American Journal of*
624 *Herpetology* **5**, 89–96 (2010).
- 625 141. Nietfeldt, J. W., Jones, S. M., Droge, D. L. & Ballinger, R. E. Rate of thermal
626 acclimation of larval *Ambystoma tigrinum*. *Journal of Herpetology* **14**, 209–211 (1980).

- 627 142. Nol, Rosemarie & Ultsch, G. R. The Roles of Temperature and Dissolved Oxygen in
628 Microhabitat Selection by the Tadpoles of a Frog (*Rana pipiens*) and a Toad (*Bufo*
629 *terrestris*). *Copeia* **1981**, 645–652 (1981).
- 630 143. Navarro, A. J. Thermal Physiology in a Widespread Lungless Salamander.
631 (University of Maryland, 2018).
- 632 144. Nowakowski, A. J. et al. Thermal biology mediates responses of amphibians and
633 reptiles to habitat modification. *Ecology Letters* **21**, 345–355 (2018).
- 634 145. Nowakowski, A. J. et al. Tropical amphibians in shifting thermal landscapes under
635 land-use and climate change. *Conservation Biology* **31**, 96–105 (2017).
- 636 146. Orille, A. C., McWhinnie, R. B., Brady, S. P. & Raffel, T. R. Positive Effects of
637 Acclimation Temperature on the Critical Thermal Maxima of *Ambystoma mexicanum* and
638 *Xenopus laevis*. *Journal of Herpetology* **54**, 289–292 (2020).
- 639 147. Oyamaguchi, H. M. et al. Thermal sensitivity of a Neotropical amphibian
640 (*Engystomops pustulosus*) and its vulnerability to climate change. *Biotropica* **50**, 326–337
641 (2018).
- 642 148. Paez Vacas, M. I. Mechanisms of population divergence along elevational gradients
643 in the tropics. (Colorado State University, 2016).
- 644 149. Paulson, B. K. & Hutchison, V. H. Blood changes in *Bufo cognatus* following acute
645 heat stress. *Comparative Biochemistry and Physiology -- Part A: Physiology* **87**, 461–466
646 (1987).
- 647 150. Paulson, B. & Hutchison, V. Origin of the stimulus for muscular spasms at the critical
648 thermal maximum in anurans. *Copeia* 810–813 (1987).
- 649 151. Percino-Daniel, R. et al. Environmental heterogeneity shapes physiological traits in
650 tropical direct-developing frogs. *Ecology and Evolution* (2021).
- 651 152. Perotti, M. G., Bonino, M. F., Ferraro, D. & Cruz, F. B. How sensitive are temperate
652 tadpoles to climate change? The use of thermal physiology and niche model tools to
653 assess vulnerability. *Zoology* **127**, 95–105 (2018).
- 654 153. Pintanel, P., Tejedó, M., Almeida-Reinoso, F., Merino-Viteri, A. & Gutiérrez-
655 Pesquera, L. M. Critical thermal limits do not vary between wild-caught and captive-bred
656 tadpoles of *Agalychnis spurrelli* (Anura: Hylidae). *Diversity* **12**, (2020).
- 657 154. Pintanel, P., Tejedó, M., Ron, S. R., Llorente, G. A. & Merino-Viteri, A. Elevational
658 and microclimatic drivers of thermal tolerance in Andean *Pristimantis* frogs. *Journal of*
659 *Biogeography* **46**, 1664–1675 (2019).
- 660 155. Pintanel, P. Thermal adaptation of amphibians in tropical mountains. Consequences
661 of global warming. (Universitat de Barcelona, 2018).

- 662 156. Pintanel, P., Tejedo, M., Salinas-Ivanenko, S., Jervis, P. & Merino-Viteri, A.
663 Predators like it hot: Thermal mismatch in a predator-prey system across an elevational
664 tropical gradient. *The Journal of animal ecology* (2021).
- 665 157. Pough, F. H. Natural daily temperature acclimation of eastern red efts,
666 *Notophthalmus v. viridescens* (rafinesque) (amphibia: caudata). *Comparative*
667 *Biochemistry and Physiology -- Part A: Physiology* **47**, 71–78 (1974).
- 668 158. Pough, F. H., Stewart, M. M. & Thomas, R. G. Physiological basis of habitat
669 partitioning in Jamaican Eleutherodactylus. *Oecologia* **27**, 285–293 (1977).
- 670 159. Quiroga, L. B., Sanabria, E. A., Fornés, M. W., Bustos, D. A. & Tejedo, M. Sublethal
671 concentrations of chlorpyrifos induce changes in the thermal sensitivity and tolerance of
672 anuran tadpoles in the toad *Rhinella arenarum*? *Chemosphere* **219**, 671–677 (2019).
- 673 160. Rausch, C. The thermal ecology of the Red-spotted toad, *Bufo punctatus*, across life
674 history. (University of Nevada, 2007).
- 675 161. Reichenbach, N. & Brophy, T. R. Natural history of the peaks of otter salamander
676 (*Plethodon Hubrichti*) along an Elevational gradient. *Herpetological Bulletin* 7–15 (2017).
- 677 162. Reider, K. E., Larson, D. J., Barnes, B. M. & Donnelly, M. A. Thermal adaptations to
678 extreme freeze–thaw cycles in the high tropical Andes. *Biotropica* **53**, 296–306 (2021).
- 679 163. Richter-Boix, A. et al. Local divergence of thermal reaction norms among amphibian
680 populations is affected by pond temperature variation. *Evolution* **69**, 2210–2226 (2015).
- 681 164. Riquelme, N. A., Díaz-Páez, H. & Ortiz, J. C. Thermal tolerance in the Andean toad
682 *Rhinella spinulosa* (Anura: Bufonidae) at three sites located along a latitudinal gradient in
683 Chile. *Journal of Thermal Biology* **60**, 237–245 (2016).
- 684 165. Ritchart, J. P. & Hutchison, V. H. The effects of ATP and cAMP on the thermal
685 tolerance of the mudpuppy, *Necturus maculosus*. *Journal of Thermal Biology* **11**, 47–51
686 (1986).
- 687 166. Rivera-Burgos, A. C. Habitat Suitability for Eleutherodactylus Frogs in Puerto Rico:
688 Indexing Occupancy, Abundance and Reproduction to Climatic and Habitat
689 Characteristics. (North Carolina State University, 2019).
- 690 167. Rivera-Ordóñez, J. M., Justin Nowakowski, A., Manansala, A., Thompson, M. E. &
691 Todd, B. D. Thermal niche variation among individuals of the poison frog, *Oophaga*
692 *pumilio*, in forest and converted habitats. *Biotropica* **51**, 747–756 (2019).
- 693 168. Romero Barreto, P. Requerimientos fisiológicos y microambientales de dos especies
694 de anfibios (*Scinax ruber* e *Hyloxalus yasuni*) del bosque tropical de Yasuní y sus
695 implicaciones ante el cambio climático (Pontificia Universidad Católica Del Ecuador,
696 2013).

- 697 169. Ruiz-Aravena, M. et al. Impact of global warming at the range margins: Phenotypic
698 plasticity and behavioral thermoregulation will buffer an endemic amphibian. *Ecology and*
699 *Evolution* **4**, 4467–4475 (2014).
- 700 170. Ruthsatz, K. et al. Thyroid hormone levels and temperature during development alter
701 thermal tolerance and energetics of *Xenopus laevis* larvae. *Conservation Physiology* **6**,
702 (2018).
- 703 171. Ruthsatz, K. et al. Post-metamorphic carry-over effects of altered thyroid hormone
704 level and developmental temperature: physiological plasticity and body condition at two
705 life stages in *Rana temporaria*. *Journal of Comparative Physiology B: Biochemical,*
706 *Systemic, and Environmental Physiology* **190**, 297–315 (2020).
- 707 172. Rutledge, P. S., Spotila, J. R. & Easton, D. P. Heat hardening in response to two
708 types of heat shock in the lungless salamanders *Eurycea bislineata* and *Desmognathus*
709 *ochrophaeus*. *Journal of Thermal Biology* **12**, 235–241 (1987).
- 710 173. Sanabria, E. et al. Effect of salinity on locomotor performance and thermal extremes
711 of metamorphic Andean Toads (*Rhinella spinulosa*) from Monte Desert, Argentina.
712 *Journal of Thermal Biology* **74**, 195–200 (2018).
- 713 174. Sanabria, E. A., González, E., Quiroga, L. B. & Tejedo, M. Vulnerability to warming in
714 a desert amphibian tadpole community: the role of interpopulational variation. *Journal of*
715 *Zoology* **313**, 283–296 (2021).
- 716 175. Sanabria, E. A. & Quiroga, L. B. Change in the thermal biology of tadpoles of
717 *Odontophrynus occidentalis* from the Monte desert, Argentina: Responses to photoperiod.
718 *Journal of Thermal Biology* **36**, 288–291 (2011).
- 719 176. Sanabria, E. A., Quiroga, L. B., González, E., Moreno, D. & Cataldo, A. Thermal
720 parameters and locomotor performance in juvenile of *Pleurodema nebulosum* (Anura:
721 *Leptodactylidae*) from the Monte Desert. *Journal of Thermal Biology* **38**, 390–395 (2013).
- 722 177. Sanabria, E. A., Quiroga, L. B. & Martino, A. L. Seasonal changes in the thermal
723 tolerances of the toad *Rhinella arenarum* (Bufonidae) in the Monte Desert of Argentina.
724 *Journal of Thermal Biology* **37**, 409–412 (2012).
- 725 178. Sanabria, E. A., Quiroga, L. B. & Martino, A. L. Seasonal Changes in the thermal
726 tolerances of *odontophrynus occidentalis* (BERG, 1896) (Anura: Cycloramphidae).
727 *Belgian Journal of Zoology* **143**, 23–29 (2013).
- 728 179. Sanabria, E. A. et al. Thermal ecology of the post-metamorphic Andean toad
729 (*Rhinella spinulosa*) at elevation in the monte desert, Argentina. *Journal of Thermal*
730 *Biology* **52**, 52–57 (2015).
- 731 180. Sanabria, E. A., Vaira, M., Quiroga, L. B., Akmentins, M. S. & Pereyra, L. C. Variation
732 of thermal parameters in two different color morphs of a diurnal poison toad,

- 733 Melanophryniscus rubriventris (Anura: Bufonidae). *Journal of Thermal Biology* **41**, 1–5
734 (2014).
- 735 181. Sanabria, E. A. & Quiroga, L. B. Thermal parameters changes in males of *Rhinella*
736 *arenarum* (Anura: Bufonidae) related to reproductive periods. *Revista de Biología Tropical*
737 **59**, 347–353 (2011).
- 738 182. Scheffers, B. R. et al. Thermal buffering of microhabitats is a critical factor mediating
739 warming vulnerability of frogs in the Philippine biodiversity hotspot. *Biotropica* **45**, 628–
740 635 (2013).
- 741 183. Scheffers, B. R., Edwards, D. P., Diesmos, A., Williams, S. E. & Evans, T. A.
742 Microhabitats reduce animal's exposure to climate extremes. *Global Change Biology* **20**,
743 495–503 (2014).
- 744 184. Schmid, W. D. High Temperature Tolerances of *Bufo Hemiophrys* and *Bufo*
745 *Cognatus*. *Ecology* **46**, 559–560 (1965).
- 746 185. Seal, er, J. A. & West, B. W. Critical Thermal Maxima of Some Arkansas
747 Salamanders in Relation to Thermal Acclimation. *Herpetologica* **25**, 122–124 (1969).
- 748 186. Seibel, R. V. Variables Affecting the Critical Thermal Maximum of the Leopard Frog,
749 *Rana pipiens* Schreber. *Herpetologica* **26**, 208–213 (1970).
- 750 187. Sherman, E. Ontogenetic change in thermal tolerance of the toad *Bufo woodhousii*
751 *fowleri*. *Comparative Biochemistry and Physiology -- Part A: Physiology* **65**, 227–230
752 (1980).
- 753 188. Sherman, E. Thermal biology of newts (*Notophthalmus viridescens*) chronically
754 infected with a naturally occurring pathogen. *Journal of Thermal Biology* **33**, 27–31
755 (2008).
- 756 189. Sherman, E., Baldwin, L., Fernandez, G. & Deurell, E. Fever and thermal tolerance in
757 the toad *Bufo marinus*. *Journal of Thermal Biology* **16**, 297–301 (1991).
- 758 190. Sherman, E. & Levitis, D. Heat hardening as a function of developmental stage in
759 larval and juvenile *Bufo americanus* and *Xenopus laevis*. *Journal of Thermal Biology* **28**,
760 373–380 (2003).
- 761 191. Shi, L., Zhao, L., Ma, X. & Ma, X. Selected body temperature and thermal tolerance
762 of tadpoles of two frog species (*Fejervarya limnocharis* and *Microhyla ornata*) acclimated
763 under different thermal conditions. *Acta Ecologica Sinica* **32**, 0465–0471 (2012).
- 764 192. Simon, M. N., Ribeiro, P. L. & Navas, C. A. Upper thermal tolerance plasticity in
765 tropical amphibian species from contrasting habitats: Implications for warming impact
766 prediction. *Journal of Thermal Biology* **48**, 36–44 (2015).
- 767 193. Simon, M. Plasticidade fenotípica em relação à temperatura de larvas de *Rhinella*
768 (Anura: Bufonidae) da caatinga e da floresta Atlântica. (Universidade de Sao Paulo,
769 2010).

- 770 194. Skelly, D. K. & Freidenburg, L. K. Effects of beaver on the thermal biology of an
771 amphibian. *Ecology Letters* **3**, 483–486 (2000).
- 772 195. Sos, T. Thermoconformity even in hot small temporary water bodies: a case study in
773 yellow-bellied toad (*Bombina v. variegata*). *Herpetologica Romanica* **1**, 1–11 (2007).
- 774 196. Spotila, J. R. Role of Temperature and Water in the Ecology of Lungless
775 Salamanders. *Ecological Monographs* **42**, 95–125 (1972).
- 776 197. Tracy, C. R., Christian, K. A., Betts, G. & Tracy, C. R. Body temperature and
777 resistance to evaporative water loss in tropical Australian frogs. *Comparative*
778 *Biochemistry and Physiology - A Molecular and Integrative Physiology* **150**, 102–108
779 (2008).
- 780 198. Turriago, J. L., Parra, C. A. & Bernal, M. H. Upper thermal tolerance in anuran
781 embryos and tadpoles at constant and variable peak temperatures. *Canadian Journal of*
782 *Zoology* **93**, 267–272 (2015).
- 783 199. Vidal, M. A., Novoa-Muñoz, F., Werner, E., Torres, C. & Nova, R. Modeling warming
784 predicts a physiological threshold for the extinction of the living fossil frog
785 *Calyptocephalella gayi*. *Journal of Thermal Biology* **69**, 110–117 (2017).
- 786 200. von May, R. et al. Divergence of thermal physiological traits in terrestrial breeding
787 frogs along a tropical elevational gradient. *Ecology and Evolution* **7**, 3257–3267 (2017).
- 788 201. von May, R. et al. Thermal physiological traits in tropical lowland amphibians:
789 Vulnerability to climate warming and cooling. *PLoS ONE* **14**, (2019).
- 790 202. Wagener, C., Kruger, N. & Measey, J. Progeny of *Xenopus laevis* from altitudinal
791 extremes display adaptive physiological performance. *Journal of Experimental Biology*
792 **224**, (2021).
- 793 203. Wang, H. & Wang, L. Thermal adaptation of the common giant toad (*Bufo*
794 *gargarizans*) at different earlier developmental stages. *Journal of Agricultural University of*
795 *Hebei* **31**, 79–83 (2008).
- 796 204. Wang, L. The effects of constant and variable thermal acclimation on thermal
797 tolerance of the common giant toad tadpoles (*Bufo gargarizans*). *Acta Ecological Sinica*
798 **34**, 1030–1034 (2014).
- 799 205. Wang, L.-Z. & Li, X.-C. Effect of Temperature on Incubation and Thermal Tolerance
800 of the Chinese Forest Frog. *Chinese Journal of Zoology* (2007).
- 801 206. Wang, L. & Li, X.-C. Effects of constant thermal acclimation on thermal tolerance of
802 the Chinese forest frog (*Rana chensinensis*). *Acta Hydrobiologica Sinica* **31**, 748–750
803 (2007).
- 804 207. Wang, L.-Z., Li, X.-C. & Sun, T. Preferred temperature, avoidance temperature and
805 lethal temperature of tadpoles of the common giant toad (*Bufo gargarizans*) and the
806 Chinese forest frog (*Rana chensinensis*). *Chinese Journal of Zoology* **40**, 23–27 (2005).

- 807 208. Warburg, M. R. On the water economy of israel amphibians: The anurans.
808 *Comparative Biochemistry and Physiology -- Part A: Physiology* **40**, 911–924 (1971).
- 809 209. Warburg, M. R. The water economy of israel amphibians: The urodeles Triturus
810 vittatus (Jenyns) and Salamandra salamandra (L.). *Comparative Biochemistry and*
811 *Physiology -- Part A: Physiology* **40**, 1055-1056,IN11,1057-1063 (1971).
- 812 210. Willhite, C. & Cupp, P. V. Daily rhythms of thermal tolerance in Rana clamitans
813 (Anura: Ranidae) tadpoles. *Comparative Biochemistry and Physiology -- Part A:*
814 *Physiology* **72**, 255–257 (1982).
- 815 211. Wu, C.-S. & Kam, Y.-C. Thermal tolerance and thermoregulation by Taiwanese
816 rhacophorid tadpoles (Buergeria japonica) living in geothermal hot springs and streams.
817 *Herpetologica* **61**, 35–46 (2005).
- 818 212. Wu, Q.-H. & Hsieh, C.-H. *Thermal tolerance and population genetics of Hynobius*
819 *fuca*. 64 (2016).
- 820 213. Xu, X. The effect of temperature on body temperature and thermoregulation in
821 different geographic populations of Rana dybowskii. (Harbin Normal University, 2017).
- 822 214. Yandún Vela, M. C. Capacidad de aclimatación en renacuajos de dos especies de
823 anuros: Rhinella marina (Bufonidae) y Gastrotheca riobambae (Hemiphractidae) y su
824 vulnerabilidad al cambio climático. (Pontificia Universidad Católica Del Ecuador, 2017).
- 825 215. Young, V. K. H. & Gifford, M. E. Limited capacity for acclimation of thermal
826 physiology in a salamander, Desmognathus brimleyorum. *Journal of Comparative*
827 *Physiology B: Biochemical, Systemic, and Environmental Physiology* **183**, 409–418
828 (2013).
- 829 216. Yu, Z., Dickstein, R., Magee, W. E. & Spotila, J. R. Heat shock response in the
830 salamanders plethodon jordani and Plethodon cinereus. *Journal of Thermal Biology* **23**,
831 259–265 (1998).
- 832 217. Zheng, R.-Q. & Liu, C.-T. Giant spiny-frog (Paa spinosa) from different populations
833 differ in thermal preference but not in thermal tolerance. *Aquatic Ecology* **44**, 723–729
834 (2010).
- 835 218. Zweifel, R. G. Studies on the Critical Thermal Maxima of Salamanders. *Ecology* **38**,
836 64–69 (1957).

837

838